LRP1 is a Negative Regulator of Oligodendrogenesis in the Adult Mouse Central Nervous System

by
Loic Francis Auderset
Bachelor of Biotechnology and Medical Research with Honours
Menzies Institute for Medical Research | College of Health and Medicine

Submitted in fulfilment of the requirements for the degree of Doctor of Philosophy
University of Tasmania, January, 2020

Declaration of Originality

This thesis contains no material which has been accepted for a degree or diploma by the University or any other institution, except by way of background information and duly acknowledged in the thesis, and to the best of my knowledge and belief no material previously published or written by another person except where due acknowledgement is made in the text of the thesis, nor does the thesis contain any material that infringes copyright.

Loic Auderset

Authority of Access

This thesis may be made available for loan and limited copying and communication in accordance with the Copyright Act 1968.

Loic Auderset

Statement Regarding Published Work Contained in Thesis

Loic Auderset

Statement of Co-Authorship

The following people and institutions contributed to the publication of work undertaken as part of this thesis:

Candidate – Mr Loic Auderset, Menzies Institute for Medical Research
Author 1 – Ms Carlie Cullen, Menzies Institute for Medical Research
Author 2 – Ms Lila Landowski, Menzies Institute for Medical Research
Author 3 – Ms Kimberly Pitman, Menzies Institute for Medical Research
Author 4 – Ms Renee Pepper, Menzies Institute for Medical Research
Author 5 – Professor Bruce Taylor, Menzies Institute for Medical Research
Author 6 – Professor Lisa Foa, School of Medicine
Author 7 – Associate Professor Kaylene Young, Menzies Institute for Medical Research

Contribution of work by co-authors for each paper:

PAPER 1: Located in Chapter 1

Auderset L, Landowski LM, Foa L, Young KM (2016b) Low Density Lipoprotein Receptor Related Proteins as Regulators of Neural Stem and Progenitor Cell Function. Stem Cells International 2016:2108495–16.

Author contributions:
Conceived and designed the review: Candidate and Author 7
Wrote the manuscript: Candidate, Author 2, Author 6 and Author 7

PAPER 2: Located in Chapter 3

Auderset L, Cullen CL, Young KM (2016a) Low Density Lipoprotein-Receptor Related Protein 1 Is Differentially Expressed by Neuronal and Glial Populations in the Developing and Mature Mouse Central Nervous System. Coulson EJ, ed. PLoS ONE 11:e0155878–22.

Author contributions:

Conceived and designed the experiments: Candidate, Author 7
Performed the experiments: Candidate, Author 1
Analysed the data: Candidate
Wrote the manuscript: Candidate, Author 1, Author 7

PAPER 3: Located in Chapter 4

Auderset L, Pitman KA, Cullen CL, Pepper RE, Taylor BV, Foa L Young KM. (2020) Low-density lipoprotein receptor-related protein 1 (LRP1) is a negative regulator of oligodendrocyte progenitor cell differentiation in the adult mouse brain. In preparation.

Author contributions:
Conceived and designed the experiments: Candidate, Author 5, Author 6, Author 7
Performed the experiments: Candidate, Author 1, Author 3, Author 4
Analysed the data: Candidate, Author 3
Wrote the manuscript: Candidate, Author 7

We, the undersigned, endorse the above stated contribution of work undertaken for each of the published (or submitted) peer-reviewed manuscripts contributing to this thesis:

Signed:

Loic Auderset	Kaylene Young	James Sharman
Candidate	Primary Supervisor	Acting Director
MIMR	MIMR	MIMR
University of Tasmania	University of Tasmania	University of Tasmania
Date: 08/01/20	**08/01/20**	**08/01/20**

Statement of Ethical Conduct

The research associated with this thesis abides by the international and Australian codes on human and animal experimentation, the guidelines by the Australian Government's Office of the Gene Technology Regulator and the rulings of the Safety, Ethics and Institutional Biosafety Committees of the University. Ethics Approval A0016151

Loic Auderset

Contribution of Candidate to Research Papers not Included in this Thesis

O'Rourke M, Cullen CL, **Auderset L**, Pitman KA, Achatz D, Gasperini R, Young KM (2016) Evaluating Tissue-Specific Recombination in a Pdgfrα-CreERT2 Transgenic Mouse Line. PLoS ONE 11:e0162858.

Cullen CL, Senesi M, Tang AD, Clutterbuck MT, **Auderset L**, O'Rourke ME, Rodger J, Young KM (2019) Low-intensity transcranial magnetic stimulation promotes the survival and maturation of newborn oligodendrocytes in the adult mouse brain. Glia 67:1462–1477.

Cullen CL, O'Rourke, Beasley S, **Auderset L**, Zhen Y, Gasperini R, Young KM. Ablating Kif3a to prevent primary cilia formation by oligodendrocyte progenitor cells reduces oligodendrogenesis and impairs motor performance. Final stages of preparation 2020.

Cullen CL, Pepper RE, Clutterbuck MT, Pitman KA, Oorschot V, **Auderset L**, Tang AD, Ramm G, Emery B, Rodger J, Jolivet RB and Young KM. Myelin and nodal plasticity modulate action potential conduction in the adult mouse. 2019 brain.(http://biorxiv.org/cgi/content/short/726760v1).

Acknowledgments

I would like to acknowledge the traditional owners of the land upon which the information contained in this thesis was gathered and subsequently written. The muwinina people are part of the oldest continuing culture in the world and I pay my respect to elders past, present and emerging, and acknowledge that sovereignty was never ceded. I would also like to thank my supervisors Kaylene, Lisa and Bruce. They were always there to provide help and feedback during the ups and downs and have been excellent mentors. As the longest serving member of the Young Lab, I am sad to leave but excited to see what lies ahead. I would like to thank all past and present members of the FLY lab groups, I have thoroughly enjoyed working alongside you all and wish you all the best for the future. Lastly, I would like to thank Susan and Leon Morrell who provided financial support during my candidature. Your kindness and generously has helped me immensely over the past 4 years and is something that I will remember forever.

Abbreviations

α2M	Alpha-2 macroglobulin
*α2M	Activated alpha-2 macroglobulin
AEP	anterior entopeduncular area
AMPA	α-amino-3-hydroxy-5-methyl-4-isoxazolepropionic acid
BACE1	Beta-secretase 1
BSA	Bovine serum albumin
cAMP	cyclic adenosine monophosphate
CC1/APC	Anti-adenomatous polyposis coli
CC	Corpus Callosum
CD91	Cluster of differentiation 91
CGE	Caudal ganglionic eminence
CNS	Central nervous system
CNTF	Ciliary neurotrophic factor
Cre	Cre Recombinase
Ctx	Cortex
DIV	Days *in vitro*
DMEM	Dulbeccos's modified eagle medium
DNA	Deoxyribonucleaic acid
DTT	Dithiothreitol
EAE	Experimental autoimmune encephalomyelitis
EBSS	Earle's balanced salt solution
EdU	5-Ethynyl-2'-deoxyuridine
FBS/FCS	Fetal bovine serum/fetal calf serum
FGF	Fibroblast growth factor

GFP	Green fluorescent protein
GPR17	G protein coupled receptor 17
HRP	Horseradish peroxidase
LGE	Lateral ganglionic eminence
LRP1	Low-density lipoprotein receptor related protein 1
LRP2	Low-density lipoprotein receptor related protein 2
MBP	Myelin basic protein
MS	Multiple Sclerosis
MyRF	Myelin regulatory factor
NAC	N-acetyl cysteine
NeuN	Neuronal Nuclear Antigen
NG2	Neural/glial antigen-2
NT3	Neurotrophin 3
OL	Oligodendrocyte
ON	Optic nerve
OPC	Oligodendrocyte progenitor cells
OLIG1	Oligodendrocyte transcription factor-1
OLIG2	Oligodendrocyte transcription factor-2
PDGF-AA	Platelet derived growth factor-AA
PDGFRα	Platelet derived growth factor receptor alpha
PDGFRβ	Platelet derived growth factor receptor beta
PDL	Poly D-lysine
pMN	Primary motor neuron
RAP	Receptor Associated Protein
RNA	Ribonucleic acid

Shh	Sonic hedgehog
SVZ	Subventricular zone
T3	Triodothyronine
TFEB	Transcription factor EB
VGCC	Voltage gated calcium channel
VLDL	Very low-density lipoprotein
YFP	Yellow fluorescent protein

Preface

Oligodendrocyte progenitor cells (OPCs) are found throughout the adult central nervous system (CNS), where they continually differentiate into oligodendrocytes. This feature of OPC behaviour makes them an attractive target for remyelination enhancing therapies aimed at treating demyelinating diseases such as Multiple Sclerosis. However, for this approach to work, further information is needed about the role of specific cell-surface receptors in directing OPC behaviour in the adult CNS. One cell surface receptor that is highly expressed by OPCs, but rapidly down regulated as they differentiate into oligodendrocytes, is the low-density lipoprotein receptor related protein (LRP1). LRP1 is a member of the low-density lipoprotein receptor family, and it is capable of signalling in a variety of ways. To investigate the role that LRP1 plays in modulating adult OPCs, I conditionally deleted *Lrp1* from OPCs in the healthy and demyelinated adult mouse CNS. In the healthy CNS, OPCs without *Lrp1* had an increased rate of proliferation and gave rise to a larger number of newborn oligodendrocytes overtime. However, the myelinating profile of individual new oligodendrocytes was unchanged. Following cuprizone induced demyelination control mice had larger demyelinated lesions when compared to *Lrp1*-deleted mice, suggesting that the blockade of LRP1 signalling by OPCs could enhance remyelination. By studying the effect of *Lrp1* deletion and the ligand activation of LRP1 on OPC behaviour *in vitro*, I determined that the effect of LRP1 on OPC proliferation was likely to be secondary to the inhibitory effect of LRP1 on OPC differentiation. These data suggest that suppressing LRP1 signalling may be useful in enhancing CNS myelin repair.

Contents

List of Figures

Chapter 1: Introduction

1.1 Glia

The central nervous system (CNS) is a highly organised structure that consists of the brain, optic nerve and spinal cord, and contains a variety of specialised cell types. These cells include neurons and glia [astrocytes, oligodendrocytes (OLs), microglia, oligodendrocyte progenitor cells (OPCs) and neural stem cells]. Historically, the study of neurons has largely dominated the field of neuroscience research, with the glial cells (glia - meaning glue), being thought of simply as support cells. However, in recent years researchers have developed a greater understanding of the functional diversity of glia, and have shown that they play a crucial role in maintaining normal CNS function. In particular, OPCs have been shown to generate new OLs throughout life.

1.2 Oligodendrocyte precursor cells (OPCs)

OPCs, also known as NG2 glia or O-2A progenitors, were first discovered in primary cell cultures derived from perinatal rat optic nerve (Stallcup, 1981; Raff et al., 1983), and were later found to be present in primary cultures derived from adult rat optic nerve (ffrench-Constant and Raff, 1986). Although their morphology can vary between development and adulthood as well as between brain regions, OPCs are normally highly ramified cells with processes extending away from their cell bodies in all directions. They can be identified by the expression of platelet derived growth factor receptor alpha (PDGFRα) (Pringle and Richardson, 1993) or the chondroitin sulphate proteoglycan NG2 (Zhu et al., 2008) (**Figure 1**), however pericytes, associated with the CNS vasculature (and inflammatory microglia) also express NG2 (Fukushi et al., 2004; Zhu et al., 2016). OPCs also express the transcription factor OLIG2, which is also crucial for the specification of OPCs from earlier progenitors (Takebayashi et al., 2002).

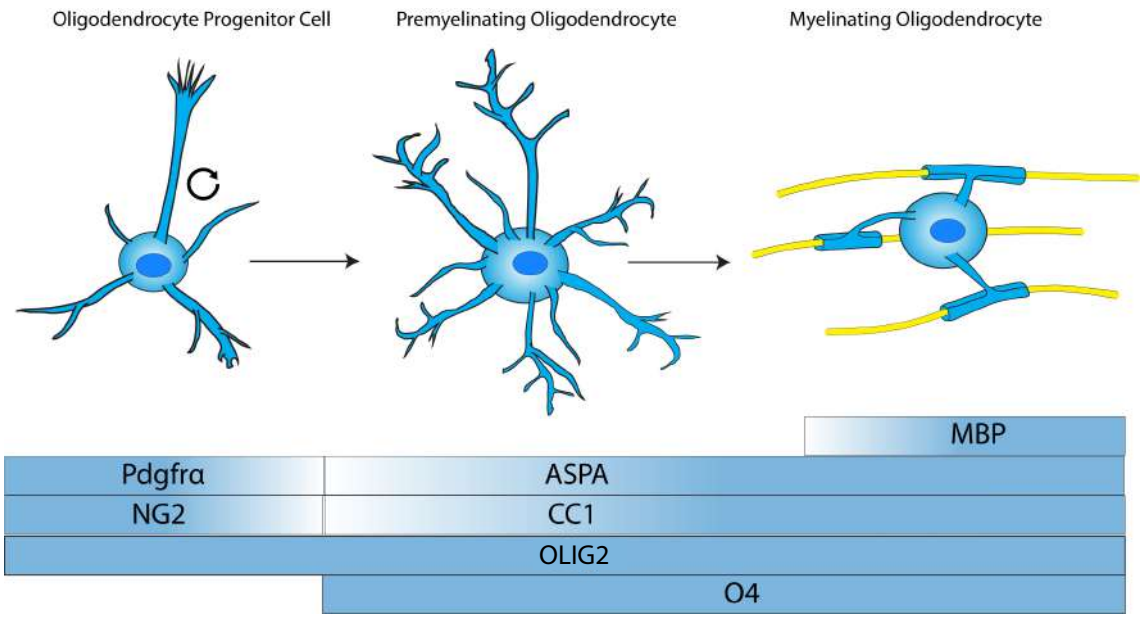

Figure 1. Markers of the oligodendrocyte lineage

OPCs can be identified by the expression of PDGFRα and NG2. As they differentiate, they lose expression of these markers and begin expressing oligodendrocyte precific markers such as ASPA and CC1. Myelinating oligodendrocytes can be indetified by the expression of MBP. All cells of the oligodendrocyte lineage can be identified by the expression of OLIG2.

1.3 OPC origins

OPCs are first generated during embryonic development in mice and around gestational week 9 in humans (Jakovcevski et al., 2009). During embryonic development, OPCs are produced from the neuroepithelial stem cells, also known as radial glial cells (Noll and Miller, 1993; Pringle and Richardson, 1993). In the spinal cord, OPC generation commences at embryonic day 12.5 (E12.5) in mice, and E16 in rats, from stem cells located in the ventral region of the neuroepithelium, known as the pre motor neuron (pMN) domain (Noll and Miller, 1993; Richardson et al., 2006). The pMN domain is named for its role prior to OPC generation, when the stem cells instead generate the spinal cord motor neurons. It is defined by the expression of two transcription factors, OLIG1 and OLIG2 (Zhou et al., 2000), both of which are highly expressed in OPCs and necessary for their production and differentiation (Dai et al., 2015). OLIG1/2 expression in the pMN domain is induced by a gradient of ventrally secreted sonic hedgehog (Shh). Examination of *Olig1/2* knockout mice confirmed the importance of these transcription factors for motor neuron and OPC generation. In the absence of OLIG1/2, stem cells in the pMN domain instead form V2 interneurons and astrocytes (Zhou and Anderson, 2002). Shortly after they first appear, OPCs begin migrating in all directions until they are evenly spread throughout the spinal cord grey and white matter by E18 in rats (Pringle and Richardson, 1993). It is estimated that approximately 85% of all spinal cord OLs originate from pMN, with other domains such as the P3 domain, ventrally adjacent to pMN (Richardson et al., 2006), and more dorsal domains (dP3 and dP6) producing the rest (Rowitch and Kriegstein, 2010). The dorsal neuroepithelial stem cells are influenced by different spatiotemporal signalling molecules and generate OPCs from ~E15 in mice (Chandran, 2003; Vallstedt et al., 2005).

Like spinal cord OPCs, forebrain OPCs have multiple origins, which were discovered by cre-lox fate mapping (Kessaris et al., 2005). Kessaris et al. (2006) found that PDGFRα^{+} OPCs are generated and migrate in three distinct waves. The initial wave of OPCs is produced from *Nkx2.1* expressing stem cells in the ventral telencephalon, specifically the medial ganglionic eminence (MGE) and the anterior entopeduncular area (AEP) at E12.5 in mice. These cells migrate along blood vessels (Tsai et al., 2016) from their ventral origins to populate all regions of the developing brain, including the developing cortex, which they reach at ~E18 (Tekki-Kessaris et al., 2001). The next wave of OPCs is initiated at E15.5 from the *Gsh2* expressing stem cells in the lateral and caudal ganglionic eminence (LGE and CGE) (Kessaris et al., 2005), and migrates to combine with the first wave in the cortex. The third and final wave of OPCs originates from the *Emx1* expressing neuroepithelial stem cells underlying the developing cortex. These newly born OPCs migrate dorsally, and can be found throughout the cortex and corpus callosum (CC) just after birth. Unexpectedly, the earliest OPCs produced by *Nkx2.1* cells are lost shortly after birth, particularly from the cortex and CC (Kessaris et al., 2005), and the purpose of these temporary OPCs is still unknown. By postnatal day 13 (P13), ~80% of OL lineage cells in the CC are derived from the cortical ventricular zone, and the remainder from the MGE/LGE (Tripathi et al., 2011).

1.4 OPC heterogeneity

The idea that the OPC population is heterogeneous stemmed from the discovery of the mixed developmental origins. However, diphtheria toxin A (DTA) ablation of a specific subpopulation of OPCs didn't change to the number of OL lineage cells at P12 or the level of myelination in adult mice, suggesting that OPCs from other origins can compensate for the loss of one population (Kessaris et al., 2005). Additionally, RNA-sequencing data has failed to identify any difference in the gene expression profile between OPCs born from separate

germinal niches (Marques et al., 2018). More recently however, Winkler et al (2018) reduced the number of dorsally-derived OPCs in embryonic mice, by conditionally deleting Smoothened (Smo), a Sonic Hedgehog (Shh) signalling effector, and found that OL number was normal at early postnatal ages, due to compensation from ventrally-derived OPCs and the proliferation of the remaining dorsal OPCs, yet the grey matter OPC population did not fully recover.

Furthermore, only a subset of OPCs express the G Protein Coupled Receptor 17 (GPR17) in the adult CNS (Lecca et al., 2008) and OPCs expressing GPR17 are less likely to differentiate into OLs (Viganò et al., 2016), suggesting that not all OPCs are equivalent. As GPR17 expressing OPCs do not localise to a specific CNS region, but are dispersed throughout the grey and white matter of the CNS, Vigano et al (2016) concluded that these OPCs act as a reserve pool, so that following white matter injury they can rapidly proliferate in order to sustain the OPC population.

1.5 OPCs in the healthy adult central nervous system

Following OPC generation and migration during development, OPCs in the adult CNS form a lattice like network and are evenly spread throughout the grey and white matter (**Figure 2**). They make up ~5% of the total number of cells and are the most proliferative cell type present in the adult CNS (Dawson, 2003). This network of cells is maintained by homotypic repulsion, most likely achieved via interactions between adhesion molecules on the filopodial extensions that are yet to be determined (Hughes et al., 2013). In mice, adult OPCs proliferate and differentiate at a slower rate than developmental OPCs (Psachoulia et al., 2009; Young et al., 2013), and in the adult human brain, the rate of generation of OLs is ~100 times lower than in rodents and is more pronounced in the grey matter (Yeung et al., 2014). However, following a demyelinating injury the rate of OPC proliferation can be increased in order to facilitate

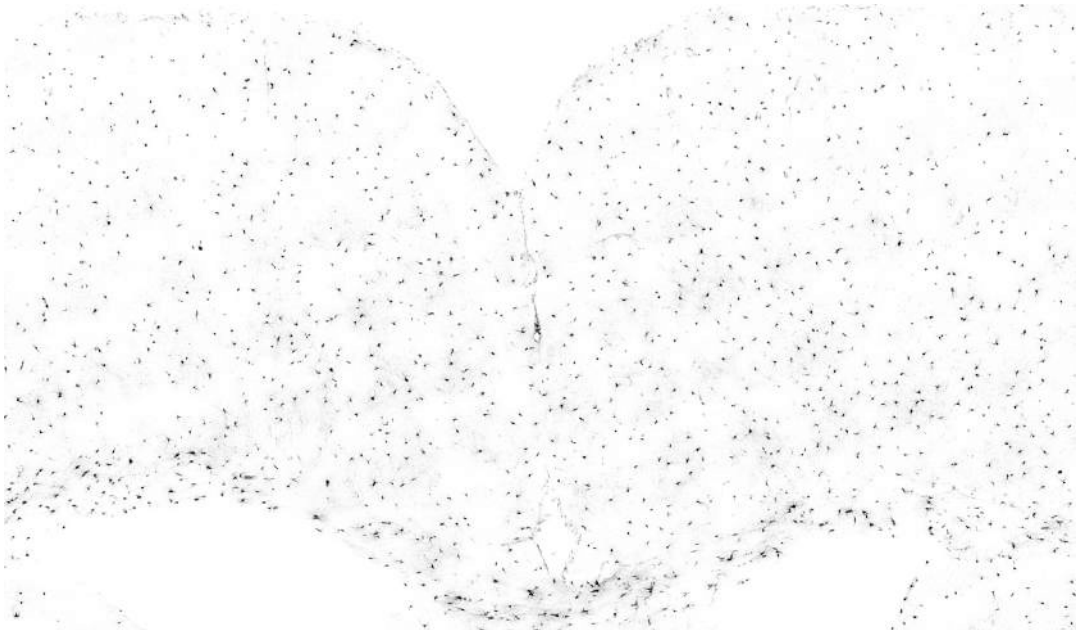

Figure 2. Distribution of OPCs in the adult CNS

Coronal brain section of pseudo-coloured YFP labeled OPCs from adult *Pdgfrα-CreER^{TM}:: Rosa26YFP* mice at 30 days post tamoxifen showing their uniform distribution throughout the cortex and corpus callosum.

repair (Franklin et al., 1997; Levine and Reynolds, 1999; Chari and Blakemore, 2002; Zawadzka et al., 2010).

1.5.1 More than just oligodendrocyte progenitors

While the best characterised function of OPCs is the lifelong addition of new OLs, they also regulate a number of other important functions within the adult CNS, [reviewed by (Pepper et al., 2018)]. For example, recent work has shown that OPCs interact with microglia and keep them in a homeostatic state (Liu and Aguzzi, 2019), and the ablation of OPCs from the adult rat brain can lead to neuronal loss from the hippocampus due to sustained microglial activation and inflammation (Nakano et al., 2017). Furthermore, OPC dysfunction may play a role in the pathology of mental illness, as the genetic ablation of OPCs from the prefrontal cortex of young adult mice leads to the development of anxiety and depressive like behaviours within 7 days, due to abnormal neuronal glutamate neurotransmission and astrocytic glutamate uptake (Birey et al., 2015). As OPCs perform a number of critical functions in the adult CNS, understanding the signalling pathways that influence OPCs behaviour could prove beneficial for the treatment of a variety of neuropathologies.

1.6 Oligodendrocytes

OLs are myelinating cells that facilitate rapid and reliable action potential conduction and provide trophic support to the underlying axons (Lee et al., 2017). Oligodendrogenesis occurs during postnatal development (Zhu et al., 2008; 2011), whereby developmental OPCs divide symmetrically to produce two OPCs or two OLs, or asymmetrically to produce one OPC and one OL (Zhu et al., 2011). OPCs differentiating into OLs go through two distinct phases, a highly ramified premyelinating phase then a mature myelinating form characterised by the elaboration of myelin internodes. During differentiation, PDGFRα and NG2 expression is lost

and the OLs acquire others markers such a APC/CC1, ASPA and myelin associated proteins such as myelin basic protein (MBP) and cyclic nucleotide phosphodiesterase (CNPase) (**Figure 1**). It is important to note that not all OPCs that differentiate go on to form myelinating OLs, as large number of the newly differentiated OLs undergo apoptosis during development and adulthood (Trapp et al., 1997; Kougioumtzidou et al., 2017). This pathway is in part due to Transcription Factor EB (TFEB), a key component of the programmed cell death pathway, as knocking out TFEB from OPCs results in more myelination by preventing apoptosis, but also results in regions that are not normally myelinated becoming myelinated (Sun et al., 2018).

1.6.1 Activity and myelination

There are a number of signalling pathways that can enhance OPC differentiation and myelination, including neurotransmission. OPCs receive direct synaptic input from neurons and express glutamate and GABA receptors, as well as voltage-gated sodium and voltage-gated calcium channels (Bergles et al., 2000; Lin and Bergles, 2004; De Biase et al., 2010; Cheli et al., 2015; Pitman et al., 2019). This allows OPCs to sense the activity of axons and previous studies have shown that neuronal activity leads to increased oligodendrogenesis and myelination *in vitro* (Demerens et al., 1996; Wake et al., 2011) and *in vivo* (Li et al., 2010; Gibson et al., 2014; Mitew et al., 2018; Cullen et al., 2019). Furthermore, sensory (Barrera et al., 2013) or social deprivation (Makinodan et al., 2012) has a negative impact on myelination. However, neurotransmission is not always necessarily required for myelination, as OLs in culture can myelinate synthetic fibres and paraformaldehyde-fixed axons (Rosenberg et al., 2008; Lee et al., 2012), suggesting that signals from axons are not essential for the formation of a myelin internodes. Additionally, the myelinating capacity of OLs is subject to intrinsic regulation as spinal cord derived OLs elaborate longer internodes than cortical OLs when cultured under equivalent conditions (Bechler et al., 2015).

1.6.2 Oligodendrocyte generation in adulthood

Even after myelin is laid down during development, some neurons within the adult CNS remain unmyelinated or sparsely myelinated (Tomassy et al., 2014). With >20% of all OLs in the mouse corpus callosum being generated after 7 weeks of age (Rivers et al., 2008). OL addition to the adult mouse CNS increases OLs density up until around 2 years of age and is associated with the continuous filling in of unmyelinated segments of partially myelinated axons. After two year of age, the level of myelin decline and signs of myelin degeneration become apparent (Hill et al., 2018). In humans, myelin degeneration has been shown to correlate with the development of age related cognitive decline and the progression of neurological disorders (Bartzokis, 2004; Safaiyan et al., 2016; Hill et al., 2018).

1.7 Myelin internode formation

Premyelinating OLs in contact with axons extend their cytoplasm to spirally wrap around the axon to form the layers of the myelin sheath (reviewed by (Snaidero and Simons, 2014). Most OLs generate somewhere between 10 and 60 myelinating processes, with each process only myelinating one axon. Given the large number of internodes formed by just one OL, the process of internode formation must be highly controlled and live imaging studies in zebrafish have shown that following initial contact, OLs make all their myelin sheaths within 5 hours and only sheath retractions are made after that time (Czopka et al., 2013). Control of sheath extension or retraction is controlled by calcium signalling as a result of local neuronal activity (Baraban et al., 2018; Krasnow et al., 2018). Along a single zebrafish axon, mature myelin internodes increase in length to compensate for an increase in body length, and ablation of a single internode leads to neighbouring internodes temporarily increasing in length until a new

internode can be made (Auer et al., 2018). Neuronal activity can also influence the number and length of individual internodes (Mensch et al., 2015; Cullen et al., 2019), for example, stimulating the mouse brain with an electromagnetic field was shown to increase internode length after 14 days of stimulation (Cullen et al., 2019). The exact mechanisms that govern the initiation of myelin internode formation from OPCs or OLs is likely regulated by a number of intrinsic and extrinsic factors (reviewed by (Osso and Chan, 2017).

1.8 Oligodendrocyte lineage cells in the damaged CNS

1.8.1 Differentiation block

Damage to CNS myelin can have severe adverse effects on CNS function and is a hallmark of neurodegenerative diseases such as Multiple Sclerosis (MS). In response to demyelination, adult OPCs can rapidly migrate to regions of demyelination and facilitate repair [reviewed by (Franklin and ffrench-Constant, 2008)]. In the mouse, OL generation from parenchymal OPCs within the CNS is accompanied by new OPC addition from neural stem cells in the subventricular zone (SVZ) (Menn et al., 2006; Xing et al., 2014). Once at a demyelinated region, OPCs will expand and differentiate into OLs where they can remyelinate.

In people with MS, remyelination is often incomplete. Chronic MS lesions often contain OPCs (Wolswijk, 2002) and some premyelinating OLs (Chang et al., 2002), however, these cells fail to terminally differentiate into myelinating OLs (Kuhlmann et al., 2009; Fancy et al., 2010), and this pathological situation has been termed differentiation block. Differentiation block, in part, results from a lack of MyRF expression, as MyRF deletion from OPCs does not impact the recruitment of OPCs to the site of lysolethicin-induced demyelination but does impair their capacity to terminally differentiate (Duncan et al., 2017). Changes in myelin biochemistry may also prevent remyelination and be a significant driver of MS progression, as the citrullination of MBP prevents the myelin sheath compacting and contributes to myelin instability (Beniac

et al., 2000), and protein hypercitrullination is a hallmark of MS (Bradford et al., 2014). However, conditional deletion of peptidylarginine deiminase 2 (PAD2) from mouse OPCs, an enzyme responsible for citrullination of MBP, reduces myelination by impairing in OPC differentiation (Falcao et al., 2019).

1.8.2 The remyelinating capacity of existing oligodendrocytes

While it has long been accepted that OPCs generate new OLs in response to an injury, and that these OPC-derived OLs are the cells responsible for remyelination (Franklin and Ffrench-Constant, 2008, Zawadzka et al., 2010), a growing body of evidence suggests that pre-existing OLs may also play a significant role in restoring myelin and consequently nervous system function (Duncan et al ., 2018, Yeung et al., 2019, Bacmeister et al,. 2020) By analysing ^{14}C incorporation by cells within the post-mortem brain, it was possible to determine that in the most aggressive cases of MS, new OLs were added to the brain, however, in the majority of MS cases, OLs present within remyelinated MS lesions were born during early life, not during adulthood, over the course of the disease (Yeung et al., 2019). By analysing the myelin internodes of OLs in the brains of large animal models, including cats and non-human primates, it was also possible to show that individual cells elaborated internodes that resembled developmental myelin as well as internodes that resembled reparative myelin (Duncan et al., 2018). Recently, Bacmeister et al. (2020) showed that surviving OLs in the CNS of cuprizone-treated mice were also able to contribute to remyelination, if the mice were subjected to a motor learning task following partial remyelination. They also showed that surviving OLs preferentially added new myelin sheathes to denuded or previously myelinated axon regions even after motor learning was complete, while newborn OLs preferentially myelinated previously unmyelinated axons (Bacmeister et al., 2020). These data suggest that

remyelination may best be achieved by promoting myelin repair from surviving OLs, as well as increasing OL generation from OPCs.

1.8.3 Disease specific oligodendrocyte lineage cells

A growing body of evidence now suggests that OL lineage cells play an active role in immunomodulation. Under inflammatory conditions, OPCs have been shown to upregulate MHC class I and class II proteins (Falcao et al., 2018), which enhances the proliferation and survival of invading immune cells. Cells of the OL lineage can also upregulate their expression of immunomodulatory chemokines (Balabanov et al., 2007) and pro-inflammatory cytokines such as IL-17A (Tzartos et al., 2008). Deleting *Act1* from NG2 glia, a key component of the IL-17 receptor signalling pathway, dramatically reduces the severity of experiment autoimmune encephalomyelitis (EAE) in mice (Kang et al., 2013). In humans with MS, different subtypes of OLs have been identified by single nucleus RNA sequencing (Jäkel et al., 2019), suggesting that OLs have different functional states within MS lesions and normal appearing white matter. These recent findings suggest that cells of the OL lineage play an important role in the regulation and propagation of the inflammatory environment.

1.9 Sequencing databases of oligodendrocyte lineage cells

Identifying candidate proteins that may be regulating OPC and OL function has become more streamlined with the availability of microarray and RNA sequencing databases. Microarray analysis comparing transcriptome of major CNS cell types was able to compare differentially expressed transcripts between OPC and mature OLs. Unsurprisingly, some of the main differentially expressed transcripts were PDGFRα and NG2, which we know are highly expressed in OPCs but not mature OLs (Cahoy et al., 2008). Another highly differentially expressed transcript is *Lrp1*, which was found to be 31.7 fold enriched in OPCs compared to

mature OLs (Cahoy et al., 2008). Over the years, additional databases have been published and the *Lrp1* transcript has been shown to be consistently expressed in OPCs but not in OL (**Figure 3**) (Zhang et al., 2014; Hrvatin et al., 2018). However, the role of LRP1 in OPCs is yet to be elucidated.

1.10 Low Density Lipoprotein Receptor Related Proteins 1 and 2

The LDL receptor family is a large family of multi-ligand receptors. Core family members include the: LDL receptor; very low density lipoprotein (VLDL) receptor (Brown and Goldstein, 1986), LDL receptor related protein (LRP1), also known as CD91 and the α-2-macroglobulin receptor (Binder et al., 2000; Liu et al., 2000; Marschang et al., 2004); LRP2, also known as GP330 and Megalin (Saito et al., 1994); LRP5 (Hey et al., 1998); LRP6 (Brown et al., 1998), and LRP8, also known as Apolipoprotein Receptor-2 (Riddell et al., 1999). Each family member is a single-pass transmembrane receptor, containing two or more extracellular cysteine-rich complement type repeats, which act as ligand binding domains (Daly et al., 1995).

At 600kDa, LRP1 and LRP2 are the largest and most promiscuous members of the LDL receptor family. Transcription of the *Lrp1* gene can be activated by a number of transcription factors including sterol regulatory element binding protein 2 (Llorente-Cortes et al., 2006), hypoxia-induced factor1α (Castellano et al., 2011), and nitric-oxide dependent transcription factors (Grana et al., 2012), but is negatively regulated by naturally occurring antisense transcripts, inversely coded within exons 5 and 6 of the *Lrp1* gene (Yamanaka et al., 2015). The *Lrp1* gene codes for a precursor protein that binds to the receptor associated protein (RAP), a chaperone that occupies the ligand binding domains of the precursor (Rudenko et al., 2002) to prevent the binding of other ligands (Willnow et al., 1995), and ensure its correct folding in the endoplasmic reticulum (Bu and Marzolo, 2000; Croy et al., 2003) (**Figure 4**). RAP remains bound to the LRP1 precursor and transports it to the Golgi apparatus. This transport

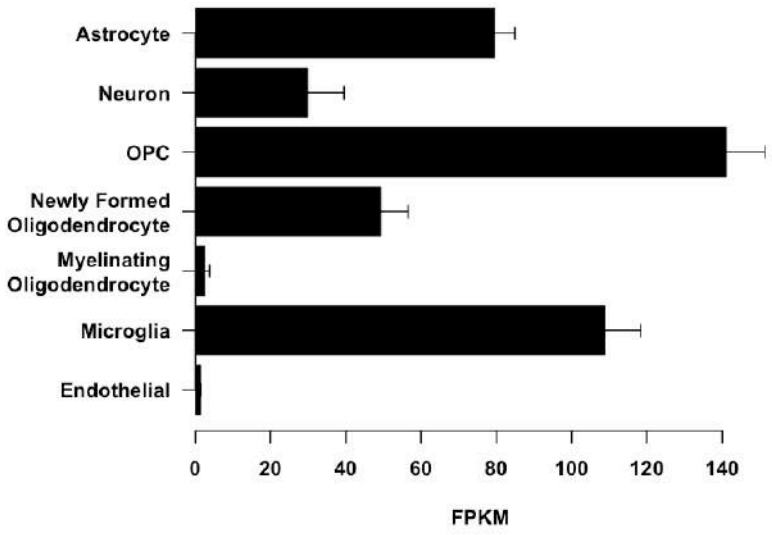

Figure 3. *Lrp1* RNA expression within the oligodendrocyte lineage

RNA sequencing database comparing the transcriptional profile of major CNS cells types shows *Lrp1* mRNA is highly express in OPCs but not mature oligodendrocytes. FPKM = fragments per kilobase million. Adapted from *Zhang et al 2014.*

Figure 4. LRP1 maturation and structural organisation

The LRP1 protein is first synthesised as a precursor protein in the endoplasmic reticulum where it is bound by the receptor associated protein (RAP) chaperone. It is then transported to the trans-Golgi network where the low pH causes RAP to dissociate. The protease Furin then cleaves the LRP1 precursor at the RX(K/R)R consensus sequence to generate a large α chain (515kDa) and a smaller β chain (85kDa) which remain non covalently linked as they shuttled to the cell membrane where they are imbedded as one functional unit. The α chain contains 4 ligand binding domains (red) that interact with a large number of ligands. The β chain contains a small extracellular region, a transmembrane region which anchors the LRP1 protein within the plasma membrane, as well as two dileucine (LL, green) motifs and two asparagine-proline-x-tyrosine (NPxY, blue) motifs, where the distal motif is contiguous with a tyrosine-x-x-leucine (YxxL, pink) motif which interact with intracellular adaptor proteins and the endocytotic machinery.

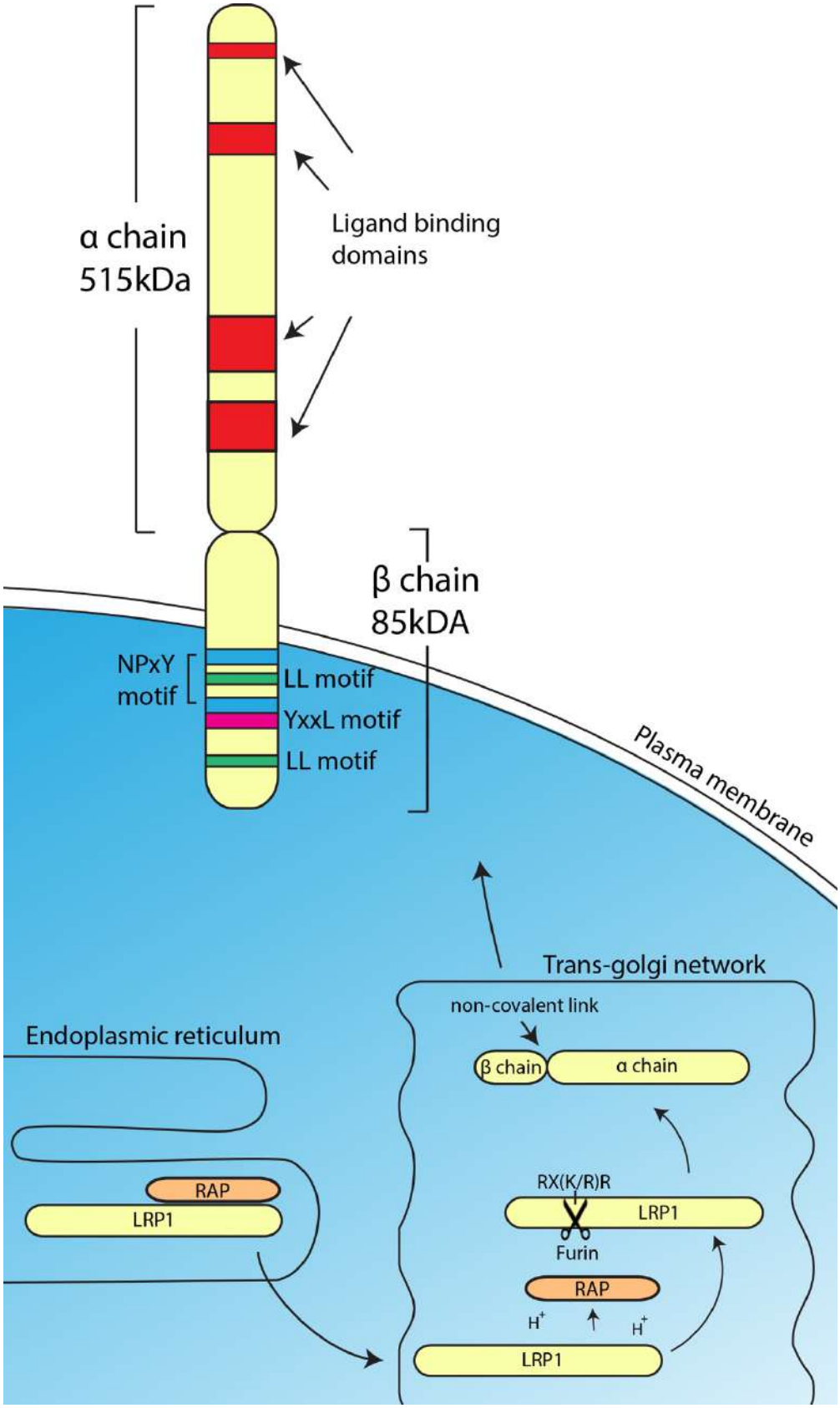
α chain
515kDa
Ligand binding
domains
β chain
85kDA
NPxY
motif
LL motif
YxxL motif
LL motif
Plasma membrane
Trans-golgi network
non-covalent link
β chain
α chain
Endoplasmic reticulum
RAP
LRP1
RX(K/R)R
LRP1
Furin
RAP
H+
H+
LRP1

involves the proximal NPXY motif in the intracellular domain of the protein (Reekmans et al., 2009). In the trans-Golgi network, the low pH of the secretory pathway causes protonation of the histidine residues in domain 3 of RAP (Lee et al., 2006), triggering its dissociation from the LRP1 precursor (Bu et al., 1995; Rudenko et al., 2002). The protease Furin then cleaves the LRP1 precursor at the RX(K/R)R consensus sequence, to generate a large α-chain (515kDa) and a smaller β-chain (85kDa) (Willnow et al., 1996b). The two fragments remain non-covalently linked on their way to the cell membrane, where they are embedded as one functional unit, comprising mature LRP1 (**Figure 4**). LRP2 is similarly chaperoned by RAP (Czekay et al., 1997), and also contains an RX(K/R)R consensus sequence, but there is no evidence that LRP2 undergoes intracellular proteolytic processing prior to its insertion into the plasma membrane (Saito et al., 1994).

1.11 Soluble LRP1 and LRP2

Once LRP1 is inserted into the plasma membrane, the soluble extracellular domain (sLRP1) can be cleaved from the cell surface by enzymes such as the beta-site APP cleaving enzyme 1 (BACE1) (Arnim et al., 2005) and metalloproteinase (Selvais et al., 2011) (**Figure 5**). sLRP1 contains the α-chain and a 55kDa fragment of the β-chain (Quinn et al., 1999), and can be detected in plasma and cerebral spinal fluid (Quinn et al., 1997; Liu et al., 2009). Similarly, soluble fragments of LRP2 have been shown to be released from cultured choroid plexus epithelial cells, and can be detected in cerebral spinal fluid (Spuch et al., 2015). LRP1 and LRP2 can then undergo intra-membrane proteolysis mediated by γ-secretase, in either the plasma or endosomal membrane (Shah et al., 2013), to liberate an intracellular fragment which reportedly enters the nucleus (May, 2002a; Biemesderfer, 2006) (**Figure 5a**). The physiological function of soluble LRP fragments in normal neural cell development is poorly understood, but they have the potential to bind LRP ligands and prevent them from binding to full-length LRPs, or in the case of the intracellular domain, modulate gene transcription.

Figure 5. Signalling mechanisms employed by LRP1

a. The extracellular domain of LRP1 can be shed following cleavage by Beta-site APP cleave enzyme 1 (BACE1) and metalloproteinases (MP) producing a soluble form of LRP1 (sLRP1). sLRP1 is thought to bind ligands of LRP1 to prevent binding to full length LRP1. Additionally, the intracellular domain can be cleaved by γ-secretase and is thought result in changes to gene transcription. **b**. Ligand binding to LRP1 can result in receptor internalisation. Once internalised, the ligand/receptor complex can be processed in a multitude of ways, including degradation by lysosomes or rescretion via trancytotic and recycling vesicles. **c**. Specific regions on the intracellular region of LRP1 may interact with a number of adaptor proteins and modulate intracellular signalling mechanisms eg Disabled 1 (Dab1) has been shown to interact with the NPXY motifs which may recruit non receptor tyrosine kinases such as Src and Abl. **d.** Activation of LRP1 by specific ligands has been shown to transactivate other receptors such as tyrosine receptor kinase A (TrkA), which can then activate downstream signalling pathways and regulate cell function.

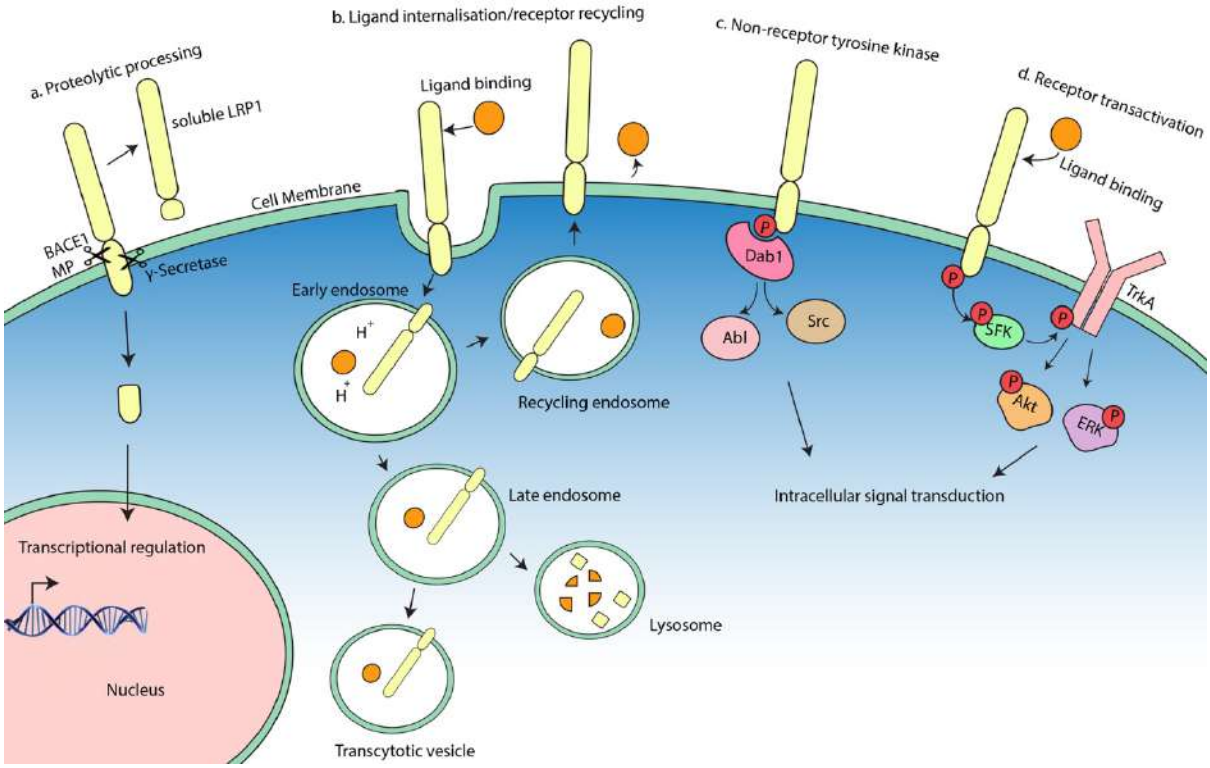
a. Proteolytic processing
soluble LRP1
BACE1
MP
γ-Secretase
Cell Membrane
Transcriptional regulation
Nucleus
b. Ligand internalisation/receptor recycling
Ligand binding
Early endosome
H+
H+
Recycling endosome
Late endosome
Lysosome
Transcytotic vesicle
c. Non-receptor tyrosine kinase
P
Dab1
Abl
Src
Intracellular signal transduction
d. Receptor transactivation
Ligand binding
P
P
SFK
P
TrkA
P
Akt
ERK
P

1.12 LRP1 and LRP2 as mediators of endocytosis

While the proteolytic processing of these receptors is becoming increasingly well understood, LRP1 and LRP2 remain best known for their role in mediating endocytosis (**Figure 5b**). Following ligand binding to mature LRP1 in the plasma membrane, it was originally believed that the two NPXY motifs of the cytoplasmic domain interacted with the endocytic machinery to mediate rapid clathrin-dependant endocytosis of the receptor-ligand complex, as has been previously shown for other members of this receptor family (Chen et al., 1990). However for LRP1, the YXXL motif and the distal di-leucine motif independently mediate endocytosis, and the NPXY motifs are not required (Li, 2000). The rate of endocytosis is regulated by cAMP-dependent Protein Kinase A, which constitutively phosphorylates LRP1, predominantly at serine 76 of the cytoplasmic tail (Li et al., 2001).

Like LRP1, LRP2 has two intracellular NPXY domains (Saito et al., 1994), however unlike LRP1, the distal NPXY motif of LRP2 has been shown to interact with the phosphotyrosine-binding domain of Disabled-2 (Oleinikov et al., 2000), a clathrin-associated sorting protein, to mediate endocytosis (Nagai, 2005; Traub, 2009; Shah et al., 2013). Interestingly, endocytosis does not occur during mitosis, due to the phosphorylation of Disabled-2, which removes it from the cell surface, so that it no longer co-localizes with clathrin, and cannot mediate this process (Chetrit et al., 2011). LRP2-directed endocytosis may still occur via clathrin-independent pathways, instead relying on the small GTPase Arf6 and Caveolin 1 (Wolff et al., 2008; Bento-Abreu et al., 2009). Furthermore, LRP1- and LRP2-mediated endocytosis can be influenced by the expression of miR199a and miR199b family members, which regulate the expression of a number of genes critical for clathrin-dependent and clathrin-independent endocytosis (Aranda et al., 2015). Following endocytosis, the extracellular beta-propeller regions of LRP1 and LRP2 facilitate ligand dissociation (Jeon et al., 2001), so that the ligands and receptors can be differentially sorted in early endosomes.

The mechanisms regulating the recycling of LRP1 back to the plasma membrane are not fully characterised, and may vary between cell types. However, it is known that this process requires binding of the adaptor protein sorting nexin 17 to the first NPXY domain of LRP1 in early endosomes (Donoso et al., 2009; Farfán et al., 2013), so that LRP1 is recycled back to the cell surface in approximately 30 minutes (Ko et al., 1998). In early endosomes, the first NPXY domain of LRP2 instead binds the phosphotyrosine-binding domain of autosomal recessive hypercholesterolemia (ARH) (Nagai et al., 2003), a clathrin-associated sorting protein that couples LRP2 to the dynein motor complex (Lehtonen et al., 2008), and transports it from the sorting endosomes to the endocytic recycling compartment (Shah et al., 2013). The constitutive phosphorylation of LRP2 by GSK3β is also involved in directing LRP2 to the endocytic recycling compartment, from which it is slowly recycled to the plasma membrane (Yuseff et al., 2007).

But what happens to the internalized ligand? LRP1 and LRP2 have been shown to bind upwards of 40 different ligands, many of which are structurally and functionally unrelated, and the list is always evolving (Spuch, 2017). They both have four LDL receptor homology regions which are the extracellular ligand-binding domains (Herz and Strickland, 2001; Marzolo and Farfán, 2011), and bind common ligands including tissue-type plasminogen activator (Willnow et al., 1992; Bu et al., 1993; Grobmyer et al., 1993; Lin et al., 2016), apolipoprotein E, lactoferrin (Willnow et al., 1992; Croy et al., 2003), and metallothioneins I and II (Ambjørn et al., 2008), however not all ligands have been shown to bind both receptors. α2-macroglobulin is a high affinity ligand for LRP1 (Hanover et al., 1983; Marynen et al., 1984), and like prion protein has only been demonstrated to bind to LRP1 (Parkyn et al., 2008), while transthyretin (Sousa et al., 2000), and the complex of vitamin D with the vitamin D binding protein have only been shown to bind LRP2 (Nykjaer et al., 1999). Once endocytosed, ligands may be degraded in lysosomes, re-secreted from recycling endosomes, or trafficked in

transcytotic vesicles from the apical to the basolateral membrane (or visa versa) before being secreted (Willnow et al., 2012) (**Figure 5b**).

1.13 LRP1 and LRP2 Intracellular Signal Transduction

The true complexity of LRP1 and LRP2 signalling lies in the fact that these receptors not only trigger endocytosis, but influence signal transduction. Upon ligand binding, the NPXY motifs can function as docking sites for intracellular adaptor proteins. LRP1 can bind cytosolic ligands in a phosphorylation-dependent manner, via two di-leucine motifs and one YXXL motif in the intracellular domain. For example, the adaptor proteins Disabled-1 and FE65 can bind to the NPXY motifs of LRP1, to recruit and activate non-receptor tyrosine kinases such as Src and Abl to the cytoplasmic tail (Trommsdorff et al., 1998) (**Figure 5c**), allowing the receptor to transduce an intracellular signal, or form signalling hubs through the binding of co-receptors (Spuch, 2017) (**Figure 5d**). A number of co-receptors of LRP1 have been identified, including platelet-derived growth factor receptor beta (PDGFRβ) (Boucher et al., 2002; Loukinova, 2002), tropomyosin-related kinase receptor A (Shi et al., 2009), amyloid precursor protein (Pietrzik, 2004) and insulin-like growth factor 1 receptor (Woldt et al., 2011). These associations increase the number of intracellular pathways by which distinct LRP ligands may elicit their effects.

1.14 LRPs as Regulators of Nervous System Development

Despite the large number of common ligands, and the structural similarities that exist between LRP1 and 2, the two genes are not functionally redundant during development. Both the *Lrp1* and *Lrp2* single knockout mice have severe developmental phenotypes. *Lrp1* knockout blastocysts fail to implant, and therefore do not develop into embryos (Herz et al., 1992). *Lrp2* knockout mice are mostly embryonic lethal, presenting with defects including a cleft palate, failure to form an olfactory bulb, and fusion of the forebrain hemispheres,

resulting in a single ventricle (holoprosencephaly) (Willnow et al., 1996a). The small number of *Lrp2* knockout mice that survive until birth experience severe vitamin D3 deficiency, as the reabsorption of vitamin D and the vitamin D binding protein from the kidney proximal tubule is LRP2-dependant, but die of respiratory failure (Willnow et al., 1996a; Nykjaer et al., 1999). Human mutations in *Lrp2* are known to cause facioocculo-acoustico-renal syndrome / Donnai-Barrow syndrome, an autosomal recessive disorder associated with disrupted brain formation, including agenesis of the corpus callosum (Kantarci et al., 2007).

The very early developmental defect observed in the *Lrp1* knockout mouse, and the gross neural phenotype of *Lrp2* knockout mouse, do not allow us to investigate the importance of these receptors for the functioning of individual neural cell types. However, a variety of expression studies performed alongside knockdown and conditional knockout approaches, have demonstrate that both receptors mediate ligand endocytosis and intracellular signalling in a number of immature neural cell types. LRP1 is more widely expressed in the CNS than LRP2, being detected in mature neurons, particularly those of the entorhinal cortex, hippocampus (Wolf et al., 1992) and cerebellum (Bu et al., 1994), and all CNS glia (Gaultier et al., 2009). In contrast, LRP2 expression is restricted to the apical surface of the neural tube, and subsequently to the forebrain, optic stalk, and otic vesicle during development (Assémat et al., 2005; Spoelgen, 2005). In the CNS of adult mice, LRP2 is predominantly expressed by cells of the choroid plexus (Chun et al., 1999) and ependymal cells (Gajera et al., 2010), but has also been detected in oligodendrocytes of the spinal cord (Wicher et al., 2005). The expression patterns of LRP1 and LRP2 are largely spatially and temporally distinct, reflecting their different roles in CNS regulation.

1.15 LRP1 and LRP2 as Regulators of Neural Stem Cell Function

1.15.1 Neural Stem Cells in the Developing and Adult CNS

The early neural tube is a pseudostratified epithelium composed of neuroepithelial precursor cells. These early neural stem cells divide symmetrically, expanding their population, before switching to include asymmetric divisions that generate neuroblasts. This switch coincides with a change in gene expression, as the neuroepithelial precursor cells transition into radial glial stem cells, which comprise two molecularly distinct subgroups in the developing human brain, corresponding to those in the outer subventricular zone, and those in the ventricular zone (Pollen et al., 2015). Following neuroblast generation, radial glia switch to glial generation starting with the production of OPCs and concluding with the production of astrocytic precursors (Kessaris et al., 2008). Towards the end of development a subset of radial glial stem cells adopt a more astrocytic gene expression profile and give rise to the adult neural stem cells (Young et al., 2007).

In adulthood neural stem cells reside in two key niches, the subventricular zone of the lateral ventricles and the dentate gyrus of the hippocampus, where they proliferate to generate intermediate progenitor cells, and ultimately neuroblasts (O'Rourke et al., 2014). Neural stem cells in the subventricular zone also produce a small number of OPCs under normal physiological conditions (Young et al., 2010). The behaviour of neural stem cells (and their intermediate progenitors) is highly controlled by mitogenic and morphogenic signalling. While key ligands and receptors for these pathways are well described, the role of LRP1 and LRP2 in these pathways has only recently been elucidated.

1.15.2 LRPs as Regulators of Cell Fate Specification

LRP1 and LRP2 have both been shown to facilitate the internalisation of the potent morphogen, sonic hedgehog (McCarthy, 2002; Morales, 2006; Capurro et al., 2012), a finding that has provided insight into the significant neurodevelopmental defects observed in patients

and mice lacking normal functioning *Lrp2* (Willnow et al., 1996a; Spoelgen, 2005; Kantarci et al., 2007). LRP2 is expressed by neuroepithelial cells, on the apical side of the neural plate, as early as E7.5 in the mouse. After neural tube closure at E9.5, LRP2 expression becomes increasingly restricted to the midline, ultimately being localised to the clathrin-coated pit regions of the apical cell membrane, clustered at the base of the primary cilium (a cellular organelle essential to sonic hedgehog signalling) (Choudhry et al., 2014), and in the sub-apical endosomes of the radial glia (Christ et al., 2012). At E8 sonic hedgehog is produced by cells of the axial mesoderm (the notochord and prechordal plate), and by E8.5 its expression expands to include the radial glia at the ventral midline of the rostral diencephalon. This expansion does not occur in *Lrp2* knockout embryos, as LRP2 is required for the radial glia to bind and sequester sonic hedgehog as it diffuses, regulating morphogen presentation to the neural stem cells (Christ et al., 2012).

Once sonic hedgehog is bound to LRP2 it can also bind its receptor patched-1, and the complex undergoes clathrin-mediated endocytosis (Christ et al., 2012). All components can then be found within early endosomes and recycling endosomes, but do not appear to be targeted to the lysosome for degradation. The internalisation of patched-1 by LRP2, results in activation of the effector smoothened, leading to changes in gene transcription mediated by the gli transcription factors. Therefore, in the absence of LRP2, radial glia show reduced expression of the sonic hedgehog target genes g*li1* and s*ix3* (Christ et al., 2012). The loss of sonic hedgehog and gli3-mediated transcriptional repression has secondary consequences for neural development, including aberrant bone morphogenic protein 4 expression in the dorsal forebrain (Spoelgen, 2005; Fuccillo et al., 2006; Christ et al., 2012), and disrupted fibroblast growth factor 8 and noggin expression (Christ et al., 2012). These data indicate that LRP2 regulates the patched-1-dependent internalisation and trafficking of sonic hedgehog (Christ

et al., 2012), which is necessary for neural stem cell specification and ventral forebrain patterning.

Later in development, the expression of LRP2 by spinal cord radial glial is also necessary for glial cell specification. *Lrp2* knockout mice completely lack OL lineage cells, and produce very few astrocytes in the spinal cord (Wicher and Aldskogius, 2008). OPC specification from radial glia in the ventral spinal cord is also directed by sonic hedgehog signalling (Poncet et al., 1996; Pringle et al., 1996; Orentas et al., 1999; Nery et al., 2001; Tekki-Kessaris et al., 2001), and so the lack of spinal cord OLs may be explained by a mechanism similar to that detailed above. However OPCs can be generated from cultured neuroepithelial precursors derived from s*onic hedgehog* and *smoothened* knockout mice (Chandran, 2003; Cai et al., 2005), indicating that LRP2 must also interact with other signalling pathways such as basic fibroblast growth factor and insulin-like growth factor I (Bolos et al., 2010), to promote OPC generation from neural stem cells. The decreased number of astrocytes observed in *Lrp2* knockout mice is also interesting. LRP2 is expressed by vimentin-positive cells in the E15 ventral spinal cord (Wicher et al., 2005), that most likely correspond to immature astrocytes (Pringle, 2003; Wu et al., 2003; Young et al., 2010). While LRP2 may play a role in regulating the behaviour of astrocytic precursors, it is more likely that the observed phenotype is the result of LRP2 being required for astrocyte specification by radial glia, as this immature glial population is not generated in *Lrp2* knockout mice. Despite these observations that strongly implicate LRP2 in glial cell specification during neural development, the ligands and signalling mechanisms are unknown.

LRP1 appears to fulfil a similar role in regulating glial generation in the brain. LRP1 is expressed by cells within the embryonic ventricular zone, and the early postnatal subventricular zone (Hennen et al., 2013). While the role of LRP1 in regulating neural stem cell function *in vivo* is poorly understood, *in vitro* studies suggest that LRP1 can regulate OPC production. Neural

stem cells can be harvested from the cortex of embryonic mice, and grown as a suspension culture termed neurospheres. When differentiated, neurospheres generate neurons, astrocytes and OLs. However, neurospheres lacking *Lrp1* generate normal numbers of neurons, but significantly fewer O4-positive OLs (Hennen et al., 2013). These data may reflect a requirement of LRP1 signalling in neural stem cells for OPC specification, but could equally result if LRP1 is necessary for the proliferation or differentiation of OPCs (see OPC section below).

1.15.3 LRPs as Regulators of Neural Stem Cell Proliferation

In the subventricular zone of the adult mouse brain, LRP2 is expressed by ependymal cells underlying the neurogenic niche (Zheng et al., 1994; Gajera et al., 2010). The importance of LRP2 expression for neural stem and progenitor cell proliferation was examined in *Lrp2*$^{267/267}$ mutant mice, which produce a truncated form of LRP2 (Zarbalis et al., 2004). *Lrp2*$^{267/267}$ mice have ~25% fewer proliferating cells in the subventricular zone relative to control mice, and a proportional reduction in the number of newborn neurons entering the olfactory bulb (Gajera et al., 2010). The absence of functional LRP2 from the neurogenic niche was accompanied by increased bone morphogenic protein 2 and 4, increased phosphorylation of the downstream effectors SMAD1, 5 and 8, and increased activation of the downstream target, Inhibitor of DNA binding 3 (Gajera et al., 2010). It is known that LRP2 can act as an endocytic receptor, sequestering and clearing bone morphogenic protein 4 (Spoelgen, 2005). However this does not appear to be the mechanism at play here, as the ventricular infusion of noggin, a potent bone morphogenic protein 4 antagonist (Lim et al., 2000), severely decreased neurogenesis, but did so in favour of oligodendrogenesis (Sabo et al., 2009), which was not the phenotype observed in the *Lrp2*$^{267/267}$ mice (Gajera et al., 2010).

The ability of LRPs to regulate proliferation may be more widespread amongst immature neural cell populations, as LRP1 also regulates the proliferation of cerebellar granular neuron precursors. Cerebellar granular neuron precursors are a temporary cell population that proliferate in the external germinal zone of the developing cerebellum, producing granule neurons from birth until ~P15 in the mouse (Marzban et al., 2014). This cell population is highly responsive to the pro-mitotic effects of sonic hedgehog (Dahmane and Ruiz i Altaba, 1999; Wechsler-Reya and Scott, 1999; Haldipur et al., 2012). However, the effect of sonic hedgehog is negatively regulated by an interaction between LRP1 and protease nexin 1, also known as SERPINE2. Protease nexin 1 complexes with its target proteases and binds to LRP1 on the surface of cultured cerebellar granule neuron precursors (Vaillant et al., 2007). Once endocytosed, protease nexin 1 antagonizes sonic hedgehog signalling, reducing the proliferation of cerebellar granule neurons. This regulation is critical for normal cerebellar development, as the absence of protease nexin 1 *in vivo* delays cerebellar granule neuron precursor differentiation, and increases the overall size of the cerebellum (Vaillant et al., 2007). We would predict that conditionally removing *Lrp1* from cerebellar granule neuron precursors would have the same effect.

1.15.4 LRPs as Regulators of Neuroblast Function

Neuroblast generation and their subsequent migration into the developing cortex has been well characterised (Stiles and Jernigan, 2010). Post-mitotic neuroblasts that are generated in the cortical ventricular zone, are destined to form cortical projection neurons (Parnavelas, 2000). They undergo radial migration out of the germinal zone, moving along the radial glial apical process. The final laminar position of a newborn neuron is determined by its birth date, with late-born neuroblasts migrating past early-born neurons, to seed progressively more superficial layers of the cortex (Kriegstein et al., 2006). In contrast, cortical interneurons are generated from radial glial cells within the ventricular zones of the medial ganglionic

eminence, the caudal ganglionic eminence, and the pre-optic area, and undergo both radial and tangential migration to populate each of the cortical layers (Lavdas et al., 1999; Letinic et al., 2002; Nery et al., 2002).

Neuroblasts born in the two neurogenic niches of the adult brain also have vastly different migratory requirements. Those born in the hippocampus are destined to be dentate granule neurons, which project from the dentate gyrus to CA3 of the hippocampus (Hastings and Gould, 1999). After birth these cells move a very short distance as they mature – migrating from the subgranular zone (the inner lip) of the dentate granule neuron layer, to their final position within the layer. On the other hand, neuroblasts born in the subventricular zone migrate tangentially, moving as neuroblast chains through the rostral migratory stream into the olfactory bulb (Doetsch et al., 1999). Upon exiting the rostral migratory stream, the neuroblasts turn and migrate radially and differentiate into granule and periglomerular neurons in the olfactory bulb (O'Rourke et al., 2014). This type of chain migration is regulated by signals that modify the actin cytoskeleton, contact-mediated signalling between the neuroblasts and the ensheathing glia (Tomasiewicz et al., 1993; Hu et al., 1996; Chazal et al., 2000; Alberti et al., 2005) as well as chemorepulsion mediated by slit and netrin (Wu et al., 1999; Murase and Horwitz, 2002; Nguyen-Ba-Charvet, 2004). Recent evidence suggests, that following neural stem cell specification and neuroblast generation, LDL family members, including LRP1 and LRP2, continue to play a significant role in regulating the successful maturation and integration of these new cells in the CNS.

1.15.5 LRP8 and the VLDL Receptor are Key Regulators of Neuroblast Migration in Development and Adulthood

Lrp8 and VLDL receptor double knockout mice have abnormalities in the layering of the brain, including the ectopic placement of neurons (Trommsdorff et al., 1999; Weeber et al., 2002), and also exhibit malformation of the cerebellum and spinal cord (Trommsdorff et al., 1999;

Su et al., 2013). LRP8 and the VLDL receptor are high affinity receptors for reelin (D'Arcangelo et al., 1997; Hiesberger et al., 1999) a large extracellular matrix protein (D'Arcangelo et al., 1997; Trommsdorff et al., 1999; Su et al., 2013). Fittingly, mice lacking *reelin* largely phenocopy the very distinct and unique cortical lamination defects seen in the *Lrp8 and VLDL receptor* double knockout mice (D'Arcangelo et al., 1997; Trommsdorff et al., 1999; Su et al., 2013). Oligomeric reelin binds to LRP8 and the VLDL receptor, activates Src family kinases, and induces phosphorylation of disabled-1. This signalling pathway enables polarisation, adhesion, stabilisation, process outgrowth, and ultimately neuroblast migration (Nichols and Olson, 2010; Sekine et al., 2012). During development reelin is first expressed in the cortical marginal zone by Cajal-Retzius cells (Frotscher, 1998; Marín-Padilla, 1998; Soriano and del Río, 2005), and later by interneurons (Alcántara et al., 1998; Drakew et al., 1998). Humans with mutations of the *VLDL receptor* gene are at increased risk of schizophrenia, which is thought to be due to subtle neuroblast migration defects within the brain (Deutsch et al., 2010).

LRP8 and the VLDL receptor can also regulate neuroblast migration when activated by an alternative ligand, thrombospondin-1. Thrombospondin-1 is expressed in the subventricular zone and throughout the rostral migratory stream (Blake et al., 2008), where it acts on LRP8 and the VLDL receptor to promote neuroblast chain migration. *Thrombospondin-1* knockout mice have defective chain migration, with fewer neuroblasts successfully migrating to the olfactory bulb (Blake et al., 2008). This phenotype is also observed in mice lacking LRP8 and VLDL receptor, or disabled-1, but is not observed in *reelin* knockout mice (Andrade et al., 2007). However, the successful migration of neurons from the subventricular zone to the olfactory bulb appears to require both ligands. Thrombospondin-1 stabilizes neuroblast chains and increases their length in the subventricular zone and rostral migratory stream, but reelin, produced by mitral cells in the olfactory bulb, is a higher affinity ligand, and

subsequently directs neuroblast dissociation, allowing them to transition to radial migration (Hack et al., 2002). Of the two ligands, only reelin activates the proteasomal degradation of disabled-1, which is necessary for neuroblast dissociation (Blake et al., 2008).

There is no evidence that reelin signalling interacts with LRP1 or LRP2. However, thrombospondins are known to interact with membrane proteins such as integrins, CD47, CD36, proteoglycans, and LRP1. Thrombospondin-1 has been shown to interact with LRP1 in combination with calreticulin to promote focal adhesion, and this interaction is an important regulator for mature oligodendrocytes (Gudz, 2006) and microglia (Le Marrec-Croq et al., 2014), but has not been demonstrated to regulate neuroblast migration.

1.15.6 LRPs, Neuroblast Migration and Neuronal Development

LRP2 regulates neuroblast migration indirectly. *In vitro* LRP2 and caveolins are expressed by astrocytes, and have been demonstrated to bind and endocytose albumin (Bento-Abreu et al., 2008; 2009). This is significant, as albumin uptake activates the transcription factor sterol regulatory binding element protein 1, inducing expression of stearoyl-coA 9-desaturase-1, the key enzyme required for synthesis of the neurotrophic factor oleic acid (Tabernero et al., 2002). In the lateral periventricular zone of the developing rat brain, oleic acid production regulates neuronal growth, migration, axon generation, and early synaptogenesis (Polo-Hernández et al., 2010; 2014), with the major neurotrophic effect being mediated by PPAR-α, protein kinase A and neuro D2 (Granda et al., 2003). When *stearoyl-coA 9-desaturase-1* is knocked down in lateral periventricular explant cultures, albumin-mediated neuroblast migration is essentially prevented (Polo-Hernández et al., 2014).

Once neuroblasts stop migrating, their journey is far from over. The immature neurons extend an axonal process to commence formation of the circuitry of the nervous system. The extending axons are tipped with a growth cone, which navigates the extracellular matrix,

guiding the axon to its target cell to ultimately form a synapse (Caudy and Bentley, 1986). A growth cone comprises a membranous, receptor-rich, fan-shaped lamellipodia that extends along finger-like projections known as filopodia. The growth cone cytoskeleton is comprised of closely interacting microtubules, and filamentous- and globular-actin (Lewis and Bridgman, 1992; Bentley and O'Connor, 1994; Suter and Forscher, 2000). Bundles of filamentous actin give structure to the filopodia, as does the cross-linked filamentous actin along the lamellipodial leading edge (Lewis and Bridgman, 1992; Korey and Van Vactor, 2000; Suter and Forscher, 2000). Microtubules are arranged as parallel bundles along the axon and splay outwards within the growth cone, providing structure and transport for proteins and organelles (Dailey and Bridgman, 1989).

Growth cones are fitted with an elaborate suite of receptors that allow for the simultaneous integration of a multitude of chemotactic cues (Tessier-Lavigne and Goodman, 1996). Binding of a chemotactic factor to its specific receptor/s on the growth cone membrane, induces an intracellular signalling cascade which manipulates the cytoskeletal elements, and dictates whether the response of the growth cone culminates in turning, extension, stasis, retraction, collapse or bifurcation (Suter and Forscher, 2000). Well defined receptors for chemotactic signals include the Eph family of receptor tyrosine kinases, Neuropilin, Roundabout, Deleted in Colorectal Cancer, L1 and Plexins (reviewed in (Dickson, 2002)).

LRP1 and LRP2 are highly expressed on the growth cones of developing neurons *in vitro*, and have been shown to signal in a co-dependent manner to promote chemotactic axon guidance within developmental neurons *in vitro* (Landowski et al., 2016). Together, LRP1 and LRP2 act as chemotactic receptors for a variety of ligands, including metallothioneins and tissue-type plasminogen activator (Landowski et al., 2016). Metallothioneins are small, highly conserved, inducible heavy metal binding proteins that are avid scavengers of reactive oxygen species

(Thornalley and Vasák, 1985). Metallothioneins I and II are widely expressed in the nervous system and elsewhere. They differ by only a few amino acids and appear to have redundant functions. Metallothionein III is highly expressed in the brain, while metallothionein IV appears to be absent from the nervous system (Hidalgo et al., 2001). In cultured growth cones from sensory neurons, the activation of LRP1 and LRP2 by metallothionein II stimulated chemo-attraction, resulting in growth cones turning towards the source of metallothionein II (Landowski et al., 2016). Metallothionein III had the opposite effect and induced chemo-repulsion. Other LRP1 ligands, such as α2-macroglobulin, and tissue-type plasminogen activator also induced chemorepulsion (Landowski et al., 2016).

The opposing responses induced by different LRP1 ligands are thought to result from differential activation of downstream signaling pathways, with metallothionein II activating Ca^{2+} / calmodulin-dependent protein kinase and other receptors such as the tropomyosin-related kinase A receptor in complex signaling hubs.

Various LRP ligands have also been shown to alter neurite outgrowth. For example, metallothionein I/II signalling has been shown to transiently activate Akt and ERK, which belong to the mitogen-activated protein kinase and the phosphoinositide-3 kinase / Akt intracellular signalling pathways (Leung et al., 2011). Myelin associated glycoprotein, an established chemorepulsive molecule, is known to interact with LRP1 (Stiles et al., 2013) and is a major constituent of the OL myelin sheath, which inhibits axonal outgrowth, and induces growth cone collapse (Henley et al., 2004; Hines et al., 2010). *In vitro* experiments have demonstrated that myelin associated glycoprotein and LRP1 form a complex with the p75 neurotrophin receptor, to activate RhoA (Stiles et al., 2013), a potent mediator of growth cone collapse and axon retraction (Wu et al., 2005). Additionally apolipoprotein E-containing lipoproteins are secreted by astrocytes and have been shown to bind LRP1 on the surface of

immature neurons to promote neurite outgrowth generally, without having an effect on directionality (Nakato et al., 2015). The complexity of LRP signalling interactions in immature neurons remains to be fully deciphered but appear to be context- and ligand- dependant (Mantuano et al., 2013a)

Mice in which *Lrp1* is selectively deleted from neurons, exhibit prominent tremor and dystonia, behavioural abnormalities, hyperactivity, motor dysfunction, age-dependent dendritic spine degeneration, synapse loss, neuroinflammation, memory loss, eventual neurodegeneration, and premature death (May et al., 2004; Mulder et al., 2004; Liu et al., 2010), clearly demonstrating that LRP1 is crucial to neuronal function. LRP1 is also found postsynaptically, where it can interact with NMDA receptors in vitro, via the intracellular scaffold postsynaptic density protein 95 (Gotthardt et al., 2000; May et al., 2004). LRP1 is able to influence the activity of NMDA receptors and regulate their distribution and internalisation (Maier et al., 2013; Nakajima et al., 2013; Mantuano et al., 2013a), as well as the NMDA-induced internalisation of the AMPA receptor subunit GluR1 (Nakajima et al., 2013). The very nature of this LRP1 / NMDA receptor relationship suggests LRP1 plays an integral role in neurotransmitter-induced calcium signalling, particularly in synaptic plasticity (Maier et al., 2013; Nakajima et al., 2013).

Another LRP family member, LRP8, has been shown to regulate synaptic plasticity (Weeber et al., 2002; Qui et al., 2006). More recently, LRP8 activation by the addition of reelin to primary mouse cortical neurons, was shown to trigger the proteolytic cleavage of LRP8 by γ-secretase. This liberated the intracellular domain, which translocated to the nucleus, and along with phosphorylated CREB, enhanced the transcription of genes associated with learning and memory (Telese et al., 2015). The ability of neurons to acquire energy for demanding tasks, may also be indirectly tied to a role of LRP1 in regulating glucose uptake.

Cultured neurons lacking *Lrp1* exhibit reduced expression of the glutamate transporters GLUT3 and GLUT4 (Liu et al., 2015).

1.16 LRP1 and LRP2 as Regulators of Oligodendrocyte Progenitor Cell Function

In the mouse spinal cord, OPC generation commences from the ventral pMN domain at E12.5 (Noll and Miller, 1993; Richardson et al., 2006). The pMN domain is named for its role in generating spinal cord motor neurons, and is defined by the expression of two transcription factors, OLIG1 and OLIG2 (Zhou et al., 2000), both of which are highly expressed by OPCs and necessary for their generation and subsequent differentiation (Lu et al., 2000; Dai et al., 2015). *Olig1/2* expression by pMN domain neural stem cells is induced by a gradient of ventrally secreted sonic hedgehog, suggesting that specification of this domain would also be LRP1/2-dependant. In the absence of *Olig1/2*, stem cells in the pMN domain instead form V2 interneurons and astrocytes (Zhou and Anderson, 2002). Shortly after their birth, OPCs differentiate into myelinating OLs in the spinal cord grey and white matter (Pringle and Richardson, 1993; Fok-Seang and Miller, 1994). It is estimated that approximately 85% of all spinal cord oligodendrocytes originate from the pMN domain, but other domains such as the P3 domain (Richardson et al., 2006), and more dorsal domains (Fogarty, 2005; Tripathi et al., 2011) also produce OPCs, just slightly later in response to different spatio-temporal cues.

1.17 LRP2 regulates OPC Proliferation and Migration during Development

One of the signalling molecules regulating OPC proliferation and migration is sonic hedgehog (Murray et al., 2002; Gao and Miller, 2006), and LRP2 appears to regulate OPC proliferation and migration by modulating sonic hedgehog availability, and contributing to the generation of a concentration gradient. In the developing mouse optic nerve, LRP2 is highly expressed by astrocytes (Ortega et al., 2012). However, LRP2 expression is not homogeneous, being highest in the caudal optic nerve at E14.5, but then changing to be highest in the rostral optic nerve

at E16.5. Blocking LRP2 signalling by optic nerve astrocytes leads to a significant reduction in OPC proliferation and migration (Ortega et al., 2012). *In vitro* studies suggest that the LRP2-mediated up-take and release of sonic hedgehog by astrocytes, promotes OPC proliferation and acts as a chemo-attractant directing their migration (Ortega et al., 2012). The temporal regulation of LRP2 expression in the caudal versus rostral regions of the optic nerve, would be predicted to 'trap' sonic hedgehog in the region being populated by OPCs at that time. The expression pattern of LRP2 in the postnatal optic nerve has not been characterised. However as LRP2 is expressed by mature oligodendrocytes in the postnatal spinal cord (Wicher et al., 2006), it might also be up-regulated by optic nerve OPCs upon differentiation.

1.18 How Might LRP1 Influence OPC Behaviour?

1.18.1 OPC migration

When examining LRP1 function in other cell types, there are a number of mechanisms by which LRP1 could feasibly influence OPC behaviour. For example OPC processes share some structural similarities with the growth cones of developing neurons (Schmidt et al., 1997; Simpson and Armstrong, 1999). In particular growth cones comprise specialised cell membrane extensions called lamellipodia and filopodia, which also extend from the cellular processes of OPCs (Schmidt et al., 1997). LRP1 signalling mediates chemo-attraction and chemo-repulsion of growth cones *in vitro* (Landowski et al., 2016), so perhaps LRP1 could regulate OPC process guidance, or even OPC migration. LRP1 is expressed by Schwann cells *in vivo*, and regulates the migration and adhesion of immature Schwann cells *in vitro*, by the activation and repression of two small Rho GTPases, Rac1 and RhoA respectively (Mantuano et al., 2010). Rac1 activation stimulates the formation of peripheral lamellae by actin remodelling in the leading process (Pankov et al., 2005). *Lrp1* knockdown decreases Rac1 activation, and increases RhoA activation, which in turn increases cell adhesion and prevents migration (Mantuano et al., 2010). This is of particular interest, as OPCs take on a bipolar

morphology when migrating (Simpson and Armstrong, 1999), and their movement has been attributed to the NG2-dependent regulation of small Rho GTPases and polarity complex proteins (Biname et al., 2013).

LRP1 also has the potential to influence OPC migration by acting as a co-receptor for PDGFRα signalling, in a similar way that it promotes fibroblast migration by co-signalling with PDGFRβ. When PDGF-BB binds to PDGFRβ on the surface of cultured mouse embryonic fibroblasts, it induces migration. However this involves the association of LRP1 with PDGFRβ (Muratoglu et al., 2010; Craig et al., 2013). The two receptors are internalized and co-localize in the endosomal compartment, where the kinase domain of PDGFRβ phosphorylates the distal NPxY motif of LRP1 (Loukinova, 2002; Newton et al., 2005; Muratoglu et al., 2010). Once phosphorylated, LRP1 has an increased affinity for the intracellular domain for SHP-2 (Rönnstrand et al., 1999; Craig et al., 2013), out competing PDGFRβ for this interaction, and preventing further activation of downstream signalling pathways (Craig et al., 2013). While OPCs do not express PDGFRβ, they express high levels of the related receptor, PDGFRα, which is also internalised following ligand binding (Avrov and Kazlauskas, 2003), suggesting an association with an unidentified endocytic receptor – which we propose could be LRP1. PDGF-AA is known to binds to PDGFRα on the surface of OPCs, and activate a phosphorylation cascade involving the Fyn tyrosine kinase and cyclin-dependant kinase 5 (Miyamoto et al., 2008), a known regulator of the actin cytoskeleton in neurons (Chae et al., 1997). By interacting with PDGFRα it is feasible that LRP1 could promote not only OPC migration, but also proliferation and cell survival (Richardson et al., 1988; Rosenkranz et al., 1999; McKinnon, 2005; Miyamoto et al., 2008). While the signalling mechanism is likely to be different, a role for LRP1 in regulating cell survival is not unprecedented, as LRP1 has been shown to protect Schwann cells against TNFα-induced cell death in a sciatic nerve crush injury model *in vivo* and *in vitro* (Campana et al., 2006).

LRP1 could be necessary for OPC migration by instead regulating lipid availability within the cell, as the establishment of cell polarity and movement of the leading edge during migration is dependent on the availability of cholesterol (Mañes et al., 1999; Mañes and Martínez-A, 2004). Most lipid-carrying proteins cannot cross the blood brain barrier, and therefore must be generated within the CNS. Apolipoprotein E is secreted by astrocytes, and functions as an effective lipid transport protein, and can bind LRP1 (Boyles et al., 1985; Beisiegel et al., 1989). Lipoproteins form non-covalent aggregates with triglycerides, phospholipids and cholesterol esters before they bind to specific receptors where they can be internalised and utilized by the cell (Morrisett et al., 1975). Upon binding of apolipoprotein E to LRP1, the complex is internalised where its lipid content is discharged, making it available to the cell (Willnow et al., 2007), before Apolipoprotein E is re-secreted (Laatsch et al., 2012). Once internalized, lipoproteins maybe utilized by OPCs for a number of functions. Forebrain neuron-specific *Lrp1* gene knockout mice have severe deficiencies in lipid metabolism, and show significant synapse loss (Liu et al., 2010), and LRP1-mediated lipid uptake may alternatively allow OPCs to sustain their post-synaptic connections with neurons. The presynaptic use of cholesterol by neurons is high, due to the requirements of lipid-rich neurotransmitter vesicles (Pfrieger, 2003). However, the postsynaptic cell also utilizes cholesterol for receptor recycling in and out of the post-synaptic membrane. Therefore, cholesterol uptake into OPCs may be critical for formation of the axon-OPC synapse, and maintenance of the OPC post-synaptic density.

1.18.2 Inflammatory response

Microglia are the resident immune cell of the CNS and become activated in response to injury, infection or in neurodegenerative disease; and express high levels of LRP1 (Marzolo et al., 2000; Auderset et al., 2016a). Microglial specific deletion of LRP1 has been shown to worsen disease severity in EAE as microglia adopt a pro-inflammatory phenotype and increase production of tissue necrosis factor alpha (TNF-α) (Chuang et al., 2016), which suggests that

normally, microglial LRP1 is required to maintain these cells in an anti-inflammatory and neuroprotective state following injury. Furthermore, knockdown of LRP1 in primary murine microglia led to enhanced sensitivity to LPS as a result of activation in NF-κβ and c-Jun N-terminal kinase (JNK) signalling pathways which again, led to the conclusion that LRP1 is required to maintain microglia in a non-activated state (Yang et al., 2016). Brifault et al found that by adding RAP to mouse microglial cultures they were able to induce LRP1 shedding from the membrane which led to the adoption of a more inflammatory phenotype and increased microglial proliferation and migration. When RAP and sLRP1 was injected directly into the dorsal horn of mouse spinal cords, significantly more microglia were observed at the injection site as well as increased expression of proinflammatory mediators such as TNF-α and IL-6 (Brifault et al., 2017).

1.19 LRP1 as a Regulator of Adult OPC Behaviour

A number of signalling pathways have been identified that are involved in regulating developmental and adult OPC behaviour, or oligodendrogenesis, including Notch1 (Genoud et al., 2002; Givogri et al., 2002; Zhang et al., 2009), FGF2 (Murtie et al., 2005; Zhou et al., 2006; Murcia-Belmonte et al., 2014), mTOR (Zou et al., 2014; Jiang et al., 2016; Grier et al., 2017) and PDGF (McKinnon, 2005; Rajasekharan, 2008; Chew et al., 2010) , however the full extent of ligand-receptor and downstream cell signalling interactions regulating OPC function is far from being fully understood. Within the OL lineage, LRP1 is exclusively expressed by OPCs, and downregulated with differentiation (Auderset et al., 2016a). LRP1 can signal in a variety of ways including ligand endocytosis (Cam et al., 2005; Parkyn et al., 2008; Liu et al., 2017; Van Gool et al., 2019), receptor trafficking (Parkyn et al., 2008; Maier et al., 2013; Kadurin et al., 2017) and cleavage and formation of a soluble product (May, 2002b; Liu et al.,

2009; Brifault et al., 2017; 2019). Previous studies have found that deleting LRP1 can also directly regulate the function of cells of the oligodendrocyte lineage, as the conditional deletion of *Lrp1* from OLIG2^{+} cells using *Olig2-Cre :: Lrp1$^{fl/fl}$* mice impaired oligodendrogenesis and myelination in the developing mouse optic nerve (Lin et al., 2017). As OPC physiology changes considerably between development and adulthood (Velez-Fort et al., 2010), and OPC behaviour can differ between CNS regions (Spitzer et al., 2019), we employed a conditional gene deletion approach to determine how LRP1 influences adult OPC behaviour and oligodendrogenesis in the adult mouse brain. The aim of this study was to determine how *Lrp1* deletion would affect OPC behaviour within the adult mouse CNS.

Chapter 2: Methods

2.1 Animal housing and mice

All animal experiments were approved by the University of Tasmania Animal Ethics (A0016151) and Institutional Biosafety Committees and were carried out in accordance with the Australian code of practice for the care and use of animals for scientific purposes. *Pdgfra-CreER^{T2} mice* (Rivers et al., 2008) were a kind gift from Prof William D Richardson (University College London). *Pdgfra-CreER^{TM}* (Kang et al., 2010a), *Pdgfrα-H2BGFP* [(*Pdgfrα-histGFP* (Hamilton et al., 2003); Jackson stock # 007669)] and *Lrp1$^{fl/fl}$* (Herz et al., 1992) mice were purchased from Jackson Laboratories. Cre-sensitive *Rosa26-YFP* (Srinivas et al., 2001) and *Tau-mGFP* (Hippenmeyer et al., 2005) reporter mice were also purchased from Jackson laboratories. Mice were maintained on a C57BL/6 background and inter-crossed to generate offspring for experimental use. All mice were weaned >P30 to ensure appropriate myelin development; were group housed with same-sex littermates in Optimice micro-isolator cages (Animal Care Systems, Colorado, USA), and were maintained on a 12-hour light / dark cycle at 20°C, with uninhibited access to food and water.

Please note that two distinct *Pdgfrα-CreER* transgenic mouse lines used in this study: the *Pdgfrα-CreER^{TM}* transgenic mouse line, generated by Kang et al. (2010b), was used for the majority of experiments, and the lower efficiency (LE) *Pdgfrα- CreER^{T2}* transgenic mouse line, generated by Rivers et al. (2008), was used to perform the *Tau-mGFP* lineage tracing experiments, as we have previously demonstrated that *Pdgfrα-CreER^{TM}* transgenic mouse are not compatible with the *Tau-mGFP* reporter [see (Pitman et al., 2019)].

2.2 DNA extraction and amplification

Ear biopsies were digested overnight in DNA extraction buffer (100mM Tris-HCl, 5mM EDTA, 200mM NaCl, 0.2% SDS and 120ng of proteinase k) at 55°C. Genomic DNA was then extracted by first precipitating cellular and histone proteins by cold incubation in 6M Ammonium Acetate (Sigma; A1542), followed by precipitation of the DNA in room temperature isopropyl alcohol (Sigma; I9516). The DNA pellet was washed in 70% Ethanol (Sigma; E7023), resuspended in sterile MilliQ water and used as template DNA to genotype the mice by polymerase chain reaction (PCR). The PCR was performed as a 25µL reaction containing: 50-100ng DNA; 0.5µL of each primer (100nmol/mL, GeneWorks); 12.5 µL GoTaq® green master mix (Promega) and MilliQ water. The following primers were used: Lrp1 5' CATAC CCTCT CAAACC CCTT CCTG and Lrp1 3' GCAAG CTCC CTGCTCA GACC TGGA ; Cre 5' CAGGT CTCAG GAGCT ATGTC CAATT TACTG ACCGTA and Cre 3' GGTGT TATAAG CAATCC CCAGAA, or GFP 5' CCCTG AAGTTC ATCTG CACCAC and GFP 3' TTCTC GTTGG GGTCT TTGCTC in a program of: 94°C for 4', and 34 cycles of 94°C for 30", 60°C for 45", and 72°C for 60", followed by 72°C for 10 minutes. To genotype mice expressing the *Rosa26-YFP* transgene we used three primers: Rosa26 wildtype 5' AAAGT CGCTC TGAGT TGTTAT, Rosa26 wildtype 3' GGAGC GGGAG AAATG GATATG and Rosa26 mutant 5' GCGAA GAGTT TGTCC TCAACC in a program of: 94°C for 4', and 37 cycles of 94°C for 30", 62°C for 45", and 72°C for 1', followed by 72°C for 10'. The DNA was then separated by gel electrophoresis (2% w/v agarose in TAE containing SYBR-safe, ThermoFisher), and imaged using an Image Station 4000M PRO gel system running Carestream software.

2.3 Tamoxifen preparation and administration

Tamoxifen (Sigma,T5648) was dissolved by sonication in corn oil (Sigma) at a concentration of 40mg/ml for 2 hours at 21°C. Adult mice were administered tamoxifen (300mg/kg) via oral gavage daily for 4 consecutive days. Mice were weighed and monitored daily. No side-effects of tamoxifen administration were observed. Our dosing regimen provides the maximal amount of tamoxifen that can be tolerated by young adult mice without observing adverse side-effects (Rivers et al., 2008).

2.4 EdU administration and labelling

For *in vivo* labelling, 5-Ethynly-2'-deoxyuridine (EdU; Thermofisher, E10415,) was administered to mice via their drinking water at a concentration of 0.2mg/ml for up to 21 consecutive days (as per Clarke et al., 2010). For *in vitro* labelling, EdU was added to complete OPC medium at a final concentration of 2.5μg/ml in complete OPC medium for 10 hours before the cells were fixed with 4% (w/v) paraformaldehyde in PBS for 15 minutes at room temperature. EdU developing cocktail was made instructions outlined in the AlexaFluor-647 Click-IT EdU kit (Invitrogen, C10340) with brain slices being exposed to the developing reagent for 45 minutes and coverslips being exposed for 15 minutes.

2.5 Generation of mixed glial cultures and purification and differentiation of OPCs

The cortices of P1-10 mice were dissected into EBSS (Invitrogen, 14155-063), diced into pieces ~1mm^3 and digested in 2ml of EBSS containing trypsin (final conc 0.06mg/ml, Sigma,T4799) at 37°C for 10 minutes. The trypsin was inactivated by the addition of foetal bovine serum (FBS) then rinsed twice in EBSS and triturated in EBSS with DNAseI (final concentration 0.12mg/ml, Sigma, 5025) and filtered through a 40μm sieve (Corning, 352340). After centrifugation at 300rcf for 5 minutes, the cells were resuspended in complete OPC medium (20ng/ml human

PDGF-AA (Peprotech), 10ng/ml bFGF (R&D Systems), 10ng/ml human CNTF (Peprotech), 5μg/ml NAC (Sigma), 1ng/ml NT3 (Peprotech), 1ng/ml Biotin (Sigma), 10μM Forskolin (Sigma), 1X Pen/Strep (Invitrogen), 2% B27 (Invitrogen), 50μg/ml Insulin (Sigma), 600ng/ml Progesterone (Sigma) 1mg/ml Transferrin (Sigma), 1mg/ml BSA (Sigma), 400ng/ml Sodium Selenite (Sigma) 160μg/ml Putrescine (Sigma) in DMEM+ Glutamax (Invitrogen, 10569069) and plated on 6 well plates coated with >30,000 MW Poly D-Lysine (PDL; Sigma, P7405).

2.5.1 Purifying OPCs by immunopanning

After 7 DIV, OPCs were purified using a modified version of the Emery and Dugas (2013) immunopanning protocol. Cells were dislodged by incubating in 1:5 TrypLE (Gibco, 12604013) in EBSS for ~10 minutes. The TrypLE was then inactivated by adding FBS then the cells were washed in EBSS prior to being collected and centrifuged for 5 minutes at 300rcf. OPCs were then immunopanned (Emery and Dugas, 2013).

2.5.2 Differentiation of purified OPCs

To differentiate OPCs, the complete OPC medium was removed and replaced with OPC differentiation medium [complete OPC medium lacking PDGF-AA and containing 4μg/ml triiodothyronine (Sigma)].

2.6 Gene deletion in vitro

Following immunopanning, purified OPCs plated at a density of 20,000 cells per 13mm coverslip were allowed to settle for two days. TAT-Cre (Excelgen, EG1001) was then added to complete OPC medium at a final concentration of 1μM for 90 minutes at 37°C and 5% CO2. The medium containing TAT-Cre was then removed and replaced with fresh complete OPC medium and returned to the incubator for 48 hours.

2.7 Western blot

2.7.1 Generation of lysates

Mouse brain lysates were produced by lysing tissue in RIPA cell lysis buffer (50mM Tris-HCL, 150mM NaCl , 1%NP-40, 1% Sodium Deoxycholate , 0.1% SDS and one phosphatase inhibitor tablet). Samples were centrifuged for 1 minute at 10,000 rpm in a bench-top centrifuge and the supernatant was collected and stored at -80°C.

2.7.2 Protein quantification

The amount of protein in each sample was quantified by performing a Bradford protein quantification assay. Six bovine serum albumin (BSA) standards (ranging from 0-2mg/mL) were prepared by diluting the 2mg/mL BSA standard (Sigma) in MilliQ water. Each brain lysate was diluted 1:10 in MilliQ water, and 5µL of each sample or standard was plated in triplicate. Twenty five microlitres of the Bio-Rad DC™ Protein Assay Reagent (Biorad; comprising1ml of Reagent A and 20µL of Reagent S) and 200µL of DC™ Protein Assay Reagent B was added to each well and the plate was placed on an orbital shaker for 15 minutes before being analysed using the FLUOstar OPTIMA microplate reader (BMG Labtech, Baden-Württemberg, Germany). Standard absorbance readings, presented as optical density, were used to calculate the protein concentration for each lysate.

2.7.3 Protein gel electrophoresis

Ten micrograms of protein lysate was combined with 10µl of 4x Bolt LDS sample buffer and 4µl of reducing agent (500mM Dithiothreitol) and made up to 40µl with MilliQ water, before each sample was incubated at 70°C for 10 minutes. Precast polyacrylamide 4%-12% Bolt Bis-Tris Plus Gels (Life Technologies) were prepared according to the manufacturer's instructions. 10µL of Seablue Plus2® (Life Technologies) protein ladder was added to the first well and 40µL of lysate to the remainder. The gel was run at 140 volts for 45 minutes at 21°C, before being

removed from it casing and left to equilibrate in 1x transfer buffer (5% Bolt Transfer buffer / 10% Ethanol / MilliQ water) for 10 minutes. The gel sandwich was constructed according to the manufacturer's instructions and the protein was transferred onto an ethanol-activated PVDF membrane (Biorad) for 60 minutes at 20 volts and 4°C. The membrane was transferred into blocking solution [5% (w/v) skim milk powder, 0.05% (v/v) tween-20 in tris buffered saline (TBS)] and incubated on the orbital shaker for 60 minutes at 21°C, before being transferred into blocking solution containing rabbit anti-LRP1 (1:40000, ab92544, Abcam) and mouse anti-GAPDH (1:40000, AB2302, Millipore). The membrane was incubated on the orbital shaker overnight at 4°C, before being washed 5 x 15 minutes in TBS /0.2% tween-20 at 21°C while agitating. The relevant horseradish peroxidase (HRP) conjugated secondary antibodies [goat anti-mouse HRP (1:20000, P044701-2, Dako) or goat anti-rabbit HRP (1:20000, P044801-2, Dako)] were diluted in TBS / 0.2% Tween20 and applied to the membrane for 1 hour on an orbital shaker at 21°C. The membrane was washed as described previously and exposed to equal volumes of Immobilon Western™ HRP Peroxidase Solution (Millipore) and Luminol Reagent (Millipore) for visualisation of the protein bands on an Image Station 4000M PRO, using Carestream software (Rochestern NY14608). Western blot band intensity was calculated by measuring integrated density and normalizing to a loading control.

2.8 Whole cell patch clamp electrophysiology

Adult (P57+30) control and LRP1-deleted mice expressing GFP selectively in OPCs were sacrificed by cervical dislocation and their brains dissected into an ice-cold sucrose solution containing: 75 mM sucrose, 87 mM NaCl, 2.5 mM KCl, 1.25 mM NaH_2PO_4, 25 mM $NaHCO_3$, 7 mM $MgCl_2$, and 0.95 mM $CaCl_2$. Coronal vibratome slices (300 µm) were prepared using a Leica VT1200s vibratome and incubated at 31.7C in artificial cerebral spinal fluid (ACSF)

containing: 119 mM NaCl, 1.6 mM KCl, 1 mM NaH_2PO_4, 26.2 mM $NaHCO_3$, 1.4 mM $MgCl_2$, 2.4 mM $CaCl_2$, and 11 mM glucose (300 ± 5 mOsm/kg), saturated with 95% O_2/5% CO_2. After 45 min, slices were transferred to ~21°C ASCF. For recording slices were transferred to a bath constantly perfused with ~21°C ACSF (2 mL/min). Recording electrodes were prepared from glass capillaries and had a resistance of 3–6 MΩ. For recording currents through voltage gated calcium channels electrodes were filled with an internal solution containing 125 mM Cs-methanesulfonate, 4mM NaCl, 3mM KCl, 1mM $MgCl_2$, 8mM HEPES, 9mM EGTA, 10 mM phosphocreatine, 5 mM MgATP, and 1 mM Na_2GTP, set to a pH of 7.2 with CsOH and an osmolarity of 290 ± 5 mOsm/kg. For AMPA/kainate receptor currents, an internal solution containing 125 mM Cs-methanesulfonate, 5mM TEA-Cl, 2mM $MgCl_2$, 8mM HEPES, 9mM EGTA, 10 mM phosphocreatine, 5 mM MgATP, and 1 mM Na_2GTP set to a pH of 7.2 with CsOH and an osmolarity of 290 ± 5 mOsm/kg was used.

Whole cell patch clamp recordings of GFP^+ cells in the motor cortex were collected using a HEKA Patch Clamp EPC800 amplifier and pCLAMP 10.5 software (Molecular devices). Upon breakthrough cells were held at −50 mV and a series of voltage steps up to +30 mV applied to determine the presence of a voltage-gated sodium channel current. Cells with a voltage-gated sodium current greater than 100pA were considered OPCs and used for further analysis. For L-Type and T-Type voltage gated calcium channel recordings the perfusate was subsequently switched to a calcium recording solution containing 20 mM $BaCl_2$, 125 mM choline Cl, 5 mM tetraethyl ammonium, 10 mM glucose, and 10 mM HEPES, set to a pH of 7.4 with CsOH and an osmolarity of 300 ± 5 mOsm/kg. To record T-type currents cells were held at −50 mV and the cell was hyperpolarised to -120mV for 200ms before voltage steps from -70mV to 30mV were applied. The current density relationship of steady state currents in the last 100ms of the voltage steps were reported from an average of 3 recordings per cell. To record L-type

currents, cells were held at −50 mV and a series of 500 ms voltage steps, from −60 to +30 mV, was applied using a P/N subtraction protocol and the current density relationship was plotted from the average of 3 recordings per cell.

For recording currents through AMPA/kainate receptors, the perfusate was switched to ACSF containing 50μm APV (Sigma) and 1μM TTX (Sigma). After 3 minutes, cells were voltage clamped at -60 mV and currents elicited by 200 ms voltage steps from -80 to 20 mV (20 mV increments) to obtain a baseline measurement. After 1 minute, the perfusate was switched to a recording solution containing 100μM kainate (Abcam), 50μm APV (Sigma) and 1μM TTX (Sigma) and currents were elicited as above to obtain the currents in the presence of kainate.

Access resistance was measured before and after all recordings and an access resistance >20 MΩ resulted in exclusion of that recording. Due to the high membrane resistance of OPCs (>1 GΩ) during calcium current recordings, recordings were made without series resistance compensation. Series resistance in AMPA current recordings was compensated 60 - 80%. Measurements were made from each data file using Clampfit 10.5.

2.9 Tissue preparation and immunolabelling

2.9.1 Embryonic tissue preparation

Female mice were mated overnight and examined the following morning for the presence of a vaginal plug, which was denoted embryonic day 0.5 (E0.5). At the required gestational stage, pregnant mice were euthanized by CO_2 exposure, the embryos removed and their brains and spinal columns removed. Postnatal mice were terminally anesthetised with pentobarbitone (i.p 30mg/kg; Ilium) and perfusion fixed with 4% (w/v) paraformaldehyde (PFA; Sigma) in PBS at a rate of 9mL per minute for ~4 minutes. The brain was removed and sliced into 2mm thick

coronal slices using a rodent brain matrix (Agar Scientific, Essex, UK), and the spinal cord was removed from the spinal column. All tissue was immersion fixed in 4% PFA (w/v) in PBS for 90 minutes at 21°C, before being cryo-protected in 20% (w/v) sucrose (Sigma) in PBS overnight at 4°C. The following day, tissue was embedded in Tissue-Tek® Cryomolds (Sakura) with Cryomatrix gel (Thermo Fisher Scientific), frozen and stored at -80°C.

2.9.2 Postnatal tissue preparation

Mice were terminally anaesthetized with an intraperitoneal (i.p) injection of sodium pentobartbital (30mg/kg, Ilium) and then perfusion fixed with 4% (w/v) paraformaldehyde (PFA; Sigma) in phosphate buffered saline (PBS). Brains were cut into 2 mm-thick coronal slices using a 1 mm brain matrix (Kent Scientific) before being post-fixed in 4% (w/v) PFA in PBS at 21°C for 90 min. Tissue was cryoprotected in 20% sucrose (Sigma) in PBS and snap frozen in OCT (ThermoFisher) for storage at −80°C.

2.9.3 Immunohistochemistry

Thirty micrometre coronal brain cryosections were collected and processed as floating sections (as per (O'Rourke et al., 2016)). Cryosections were exposed to primary antibodies diluted in blocking solution [10% (v/v) fetal calf serum and 0.1% (v/v) triton x100 in PBS] and incubated overnight at 4°C on an orbital shaker. Primary antibodies included rabbit anti-LRP1 (1:500, ab92544, Abcam), goat anti-PDGFRα (1:100, AF1062, R&D Systems), rabbit anti-ASPA (1:200, AB97454, Abcam), rabbit-anti-LRP2 (1:100, AB76967, Abcam), rat-anti-GFP (1:2000, 04404-26, Nacalaitesque) rat anti-MBP (1:100, MAB386, Millipore), rabbit anti-OLIG2 (1:400, AB9610, Abcam), mouse anti-PSANCAM (1:500, MAB5324, Millipore), mouse anti-RC2 (1:100, MAB5740, Millipore), mouse anti-GFAP (1:2000, 556327, BD Pharmigen), guinea-pig anti-IBA1 (1:250, 234004, Synaptic Systems), mouse anti-CC1 (1:200, MABC200 Millipore), mouse anti-NeuN (1:200, MAB377, Millipore) and mouse anti-parvalbumin (1:1000, MAB1572, Millipore).

2.9.4 Immunocytochemistry

Primary OPCs grown on glass 13mm glass coverslips were fixed in 4% PFA for 15 minutes at room temperature. The coverslips were then rinsed 3 times with PBS and the cells were then exposed to blocking solution containing the relevant antibodies and (as stated above).

2.10 Cuprizone administration and Black gold staining

Cuprizone powder (Sigma, C9012) was added to crushed mouse food (Barrastock) at a concentration of 0.2% w/w and changed every 2 days for 35 days. Tissue from cuprizone fed mice was collect as stated above (Tissue Preparation and immunohistochemistry). Thirty micrometre μm brain sections were cut using a Leica CM1860 UV cryostat into PBS then floated onto superfrost glass slides. Once dry, the sections were rehydrated in milliQ for 3 minutes. MilliQ was removed and preheated (60°C) 0.3% Black Gold II stain (Millipore, AG105) was added to the slide and incubated in an oven at 60°C for 60 minutes. Slides were the removed from oven and rinsed twice with milliQ before a preheated 1% v/v sodium thiosulphate solution was added and incubated for 3 minutes at 60°C. The slides were then rinsed prior to dehydration using a series of graded alcohol steps then submerged in xylene (Sigma, 214736) for 3 minutes prior to being mounted using DPX mounting media (Sigma, 06522)

2.11 Microscopy and Statistical Analysis

Fluorescently labelled sections were examined using an UltraView Spinning Disc Confocal microscope with Volocity Software (Perkin Elmer, Waltham, USA). Images were collected as z stacks with 2μm spacing using standard excitation and emission filters for DAPI, FITC (Alexa Fluor-488), TRITC (Alexa Fluor-568) and CY5 (Alexa Fluor-647). Images for quantification were collected using a 10x or 20x objective and images spanning each region of interest were stitched together using Volocity software. Images used to quantify cellular morphology were

collected using a 20x, 40x or 60x water objective. Black gold stained sections were captured on a light microscope using a 2.5x objective and were stitched together using Adobe Photoshop CS6. All images were analysed with Photoshop CS6 (Adobe, San Jose, USA) or Image J (NIH, Bethesda, Maryland).

All images were analyzed with Photoshop CS6 (Adobe, San Jose, USA) or Image J (NIH, Bethesda, Maryland). Statistical comparisons were carried out using Prism (Graph Pad, La Jolla, USA).

Chapter 3 – LRP1 Expression in the Developing and Adult CNS

Some of the immunohistochemical data for this Chapter were collected out prior to commencing postgraduate studies, however additional data were generated during my PhD. Most of the data were analysed and the manuscript written after commencing my PhD.

3.1 Introduction

Low density lipoprotein receptor related protein 1 (LRP1) is one of the largest members of the low-density lipoprotein receptor family, and binds a large variety of ligands to influence a range of cellular behaviors [reviewed (Auderset et al., 2016b). While LRP1 is best known for its ability to mediate endocytosis (Li, 2000; Pi et al., 2012), it can also operate as a co-receptor (Gopal et al., 2011), or recruit non-receptor tyrosine kinases to its intracellular domain to mediate intracellular signal transduction (Shi et al., 2009). Furthermore LRP1 can undergo proteolytic cleavage, reminiscent of notch or the amyloid precursor protein cleavage, to generate a soluble extracellular fragment (Arnim et al., 2005; Selvais et al., 2011) or a free intracellular domain, which has been shown to enter the nucleus and influence gene transcription (May, 2002a; Kinoshita et al., 2003; Zurhove et al., 2008). Utilizing these signaling mechanisms, LRP1 performs unique tissue-specific functions [reviewed (Lillis et al., 2008)], and it is highly likely that it mediates cell-type specific functions in the central nervous system (CNS).

LRP1 is widely expressed throughout the CNS. The majority of research examining LRP1 function in the brain has focused on its role in regulating amyloid precursor protein trafficking (Ulery et al., 2000; Pietrzik et al., 2002), amyloid β clearance from the brain parenchyma [reviewed (Ramanathan et al., 2015)], and blood brain barrier permeability (Yepes et al., 2003). However LRP1 is also detected in mature neurons, particularly those of the entorhinal

cortex, hippocampus (Wolf et al., 1992) and cerebellum (Bu et al., 1994), and is critical for neuronal function. The selective deletion of *Lrp1* from differentiated neurons during mouse development, leads to behavioural and motor defects including hyperactivity, tremor and dystonia (May et al., 2004). These effects are primarily due to the importance of LRP1 for regulating synaptic function, specifically at the post-synaptic density where it is thought to regulate the turnover and recycling of synaptic proteins (May et al., 2004; Nakajima et al., 2013). More recently LRP1 was also shown to mediate the chemo-attraction and -repulsion of sensory neuron growth cones *in vitro* (Landowski et al., 2016), and there is some evidence that LRP1 is expressed by astrocytes (Casse et al., 2012) , microglia (Zhang et al., 2017) and oligodendrocytes (Gaultier et al., 2009) *in vitro,* and by a sub population of radial glia in the embryonic mouse brain (Hennen et al., 2013).

Studies reporting the expression of LRP1 in the CNS have often focused on a single stage of development, and examined gross regional expression or a single cell type, often *in vitro* (Auderset et al., 2016b). Therefore, when reading the literature, it is unclear which cells within the CNS actually express this receptor, and which do not. Recent microarray and RNA sequencing data have shown that *Lrp1* mRNA is highly expressed by neurons, astrocytes and microglia, as well as oligodendrocyte progenitor cells (OPCs) and newly formed oligodendrocytes in the early postnatal brain, but indicate that it is down-regulated as the cells differentiate into mature myelinating oligodendrocytes (Cahoy et al., 2008; Zhang et al., 2014). This is the first indication that LRP1 may be expressed by oligodendrocyte lineage cells in the healthy nervous system, but has not been verified at the protein level. Herein we characterise LRP1 expression within the developing and mature mouse brain and spinal cord. We report that LRP1 is expressed extensively throughout the CNS, being expressed at high levels by radial glia, neuroblasts, neurons, microglia, astrocytes and OPCs. However LRP1 was not expressed by mature oligodendrocytes in the brain or spinal cord, and was not expressed

by parvalbumin-positive cortical interneurons – indicating that LRP1 is not generically expressed by all neural cell types.

3.2 Results

3.2.1 LRP1 is expressed in the developing and adult mouse brain

The LRP1 protein is highly expressed in the brain (Bu et al., 1994). However, the differential expression of LRP1 across development has not been investigated. To determine the relative expression of LRP1 from embryonic to postnatal development, and into adulthood, we performed a western blot analysis to detect LRP1 in protein lysates generated from E13.5, P5, and P60 C57Bl6 mouse brain (n=3 mice per age). A single 85kDa band was detected in each lysate, corresponding to the size of the beta chain of LRP1 (**Figure 6a**). LRP1 expression was normalised to GAPDH expression levels (**Figure 6a**). We found that LRP1 expression peaked during early postnatal brain development, before decreasing in adulthood (**Figure 6b**). From these data it is not possible to determine whether cells within the postnatal CNS reduce their expression of LRP1 with age, or whether this is the result of the changing cellular composition of the brain over this time period. To look at this more closely, and determine which cell types specifically express LRP1 in the CNS, we next undertook an immunohistochemical characterisation of LRP1 expression in the brain and spinal cord.

3.2.2 LRP1 is highly expressed by radial glia in the developing CNS

In the embryonic brain and spinal cord, radial glial cell marker-2 (RC2) is a protein that binds to intermediate filament proteins in the radial glial stem cells (Chanas-Sacré et al., 2000), allowing identification of their cell bodies as well as their processes that project outwards from the neuroepithelium to the pial surface. In the E13.5 mouse brain, all radial glia ($RC2^{+}$)

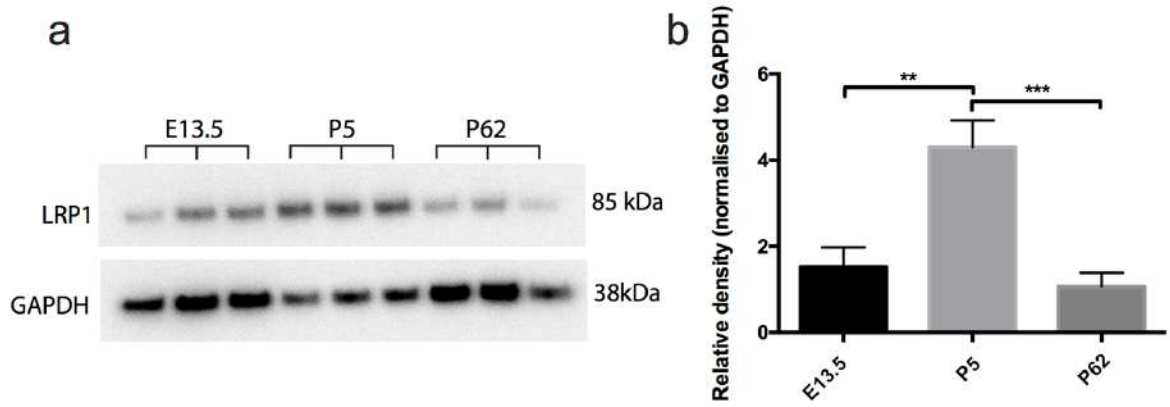

Figure 6: LRP1 is highly expressed in the brain

Whole brain lysates from E13.5, P5 and P60 wildtype mice were collected. Western blot was performed to examine LRP1 expression in the embryonic (E), postnatal (P) and adult (A) mouse brain and GAPDH protein expression. (**c**) Quantification of band pixel intensity normalised to loading control (GAPDH) shows that LRP1 expression is significantly elevated in the postnatal brain compared to the embryonic (P=0.001) and adult (P=0.0004) brain. Results were compared using a one-way ANOVA with a Tukey's post-hoc test, expressed as means ± SEM and are representative of three independent experiments. **P<0.01, ***P<0.001.

were LRP1-positive (**Figure 7a**; 117 of 117 cells counted). Similarly, at E15.5 100% of radial glia examined in the MGE of the brain (**Figure 7c**; n=125 cells counted), and in the spinal cord (**Figure 7e,** n=112 cells counted) expressed LRP1 throughout the cell. At E18, $LRP1^+$ cells continued to occupy the ventricular zone of the brain (**Figure 7g**). While it was not possible to demonstrate LRP1 co-localisation with RC2 at the cell body, due to the down-regulation of RC2, LRP1 and RC2 were still present together within the processes of these cells (**Figure 7g**). These data suggest that LRP1 is expressed by radial glia in the brain and spinal cord, and is sustained throughout embryonic development. Even at these early developmental stages it was already clear that LRP1 expression was not restricted to the radial glia, as the $LRP1^+$ radial glia wrapped around and made contact with other $LRP1^+$ cells (**Figure 7e**).

3.2.3 LRP1 is highly expressed by $GFAP^+$ astrocytes in the postnatal CNS

Radial glia are only present during development, replaced by a population of neural stem cells in the subventricular zone (SVZ) of the lateral ventricles in the postnatal brain. These neural stem cells share a number of markers that identify them as being closely related to astrocytes. For example, fibrous astrocytes and neural stem cells both express glial fibrillary acidic protein (GFAP) (Young et al., 2010). $GFAP^+$ cells in the SVZ of the adult brain likely comprise both of these cell populations, and were found to express LRP1 (**Figure 8a**; 33 of 33 cells counted). Furthermore $GFAP^+$ fibrous astrocytes in the corpus callosum of the P5 mouse brain also expressed LRP1 in the soma and along their processes (**Figure 8c**; 73 of 73 cells counted), and this expression was retained in adulthood (**Figure 8e**; 99.20% ± 1.37%; avg ± std, n=3 mice). In the spinal cord of adult mice, essentially all fibrous astrocytes were LRP1-postive (**Figure 8g**; 108 of 109 cells counted). While the majority of astrocytes in the adult mouse cortex are protoplasmic astrocytes and do not express GFAP (Young et al., 2010), the small number of

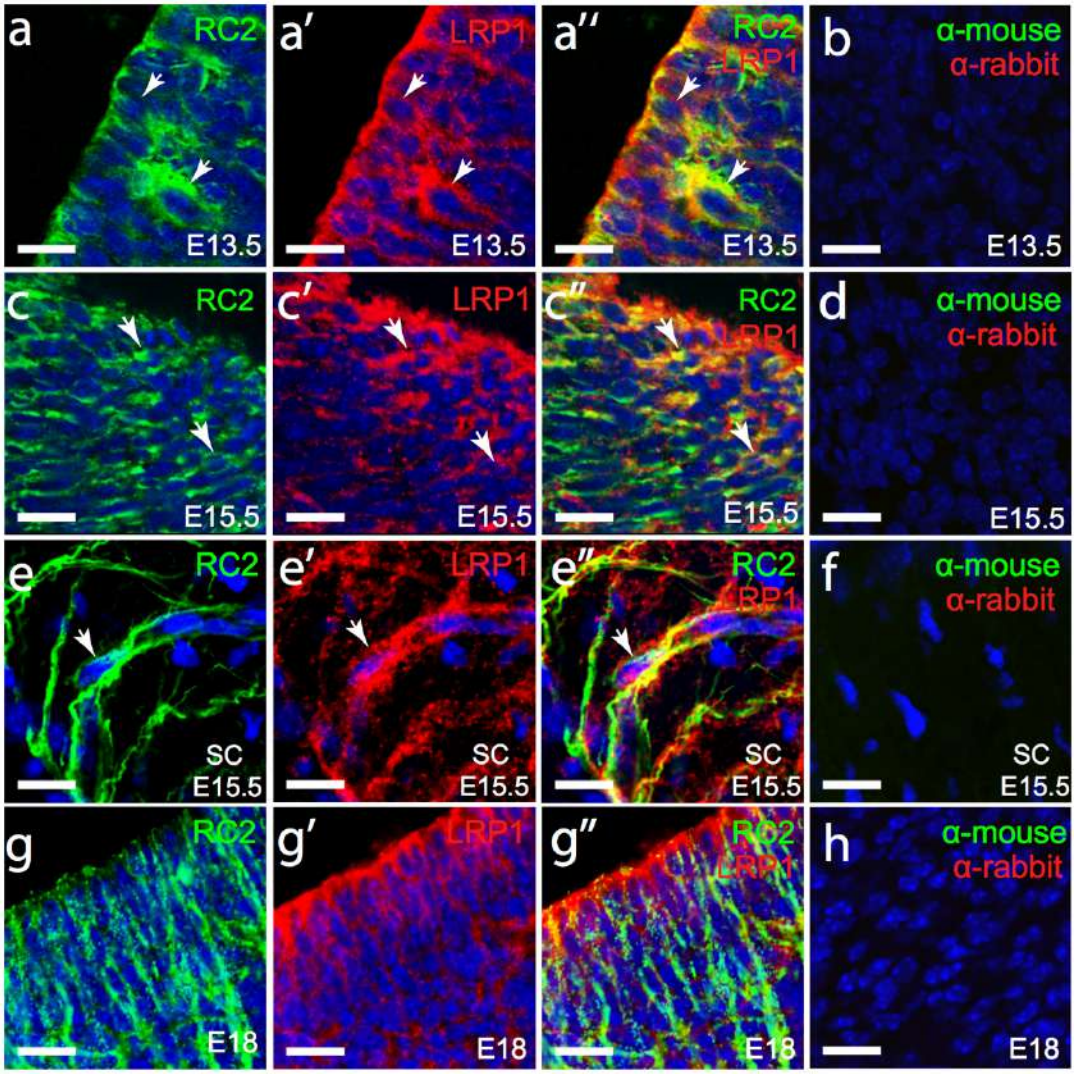

Figure 7: LRP1 is expressed by radial glial in the developing brain and spinal cord

Coronal and transverse sections of embryonic brain (E13.5 **a**, E15.5 **c** and E18 **g**) and spinal cord (E15.5 **e**) were immunolabelled to detect radial glia (RC2, green) and LRP1 (red). The nuclear marker Hoechst 33342 was used to label cell nuclei (blue). (**b**,**d**,**f**,**h**,**j**) secondary alone controls. White arrows represent cell bodies and yellow arrows represent co-localisation. Scale bar represents 17µm. SC= spinal cord.

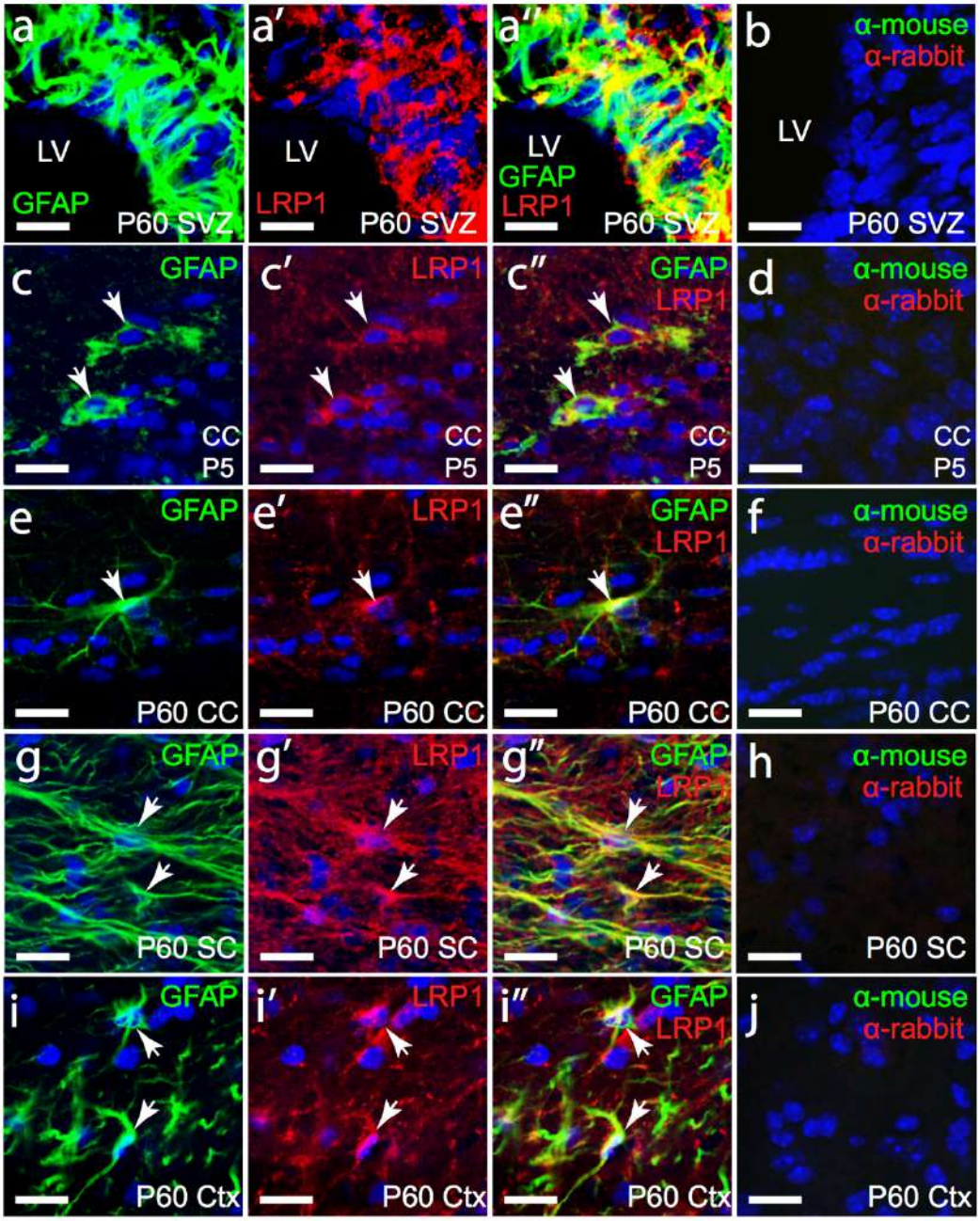

Figure 8: LRP1 is highly expressed by fibrous astrocytes

Coronal and transverse sections of early postnatal (P5 **a**) and adult (P60) brain (**c**,**g**,**i**) and spinal cord (**e**) were immunolabelled to detect astrocytes (GFAP, green) and LRP1 (red). The nuclear marker Hoechst 33342 was used to label cell nuclei (blue). (**b**,**d**,**f**,**h**,**j**) secondary alone controls. White arrows represent cell bodies and yellow arrows represent co-localisation. Scale bar represents 17μm. CC= corpus callosum, SC= spinal cord, Ctx= cortex, SVZ=subventricular zone and LV= lateral ventricle.

fibrous astrocytes present in layer I of the motor cortex were LRP1-positive (**Figure 8i**; 46 of 48 cells counted). These data are consistent with microarray (Cahoy et al., 2008) and RNA sequencing (Zhang et al., 2014) data which indicate that *Lrp1* mRNA can be detected in astrocytes in the early postnatal mouse brain.

3.2.4 LRP1 is highly expressed by neuroblasts and neurons in the developing and adult CNS

During development, neurons are the first cell type produced by radial glia. At E13.5, E15.5 and E18, PSA-NCAM$^+$ neuroblasts are present throughout the telencephalon. It is important to note that while all neural progenitors express PSA-NCAM, as well as a number of glial progenitors (Marmur et al., 1998). This high density of neuroblasts in the MGE made quantification extremely difficult. However, at E13.5 all PSA-NCAM$^+$ cells examined in the MGE of the developing brain, were found to express LRP1 (57 of 57 cells counted; **Figure 9a**), and continued to express LRP1 at E15.5 (108 of 110 cells counted; **Figure 9c, e**) and E18 (111 of 111 cells counted; **Figure 9g**).

Many of these neuroblasts mature into functional neurons in the postnatal CNS, and the fact that LRP1 is expressed by neurons is well established (May et al., 2004; Lillis et al., 2008; Liu et al., 2010). NeuN is a perinuclear protein expressed by the majority of mature CNS neurons, including all excitatory neurons (Mullen et al., 1992). We determined that LRP1 was expressed by essentially all NeuN$^+$ neurons in the P5 mouse cortex (111 of 113 NeuN$^+$ cells counted; **Figure 10a**). Furthermore 98.44% ± 0.99% of NeuN$^+$ cells expressed LRP1 in the adult mouse cortex (**Figure 10c**; n=3 mice, avg ± std). Similarly in the spinal cord grey matter 97.7% ± 0.76% of NeuN$^+$ neurons expressed LRP1 (**Figure 10e**; n=3 mice, avg ± std). However not all neurons express NeuN. Interneurons are the GABAergic inhibitory neurons of the CNS, and they comprise a number of morphologically and functionally distinct cell populations, many of

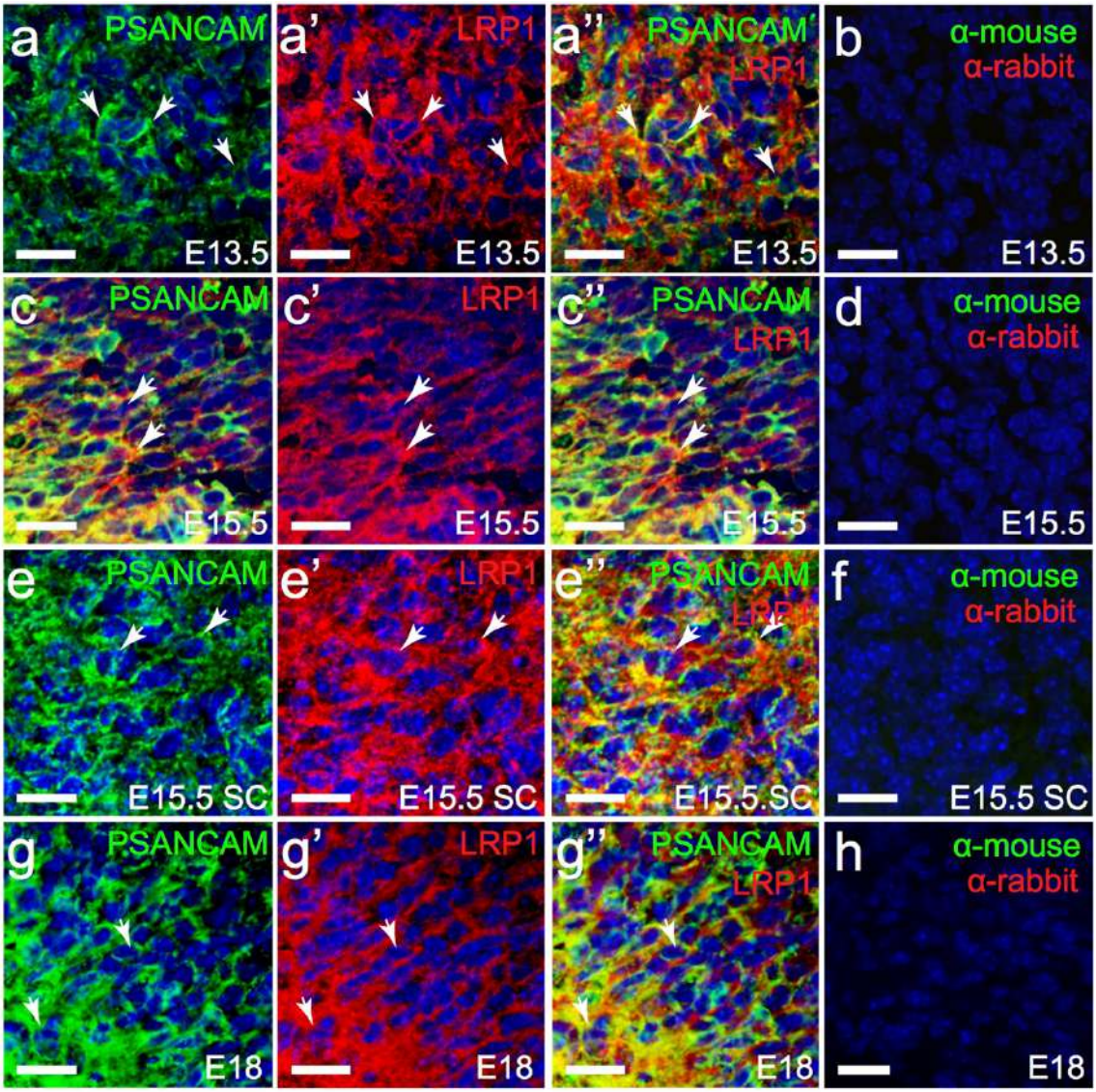

Figure 9: Neuroblasts express LRP1 in the embryonic brain and spinal cord

Coronal and transverse sections of embryonic brain (E13.5 **a**, E15.5 **c** and E18 **g**) and spinal cord (E15.5 **e**) were immunolabelled to detect neuroblasts (PSANCAM, green) and LRP1 (red). The nuclear marker Hoechst 33342 was used to label cell nuclei (blue). (**b**,**d**,**f**,**h**,**j**) secondary alone controls. White arrows represent cell bodies and yellow arrows represent co-localisation. Scale bar represents 17μm. SC= spinal cord

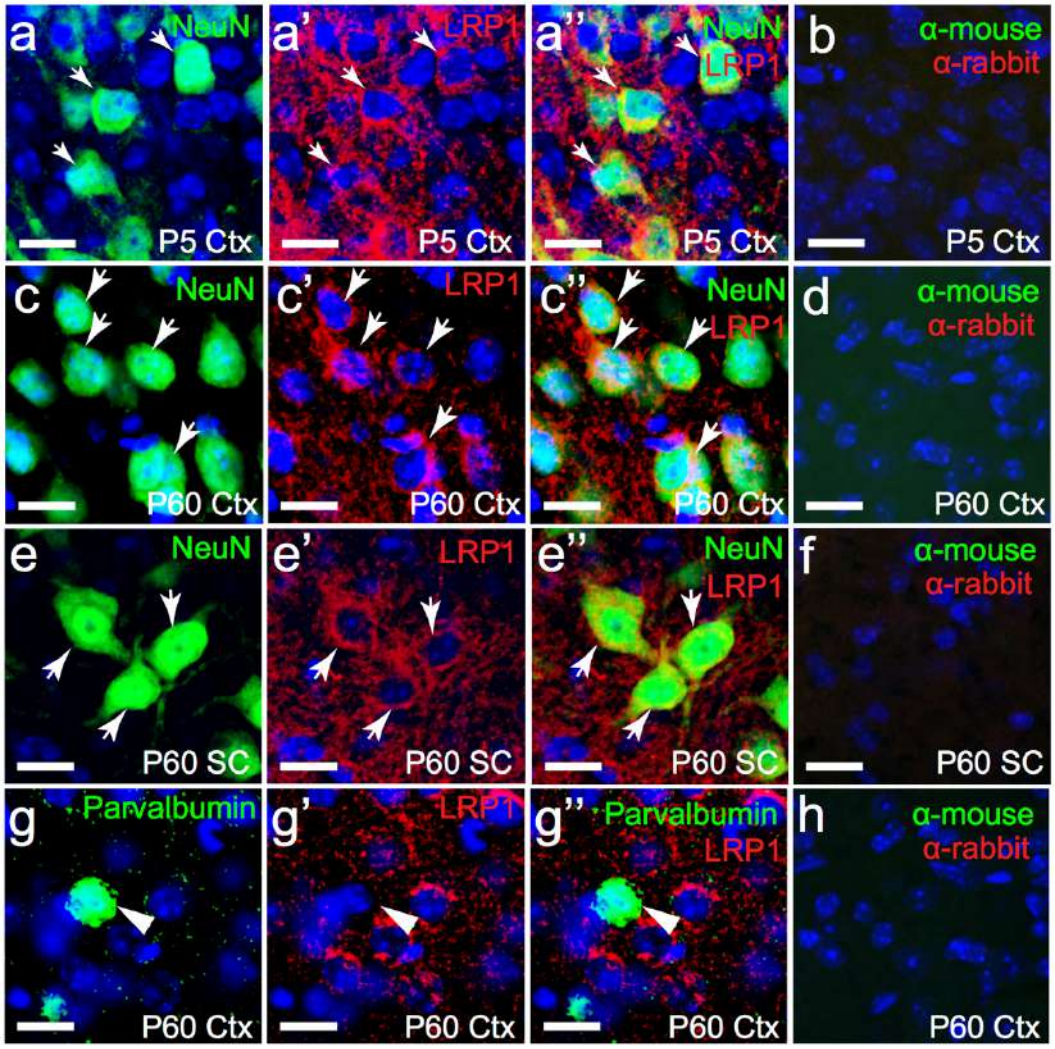

Figure 10: NeuN-positive neurons express LRP1, but not parvalbumin-positive interneurons

Coronal sections of early postnatal (P5, **a**) and adult (P60, **c**) brain and spinal cord (**e**) were immunolabelled to detect mature neurons (NeuN, green) and LRP1 (red), as well as a subpopulation of interneurons (parvalbumin, green, **e**). The nuclear marker Hoechst 33342 was used to label cell nuclei (blue). (**b**,**d**,**f**,**h**) secondary alone controls. White arrows represent cell bodies and yellow arrows represent co-localisation. Scale bar represents 17µm. Ctx= cortexand SC= spinal cord.

which do not express NeuN (Clarke et al., 2012). However, in the cortex a large proportion of interneurons, specifically the chandelier and basket cells, can be identified by their expression of the calcium binding protein parvalbumin (Kawaguchi and Kubota, 1987). To determine whether interneurons also express LRP1, we processed P60 mouse brain cryosections to detect LRP1 and parvalbumin (**Figure 10g**), and were surprised to find that only 3.02% ± 2.68% of parvalbumin^{+} interneurons expressed LRP1 (n=3 mice, avg ± std). These data indicate that LRP1 does not play a generic role in regulating neuron function in the CNS, and is not required for the normal functioning of parvalbumin-positive interneurons.

3.2.5 LRP1 is highly expressed by microglia in the CNS

Microglia are the resident immune cells of the CNS and act as the first line of defence against CNS damage. Following an event such as CNS injury or infection, microglia alter their morphology and function to a proinflammatory, phagocytic state which allows for the clearance of cellular debris and invading pathogens (Kim and de Vellis, 2005). *Lrp1* mRNA has been previously shown to be highly expressed in microglia (Cahoy et al., 2008; Zhang et al., 2014) and LRP1 has also been shown to be expressed by microglia *in vitro* (Jeon et al., 2012; Zhang et al., 2017). To determine whether microglia express LRP1 across development and during adulthood we performed immunohistochemistry on coronal mouse brain and transverse spinal cord cryosections to detect LRP1 (red) and the specific marker of activated microglia, Iba-1 (Ito D et al., 1998) (green) (**Figure 11**). Microglia were readily detected in the CNS at all ages, and strongly expressed LRP1 at E13.5 (**Figure 11a**), E15.5 (**Figure 11c**), E18 (**Figure 11e**), P5 (**Figure 11g, i**) and P60 (**Figure 11k, m**). Quantification of the proportion of microglia that express LRP1 revealed that ~96-98% of brain microglia expressed LRP1 at each age (**Figure 11o**). Microglia in the embryonic (**Figure 12a**) and postnatal (**Figure 12b**) spinal

Figure 11: Microglia in the brain stably express LRP1 throughout life

Coronal sections of embryonic (E13.5 **a,** E15.5 **c** and E18 **e**), early postnatal (P5, **g,i**) and adult (P60, **k,m**) brain were immunolabelled to detect microglia (Iba1, green) and LRP1 (red). The nuclear marker Hoechst 33342 was used to label cell nuclei (blue). (**o**) The percentage of $Iba1^{+}$ cells that also expressed LRP1 remained high across all time points examined. Results were compared using a one-way ANOVA with a Bonferroni's post-hoc test, expressed as means ± SEM and are representative of three independent experiments. (**b**,**d**,**f**,**h**,**j,l,n**) secondary alone controls. White arrows represent cell bodies and yellow arrows represent co- localisation. Scale bar represents 17µm. Ctx= cortex and CC= corpus callosum.

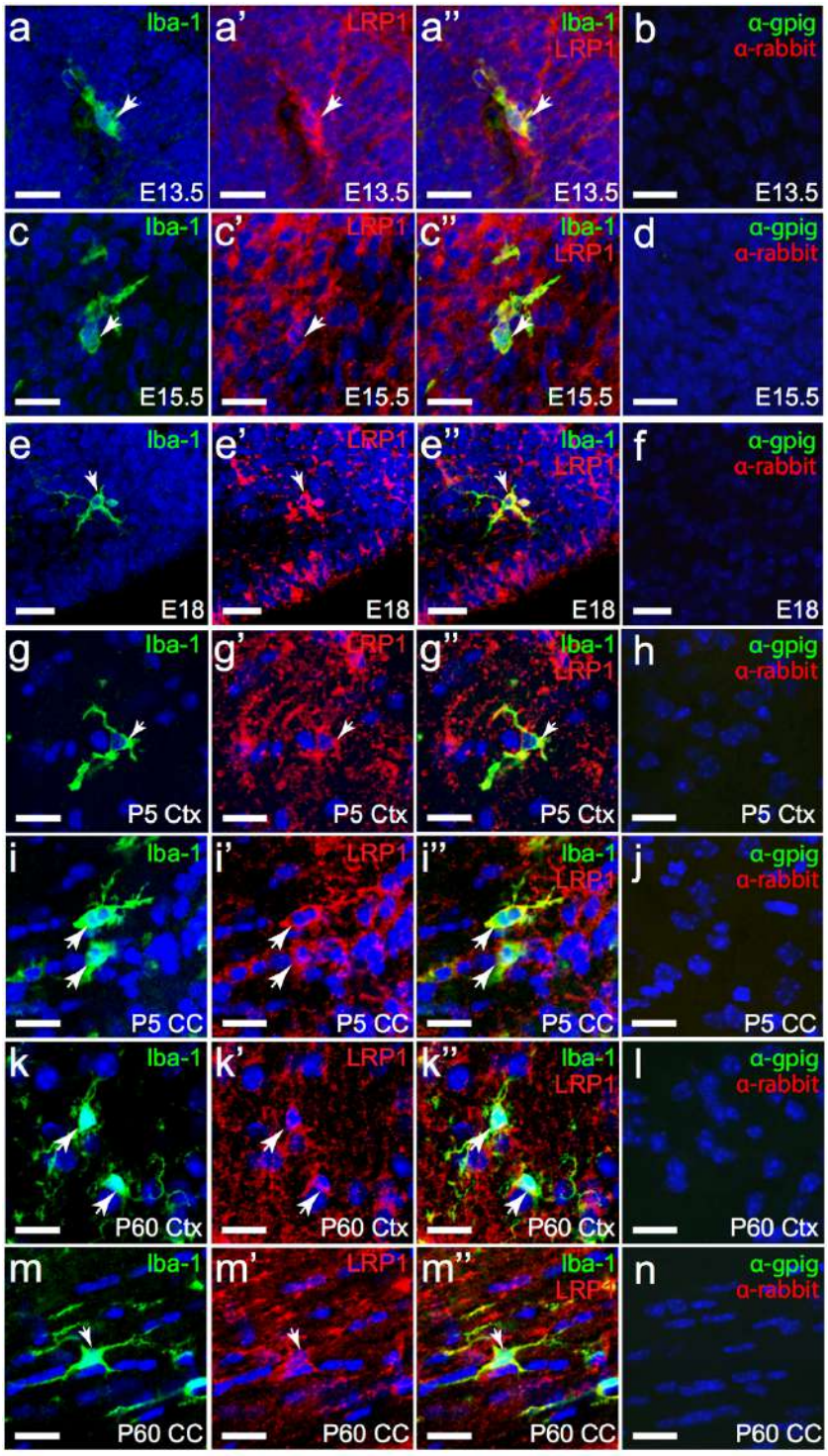
a
Iba-1
E13.5
a'
LRP1
E13.5
a''
Iba-1
LRP1
E13.5
b
α-gpig
α-rabbit
E13.5
c
Iba-1
E15.5
c'
LRP1
E15.5
c''
Iba-1
LRP1
E15.5
d
α-gpig
α-rabbit
E15.5
e
Iba-1
E18
e'
LRP1
E18
e''
Iba-1
LRP1
E18
f
α-gpig
α-rabbit
E18
g
Iba-1
P5 Ctx
g'
LRP1
P5 Ctx
g''
Iba-1
LRP1
P5 Ctx
h
α-gpig
α-rabbit
P5 Ctx
i
Iba-1
P5 CC
i'
LRP1
P5 CC
i''
Iba-1
LRP1
P5 CC
j
α-gpig
α-rabbit
P5 CC
k
Iba-1
P60 Ctx
k'
LRP1
P60 Ctx
k''
Iba-1
LRP1
P60 Ctx
l
α-gpig
α-rabbit
P60 Ctx
m
Iba-1
P60 CC
m'
LRP1
P60 CC
m''
Iba-1
LRP1
P60 CC
n
α-gpig
α-rabbit
P60 CC
O
100
50
0
% LRP1+ Iba1+ cells
E13.5
E15.5
E18
P60

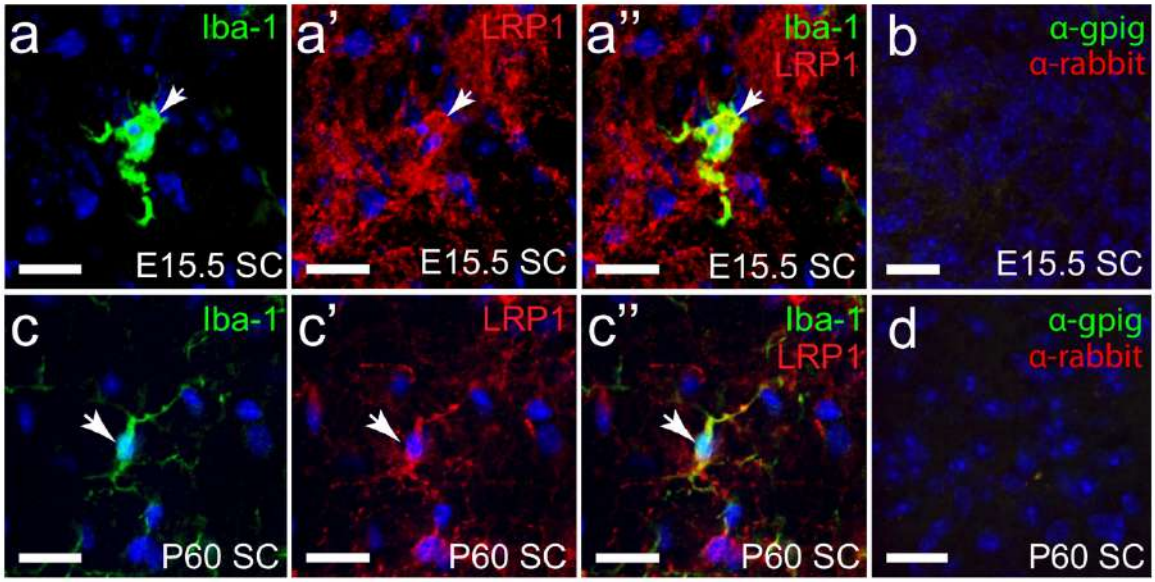

Figure 12: Microglia in the spinal cord express high levels of LRP1

Transverse sections of embryonic (E15.5, a) and adult (P60, c) spinal cord were immunolabelled to detect microglia (Iba1, green) and LRP1 (red). The nuclear marker Hoechst 33342 was used to label cell nuclei (blue). (b,d) secondary alone controls. White arrows represent cell bodies and yellow arrows represent co-localisation. Scale bar represents 17µm. SC= spinal cord

cord also expressed LRP1. In fact the proportion of microglia that express LRP1 in the brain and spinal cord was remarkably similar, with 98.66 ± 1.33% of microglia in the adult spinal cord labelling with anti-LRP1 (n=3 mice, avg ± std). These data demonstrate that microglia consistently express LRP1 throughout development.

3.2.6 LRP1 is expressed by OPCs, but not oligodendrocytes in the CNS

As their name suggests, oligodendrocyte progenitor cells (OPCs) are immature cells that give rise to the myelin-forming oligodendrocytes in the developing and adult CNS. In the mouse, the majority of oligodendrocytes are born in the first month following birth, however the life-long addition of new oligodendrocytes has been implicated in CNS repair as well as learning and memory [reviewed (Wang and Young, 2014)]. A recent RNA sequencing study indicated that *Lrp1* mRNA was highly expressed by OPCs, but not by oligodendrocytes (Zhang et al., 2014). However, the expression of LRP1 protein by OPCs or oligodendrocytes has never been reported.

To determine whether OPCs express LRP1 we processed cryosections to detect platelet-derived growth factor receptor α (PDGFRα; green), a protein uniquely expressed by OPCs within the CNS (Richardson et al,. 1988), and LRP1 (red) (**Figure 13**). By E15.5 a chain of PDGFRα$^+$ OPCs extended from the MGE to the developing cortex, and ~70% of them were found to express LRP1 (**Figure 13a, l**). By E18, OPCs had populated the entire CNS (Kessaris et al., 2005), and the proportion that labelled with anti-LRP1 increased to ~83% (**Figure 13c, l**). Furthermore, LRP1 expression was detected in the cell soma, and throughout the processes (**Figure 13c**). In the P5 mouse brain, ~98% of OPCs in the corpus callosum (**Figure 13e, l**) and ~99% of OPCs in the cortex (**Figure 13g, l**) labelled with anti-LRP1. Similarly, at P60, ~99% of OPCs expressed LRP1 in the corpus callosum (**Figure 13g)** and cortex (**Figure 13**i). The fraction of OPCs that expressed LRP1 was significantly less at E15.5 ($p<0.0001$) and E18 ($p<0.05$)

Figure 13: LRP1 is developmentally upregulated on OPCs

Coronal sections of embryonic (E15.5 **a** and E18 **c**), early postnatal (P5, **e,i**) and adult (P60, **k,m**) brain were immunolabelled to detect oligodendrocyte progenitor cells (Pdgfrα, green) and LRP1 (red). The nuclear marker Hoechst 33342 was used to label cell nuclei (blue). (**b**,**d**,**f**,**h**,**j**) secondary alone controls. (**k**) The percentage of OPCs that express LRP1 was significantly less in the embryonic brain. Results were compared using a one-way ANOVA with a Bonferroni's post-hoc test, expressed as means ± SEM and are representative of three independent experiments. *=P<0.05, ****=P<0.0001. Scale bar represents 17μm. CC= corpus callosum and Ctx= cortex.

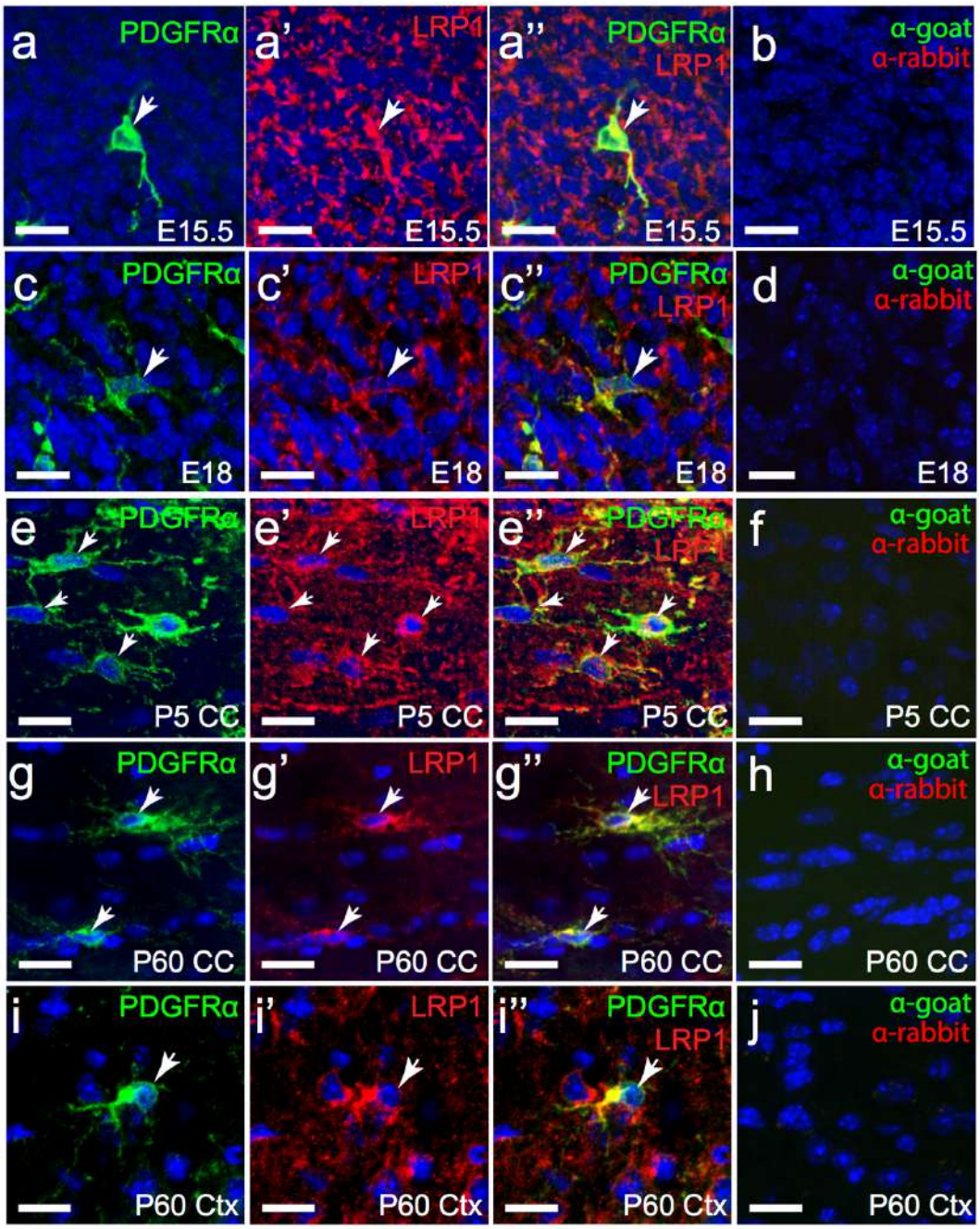
a
PDGFRα
E15.5
a'
LRP1
E15.5
a''
PDGFRα
LRP1
E15.5
b
α-goat
α-rabbit
E15.5
c
PDGFRα
E18
c'
LRP1
E18
c''
PDGFRα
LRP1
E18
d
α-goat
α-rabbit
E18
e
PDGFRα
P5 CC
e'
LRP1
P5 CC
e''
PDGFRα
LRP1
P5 CC
f
α-goat
α-rabbit
P5 CC
g
PDGFRα
P60 CC
g'
LRP1
P60 CC
g''
PDGFRα
LRP1
P60 CC
h
α-goat
α-rabbit
P60 CC
i
PDGFRα
P60 Ctx
i'
LRP1
P60 Ctx
i''
PDGFRα
LRP1
P60 Ctx
j
α-goat
α-rabbit
P60 Ctx

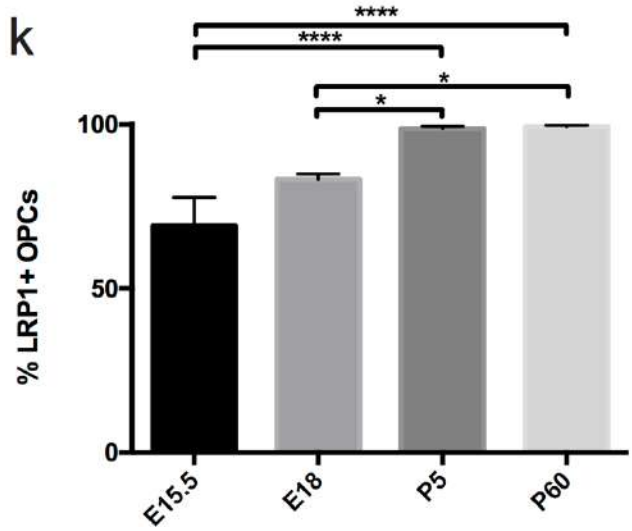
k
****
****
*
*
100
50
0
% LRP1+ OPCs
E15.5
E18
P5
P60

relative to both postnatal time points examined (**Figure 13k;** one-way ANOVA with Bonferroni). These differences may be due to the proportion of OPCs present from specific germinal zones at the time of analysis, for example at E15 OPCs derived from the MGE and AEP may not express LRP1, but as this population dies shortly after birth (Kessaris et al., 2005), the percentage of OPCs that express LRP1 increases. The proportion of OPCs that expressed LRP1 in the embryonic and postnatal brain, was mirrored in the spinal cord, with only 77.11% ± 0.72% of OPCs expressing LRP1 at E15.5 (n=3 mice, avg ± std; **Figure 14a**), but 100% ± 0% of spinal cord OPCs expressing LRP1 by adulthood (n=3 mice, avg ± std; **Figure 14c**). These data suggest that OPCs acquire LRP1 expression during development, but then retain this expression throughout postnatal life.

Individual OPCs appeared to express a high level of LRP1 protein by immunohistochemistry. To examine this directly, we determined the maximum pixel intensity for LRP1 at the microglia (236 ± 8.37 arbitrary units, mean ± SEM, n=19 cells), OPC (208 ± 12.24 arbitrary units, mean ± SEM, n=14 cells) and neuronal somas (125 ± 6.68 arbitrary units, mean ± SEM, n=14 cells) in the P60 mouse cortex. Microglia and OPCs expressed an equivalent level of LRP1, while $NeuN^+$ neurons expressed significantly less LRP1 than both of these cell types ($p<0.05$, Kruskal-Wallis).

When OPCs mature into oligodendrocytes they no longer express PDGFRα. Therefore, the OL-specific antibody CC1 (Bhat et al,. 1996), also known as APC, was used to label oligodendrocytes in the P60 mouse corpus callosum and spinal cord white matter (**Figure 15**). Oligodendrocytes in the corpus callosum assemble themselves in series, running parallel with the axons that traverse the two cerebral hemispheres. We found that 0.0% ± 0.0% of $CC1^+$ oligodendrocytes present in the corpus callosum were $LRP1^+$ (n=3 mice, avg ± std). Similarly,

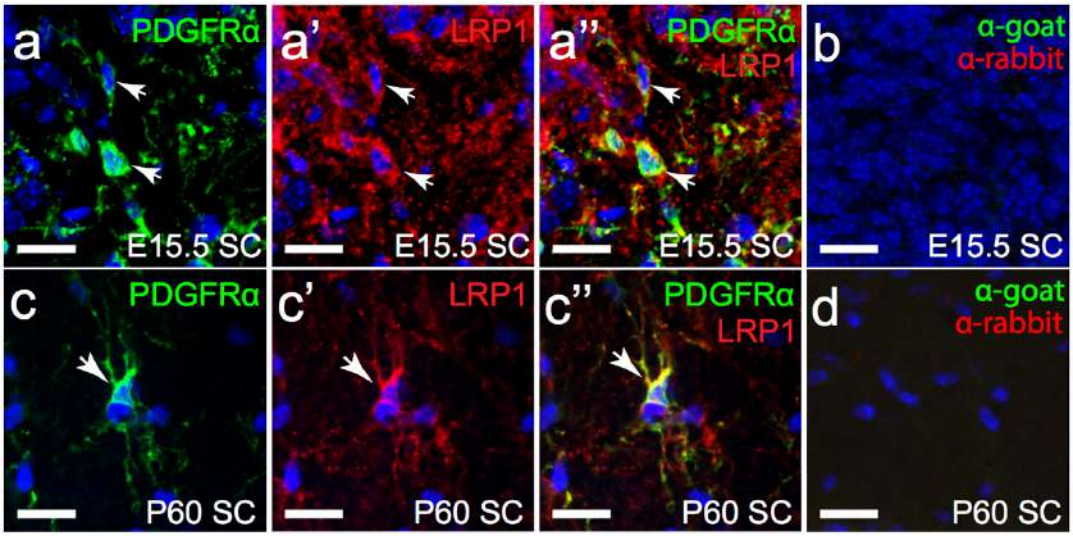

Figure 14: OPCs in the spinal cord express LRP1 in the cell body and processes

Transverse sections of embryonic (E15.5, **a**) and adult (P60, **c**) spinal cord were immunolabelled to detect oligodendrocyte progenitor cells (Pdgfrα, green) and LRP1 (red). The nuclear marker Hoechst 33342 was used to label cell nuclei (blue). (**b**,**d**) secondary alone controls. White arrows represent cell bodies and yellow arrows represent co-localisation. Scale bar represents 17µm. SC= spinal cord.

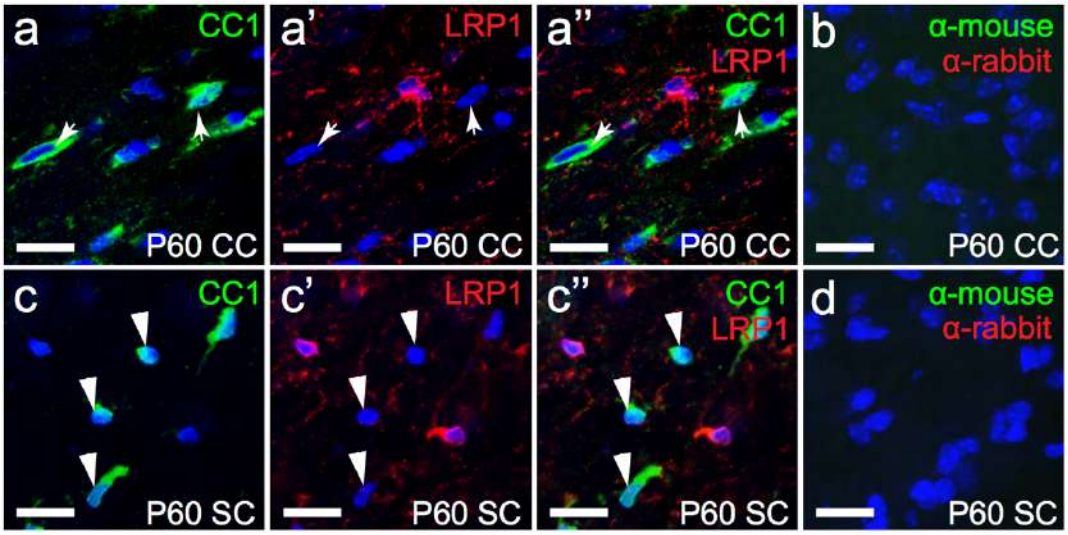

Figure 15: Oligodendrocytes do not express LRP1

Coronal and transverse sections of adult (P60) brain (**a**) and spinal cord (**c**) were immunolabelled to detect oligodendrocytes (CC1, green) and LRP1 (red). The nuclear marker Hoechst 33342 was used to label cell nuclei (blue). (**b**,**d**) secondary alone controls. White arrows represent cell bodies and yellow arrows represent co-localisation. Scale bar represents 17µm. CC=corpus callosum and SC= spinal cord.

none of $CC1^+$ cells in the spinal cord expressed LRP1 (122 cells counted). These data indicate that oligodendrocytes do not require LRP1 for their CNS function.

3.2.7 Newly formed oligodendrocytes do not express LRP1

Given that OPCs highly expressed LRP1, but oligodendrocytes did not, we wanted to determine the point in oligodendrocyte maturation when LRP1 was down-regulated. RNA sequencing data suggest that *Lrp1* mRNA is expressed by OPCs, but is still present, albeit at a lower level, in newly formed oligodendrocytes (Zhang et al., 2014). To look at this more closely we performed cre-lox transgenic lineage tracing of OPCs in adulthood. *Pdgfra-CreER^{T2} :: Rosa26-YFP* mice were given tamoxifen at P57 to turn on YFP expression in PDGFRα^+ OPCs. Mice were perfusion fixed one week later and coronal brain sections processed to detect YFP, LRP1 and either PDGFRα or CC1. As expected, we found that YFP^+ PDGFRα^+ OPCs in the corpus callosum had given rise to YFP^+ PDGFRα-negative newborn oligodendrocytes in the one week tracing period (Rivers et al., 2008; Kang et al., 2010b). Consistent with our earlier data, all YFP^+ PDGFRα^+ OPCs expressed LRP1 (**Figure 16a**, 100% ± 0%, n=3 mice) and all YFP^+ $CC1^+$ oligodendrocytes did not express LRP1 (**Figure 16b**, 0% ± 0%; avg ± std, n=3 mice). Furthermore, all YFP^+ PDGFRα-negative newborn oligodendrocytes were LRP1-negative (**Figure 16c**). Therefore LRP1 protein expression is not retained by any new YFP-labelled oligodendrocytes, even in a population that would comprise both premyelinating and myelinating cells. These data strongly indicate that LRP1 is rapidly down-regulated alongside PDGFRα at the onset of differentiation and is not retained beyond the progenitor stage in the oligodendrocyte lineage.

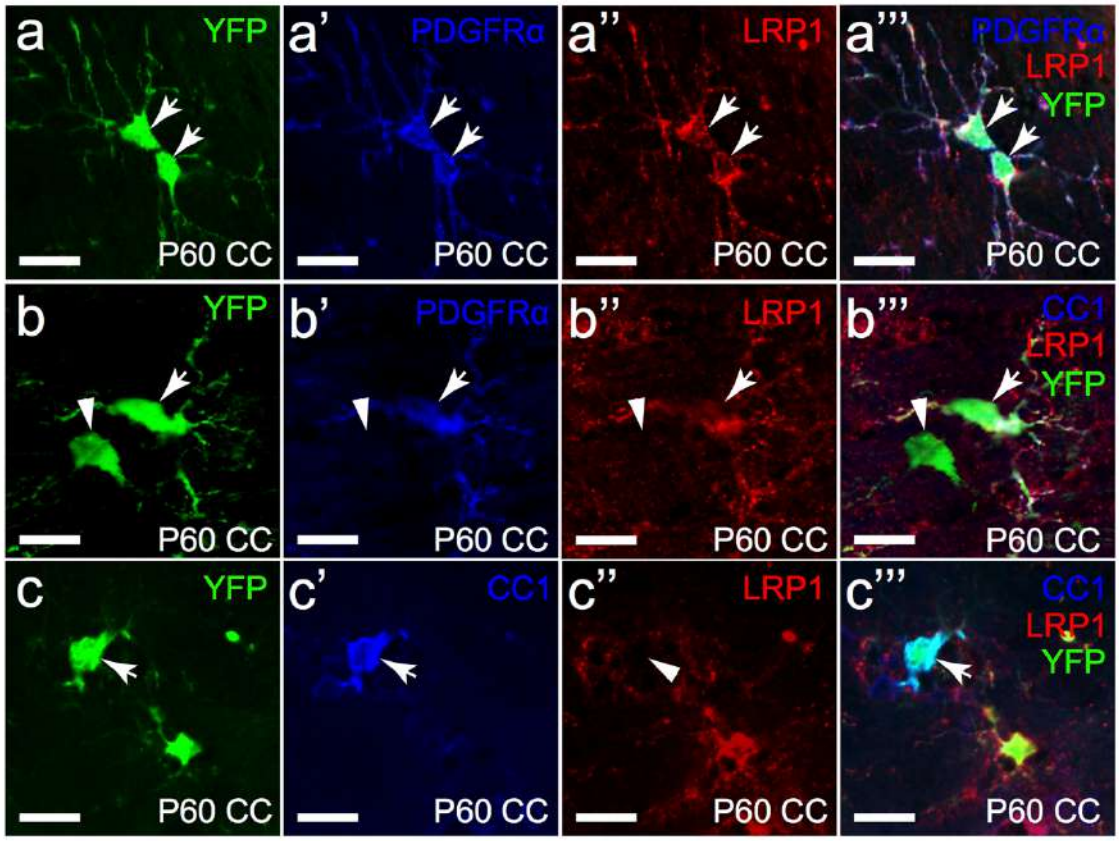

Figure 16. Newly formed oligodendrocytes do not express LRP1.

Tamoxifen was administered to Pdgfra-CreER^{T2}:: Rosa26-YFP transgenic mice at P57 to label OPCs and trace them as they generate new oligodendrocytes until P64. Single scan confocal images were collected through the corpus callosum (CC) following immunolabelling with YFP (green), LRP1 (red) and either PDGFRα or CC1 (blue). a-a''' YFP^{+}, PDGFRα^{+} cells were also LRP1^{+}. b-b''' YFP^{+}, PDGFRα-negative cells were also negative for LRP1. c-c''' YFP^{+} CC1^{+} cells were found to be LRP1-negative. White arrows indicate regions of co-localisation. Arrowheads indicate oligodendrocyte cell bodies, which do not express LRP1. Scale bars represent 17µm. CC = corpus callosum.

3.3 Discussion

Our data indicate that LRP1 protein is present in the brain of embryonic, early postnatal and adult mice. Specifically, LRP1 is expressed by radial glia, immature and mature neurons, excluding parvalbumin-positive interneurons, and is also expressed by microglia, astrocytes and OPCs, but not newly formed and mature oligodendrocytes. These data are largely consistent with previously published microarray and RNA sequencing studies comparing the expression of *Lrp1* mRNA by neurons, microglia, astrocytes and oligodendrocyte-lineage cells (Cahoy et al., 2008; Zhang et al., 2014) with the exception of newly formed oligodendrocytes. The absence of LRP1 expression from oligodendrocytes may also contribute to the overall decrease in LRP1 expression detected in the brain between P5 and P60. Oligodendrocytes are largely generated after P5 in the mouse, and while this is unlikely to be the sole explanation, it would certainly be a contributing factor.

3.3.1 Neuronal populations differentially express LRP1 in the mature CNS

Given that LRP1 has been implicated in neuronal development (Landowski et al., 2016), it is not surprising that we observed a high level of LRP1 expression in immature neurons in the embryonic CNS. However by the time the neurons matured into $NeuN^+$ or $parvalbumin^+$ neurons there was a clear divergence in LRP1 expression, with $NeuN^+$ neurons expressing LRP1 while $parvalbumin^+$ neurons did not. Parvalbumin-positive interneurons comprise approximately 40% of interneurons in the mature mouse cortex (Rudy et al., 2010), and include interneuron subtypes such as basket and chandelier cells (Kawaguchi and Kubota, 1997). While this is the first study to examine the expression of LRP1 in parvalbumin-positive interneurons, a previous study did report LRP1 expression in somatostatin-positive interneurons in the hippocampus and parietal cortex (Van Uden et al., 1999). Somatostatin-positive interneurons comprise approximately 30% of interneurons in the mature mouse

cortex (Rudy et al., 2010), and are made up predominately of Martinotti cells as well as a small number of X94 cells (Kawaguchi and Kubota, 1997; Ma, 2006). We hypothesised that LRP1 may be expressed by somatostatin$^+$ but not parvalbumin$^+$ interneurons, due to their distinct developmental origins. Parvalbumin-positive interneurons arise from *Nkx2.1*-expressing precursors in the MGE, while the somatostatin-positive interneurons arise from the *Nkx6.2* expressing precursors in the dorsal MGE (Butt et al., 2005; Fogarty et al., 2007). However this is unlikely to be the reason why parvalbumin$^+$ interneurons do not express LRP1, as neuroblasts arising from the MGE at each embryonic stage examined, were LRP1-positive. Therefore, these neurons must downregulate LRP1 upon differentiation, suggesting instead that parvalbumin$^+$ interneurons do not require LRP1 for their function.

We report that LRP1 is consistently expressed by NeuN-positive neurons throughout the cortex and spinal cord. These data are consistent with previous studies reporting that LRP1 expression is particularly pronounced in the cell body and proximal processes of cortical and CA1 pyramidal neurons (Wolf et al., 1992; Bu et al., 1994; May et al., 2004), which are neuronal populations known to express NeuN. While this study does not examine the functional role of LRP1 in these neuronal populations, the conditional deletion of *Lrp1* from forebrain neurons *in vivo* previously revealed that LRP1 is important for synapse maintenance, as its absence resulted in synaptic loss and neurodegeneration. This was largely attributed to impaired lipid metabolism (Liu et al., 2007; 2010). However *in vitro* studies also indicate that LRP1 interacts with post-synaptic receptors, and can thereby regulate synaptic function (Maier et al., 2013; Nakajima et al., 2013; Gan et al., 2014).

3.3.2 LRP1 as a critical regulator of microglia in the CNS

The consistent and high level of LRP1 expression that we observed in microglia at all ages examined, points to this receptor playing an important role in this cell type across the life-

span. Previous studies have shown that LRP1 is expressed in primary microglial cultures derived from rats (Marzolo et al., 2000) and mice (Pocivavsek et al., 2009). However, what could be the function of LRP1 in regulating microglial function? *In vitro*, the transition of microglia from a "resting" or surveillance state to an "activated" or pro-inflammatory state can be triggered by activation of LRP1 by one of its ligands, tissue plasminogen activator (tPA), and this same ligand was found to promote the migration of microglia-like BV-2 cells (Jeon et al., 2012). *In vivo*, when *Lrp1* was conditionally ablated from microglia, the cells were less responsive to cerebral ischemia (Zhang et al., 2017). However regulating activation and migration may not be the only microglial functions regulated by LRP1, as the knockdown of Lrp1 *in vitro*, using siRNA, reduced their phagocytic capacity, decreasing their internalisation of amyloid β (N'songo et al., 2013). These data indicate that LRP1 may be important for the initial activation of microglia, followed by migration to the site of injury and the subsequent clearing of cellular debris or foreign pathogens. However how LRP1 differentially regulates these functions is far from understood.

3.3.4 What is the function of LRP1 in astrocytes?

LRP1 expression was observed in astrocytes at each postnatal age examined. These data are consistent with previous findings that demonstrated LRP1 is expressed by human cerebral and cerebellar astrocytes (Moestrup et al., 1992) , rat astrocytes (Bu et al., 1994) and mouse primary astrocyte cultures (Marzolo et al., 2000). *Lrp1* mRNA has also been shown to be present in mouse astrocytes (Zhang et al., 2014). The role that LRP1 plays in regulating astrocytic function has not been extensively studied. However one potential function is that LRP1 regulates the availability of its ligand, tissue plasminogen activator, at the synapse by facilitating clathrin dependant endocytosis (Casse et al., 2012). Additionally, LRP1 is expressed by perivascular astrocytes, and may be involved in the regulation of blood brain barrier

permeability in the early stages of cerebral ischemia (Samson et al., 2008). Given the diverse range of functions that astrocytes perform, and the high level of LRP1 that we detect in these cells, further investigation into the function of LRP1 in this cell type would be warranted.

3.3.5 What is the function of LRP1 in OPCs?

Our data raise a number of questions relating to the role played by LRP1 in regulating the behaviour of OPCs. A previous study examining cultured neurospheres found that upon differentiation, cultures that lacked *Lrp1* produced significantly fewer oligodendrocytes compared to control neurospheres (Hennen et al., 2013). The authors suggested that these data reflected a critical role for LRP1 in regulating the generation of OPCs from neural stem cells. However, an equally plausible explanation could be that LRP1 is required for the expansion of OPCs or their differentiation into oligodendrocytes.

OPCs are continuously producing new oligodendrocytes throughout life (Dimou et al., 2008; Rivers et al., 2008; Kang et al., 2010b; Zhu et al., 2011; Young et al., 2013), and in young adult mice, the rate of oligodendrogenesis is still remarkably high (Rivers et al., 2008). By tracing the fate of OPCs using a transgenic reporter mouse, we were able to selectively identify newborn oligodendrocytes that were born during the one week tracing period. We found that the YFP-labelled newborn oligodendrocytes (PDGFRα-negative cells) were devoid of LRP1 expression. Furthermore, no $CC1^+$ oligodendrocytes expressed LRP1. Our observation that newly formed oligodendrocytes did not express LRP1 was surprising due to the moderately high *Lrp1* mRNA levels identified by RNA sequencing (Zhang et al., 2014), and indicate that the mRNA levels do not necessarily correlate with protein abundance [reviewed (Vogel and Marcotte, 2012)]. The rapid down-regulation of LRP1 following OPC differentiation demonstrates that LRP1 is only necessary for normal function in OPCs, and that its expression is not required for oligodendrocyte maturation. Given that LRP1 expression in OPCs appears

to co-localise strongly with PDGFRα (**Figure 16 a'-a''**), it is possible that these receptors form a signalling complex and the loss of PDGFRα is accompanied by a down-regulation in LRP1 expression. There is some foundation for speculating that LRP1 may interact with PDGFRα, as it has been previously shown to interact with the related PDGFRβ in fibroblasts cell lines (Newton et al., 2005; Takayama et al., 2005; Craig et al., 2013). However the role of LRP1 in OPCs has not yet been investigated.

Conclusions

LRP1 protein is present in the brain of embryonic, early postnatal and adult mice. On a cellular level, LRP1 is highly expressed by some glial and neuronal cell populations. In particular, LRP1 is expressed by radial glia, immature and mature neurons (excluding parvalbumin-positive interneurons), microglia, astrocytes and OPCs. However, LRP1 is down-regulated early in OPC differentiation, as LRP1 is not expressed by newly formed or mature oligodendrocytes. Overall, these data indicate that CNS glia are highly susceptible to LRP1 signalling, a possibility that has been largely unexplored to date.

Chapter 4 - LRP1 is a negative regulator of oligodendrocyte progenitor cell differentiation in the adult mouse brain

4.1 Introduction

Oligodendrocytes myelinate the central nervous system (CNS) to facilitate the rapid and reliable propagation of action potentials along axons, and to provide axons with essential metabolic support [reviewed by (Philips and Rothstein, 2017)]. While the majority of OLs are produced during development, new OLs are continuously produced from oligodendrocyte progenitor cells (OPCs) (Dimou et al., 2008; Rivers et al., 2008; Zhu et al., 2008; Kang et al., 2010a; Hughes et al., 2013; Young et al., 2013; Hill et al., 2018), and add myelin internodes to the CNS throughout life (Hill et al., 2018; Hughes et al., 2018). A number of signalling pathways have been identified that regulate different aspects of developmental and adult OPC behaviour, and oligodendrogenesis, including pathways involving Notch1 (Genoud et al., 2002; Givogri et al., 2002; Zhang et al., 2009), fibroblast growth factor 2 (Murtie et al., 2005; Zhou et al., 2006; Murcia-Belmonte et al., 2014), mammalian target of rapamycin (Zou et al., 2014; Jiang et al., 2016; Grier et al., 2017) and platelet-derived growth factor A (McKinnon, 2005; Rajasekharan, 2008; Chew et al., 2010). However, microarray (Cahoy et al., 2008) and RNA sequencing (Zhang et al., 2014; Hrvatin et al., 2018) experiments have uncovered a number of mRNA transcripts that are differentially expressed across oligodendrocyte

development, but have no known regulatory function in this lineage. One such gene is the *low-density lipoprotein receptor related protein 1* (*Lrp1*).

LRP1, also known as CD91, or the α2 macroglobulin receptor (α2MR), is highly expressed by OPCs, and is rapidly downregulated with OL differentiation (Auderset et al., 2016a). This large cell surface receptor, comprising a 515kDa extracellular α-chain and an 85kDa β-chain, can interact with a large variety of ligands, as well as extracellular and intracellular proteins (reviewed by (Bres and Faissner, 2019). Consequently, LRP1 can signal in a variety of ways including ligand endocytosis and processing (Cam et al., 2005; Parkyn et al., 2008; Liu et al., 2017; Van Gool et al., 2019), receptor trafficking (Parkyn et al., 2008; Maier et al., 2013; Kadurin et al., 2017) and cleavage and formation of a soluble product (May, 2002b; Liu et al., 2009; Brifault et al., 2017; 2019). *Lrp1* knockout is embryonic lethal due to a failure in blastocyst implantation (Herz et al., 1992) and the conditional deletion of *Lrp1* from cultured mouse neural stem and progenitor cells (NSPCs) has been shown to impair NSPC proliferation and reduce the number of oligodendrocyte lineage cells they produce (Hennen et al., 2013; Safina et al., 2016). Furthermore, the conditional deletion of *Lrp1* from *Olig2*$^{+}$ cells in development (*Olig2-Cre :: Lrp1*$^{fl/fl}$ mice) impairs oligodendrogenesis and myelination in the optic nerve by postnatal day 21 (Lin et al., 2017).

OPC physiology changes considerably between development and adulthood and can also differ between CNS regions (Velez-Fort et al., 2010; Pitman et al., 2020; Spitzer et al., 2019). Therefore, to explore the potential role that LRP1 plays in adult OPCs, we employed a conditional gene deletion approach to evaluate the capacity for LRP1 to regulate OPC behaviour and oligodendrogenesis in the adult mouse brain. We report that LRP1 is a negative regulator of OPC differentiation in the healthy CNS and that *Lrp1* deletion prior to cuprizone induced demyelination results in smaller lesions.

4.2 Results

4.2.1 LRP1 can be successfully deleted from OPCs in the adult mouse brain

In order to determine the role that LRP1 plays in regulating adult myelination, *Lrp1* was conditionally deleted from OPCs in young adult mice. Tamoxifen was administered to P50 control (*Lrp1*$^{fl/fl}$) and *Lrp1*-deleted (*Pdgfrα-CreER*^{TM} *:: Lrp1*$^{fl/fl}$) mice and brain tissue examined 7 or 30 days later (at P50+7 and P50+30, respectively). Coronal brain cryosections from control (**Fig. 17a**) and *Lrp1*-deleted mice (**Fig. 17b**) were immunolabelled to detect LRP1 (red) and OPCs (PDGFRα, green). Consistent with Auderset et al. (2016), essentially all OPCs in the corpus callosum of control mice expressed LRP1 (**Fig. 17c**: P50+7, 99% ± 0.6%; P50+30, 99.7% ± 0.3%). However, in the corpus callosum of P50+7 *Lrp1*-deleted mice, only 2% ± 0.8% of PDGFRα^{+} OPCs expressed LRP1, and at P50+30, only 0.5% ± 0.5 of OPCs expressed LRP1 (**Fig. 17c**), confirming the successful deletion of *Lrp1* from adult OPCs. Similar results were found in the motor cortex at P50+7, with 100% ± 0% of PDGFRα^{+} also expressing LRP1 in control mice, while only 0.4% ± 0.4% of PDGFRα^{+} cells in the *Lrp1* deleted mice expressed LRP1. Deletion of the extracellular portion of the *Lrp1* gene was also confirmed by PCR, as gene deletion enabled the amplification of a recombination-specific DNA product from genomic DNA extracted from *Lrp1*-deleted brain tissue that was not amplified from control mouse genomic DNA (**Fig. 17d**).

4.2.2 *Lrp1*-deletion increases adult OPC proliferation

OPCs divide more frequently in white matter than grey matter regions of the adult mouse CNS (Psachoulia et al., 2009), and it has been reported that adult OPCs divide to self-renew, ensuring the homeostatic maintenance of a stable pool of cells (Hughes et al., 2013). To determine whether LRP1 regulates the rate at which OPCs enter the cell cycle, or the fraction

Figure 17: LRP1 can be deleted from the vast majority of OPCs

Coronal brain sections from P57+7 and P57+30 control (*Pdgfrα-CreER^{TM}) and Lrp1*-deleted *(Pdgfrα-CreER^{TM} :: Lrp1$^{fl/fl}$*) mice were immunolabelled to detect OPCs (PDGFRα, green) and LRP1 (red). (**a**) Confocal image of LRP1^{+} OPCs in the corpus callosum (CC) of a P50+7 control mouse (yellow arrow heads). (**b**) Confocal image of LRP1-neg OPCs in the CC of a P50+7 *Lrp1*-deleted mouse (white arrow heads). (**c**) The proportion (%) of PDGFRα^{+} OPCs that express LRP1 in P50+7 and P50+30 control and *Lrp1*-deleted mice (n=3-4 mice per genotype per time-point; [2-way ANOVA *genotype F (1,10)=2.8, p = <0.0001; days post tamoxifen (F 1,10) =0.52, p = 0.5; interaction F(1, 10)= 3.44, p = 0.09]* with Bonferroni multiple comparisons, **** p ≤ 0.0001). (**d**) PCR amplification of genomic DNA from the brain of P50+7 control (*Pdgfrα-CreER^{TM}*) and *Lrp1$^{fl/fl}$* (*Pdgfrα-CreER^{TM} :: Lrp1$^{fl/fl}$*) mice indicates that recombination (producing the *Lrp1* reco band) only occurs in *Lrp1$^{fl/fl}$* mice. The nuclear marker Hoescht 33342 was used to label cell nuclei. Scale bar represents 17μm. CC = corpus callosum

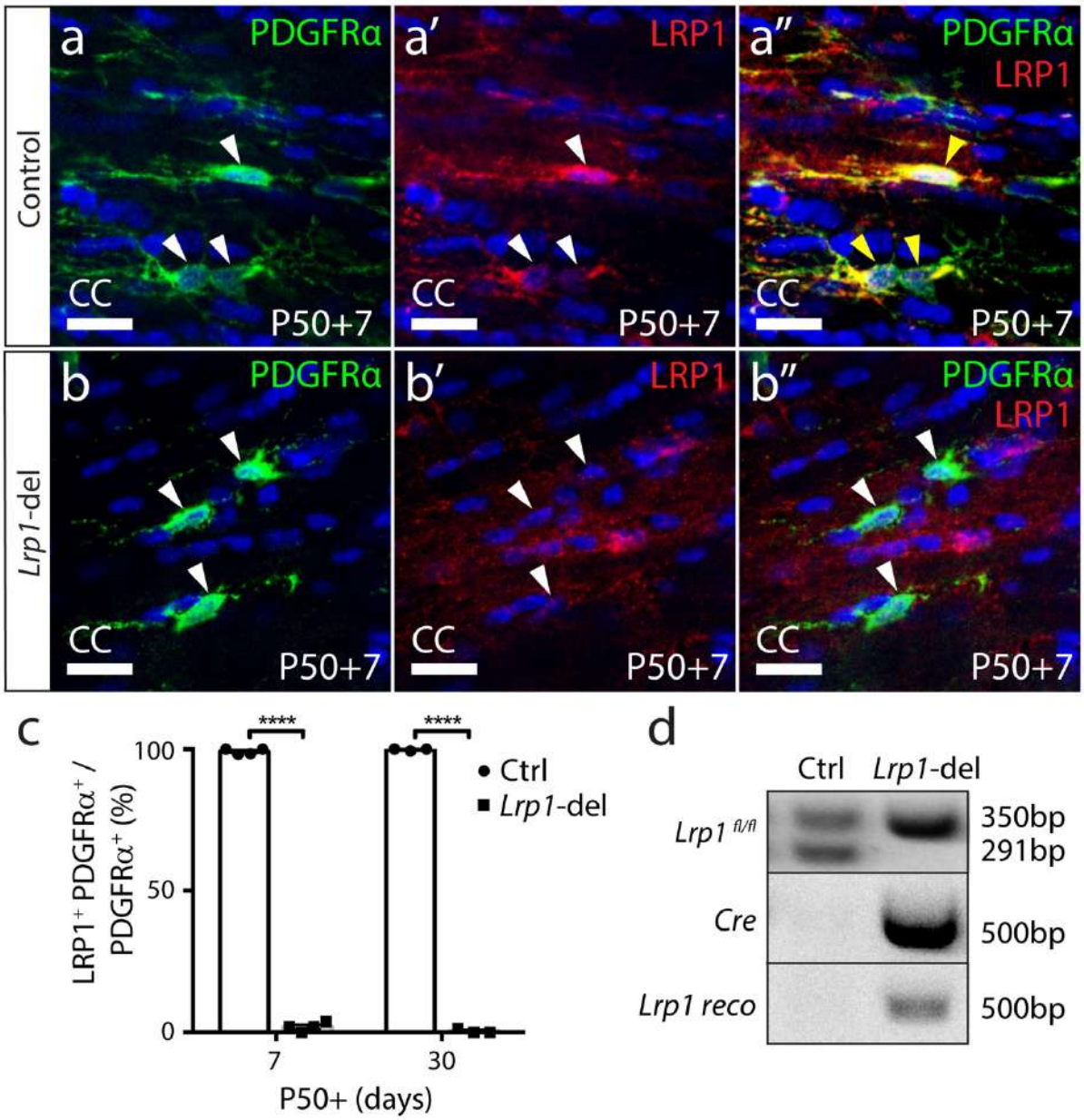
Control
Lrp1-del
a
PDGFRα
a′
LRP1
a″
PDGFRα
LRP1
b
PDGFRα
b′
LRP1
b″
PDGFRα
LRP1
CC
P50+7
c
LRP1+ PDGFRα+ / PDGFRα+ (%)
100
50
0
****
****
Ctrl
Lrp1-del
7
30
P50+ (days)
d
Ctrl
Lrp1-del
Lrp1 fl/fl
350bp
291bp
Cre
500bp
Lrp1 reco
500bp

of OPCs that proliferate, we delivered a thymidine analogue, EdU, to P57+7 control and *Lrp1*-deleted mice, via the drinking water, for 2, 4, 6 or 20 days. Coronal brain cryosections from control (**Fig. 18a-d**) and *Lrp1*-deleted (**Fig. 18e-h**) mice were processed to detect PDGFRα$^+$ OPCs (green) and EdU (red). When quantifying the proportion of OPCs that became EdU labelled over time, we found that 20 days of EdU-delivery resulted in EdU uptake by all OPCs in the corpus callosum of control and *Lrp1*-deleted mice (100% ± 0% and 100% ± 0% respectively; **Fig. 18d, h**), indicating that the proportion of OPCs that can proliferate is not influenced by LRP1 signalling. Furthermore, the rate of EdU incorporation by OPCs was equivalent in the corpus callosum of control or *Lrp1*-deleted mice (**Fig. 18i**), suggesting that LRP1 does not influence the rate at which OPCs enter the cell cycle and become labelled. While OPCs in the motor cortex entered the cell cycle less frequently than those in the corpus callosum i.e. EdU labelling occurred at a slower rate (compare the slope of the regression lines in **Fig. 18i** and **Fig. 18j**), OPC proliferation in the motor cortex was also not affected by *Lrp1*-deletion (**Fig. 18j**).

While these data indicate that LRP1 does not influence OPC proliferation immediately after deletion, one potential function of LRP1 can be the delivery or removal of signalling receptors and channels to the cell membrane (Takayama et al., 2005; Liu et al., 2010; Pi et al., 2012; Maier et al., 2013; Nakajima et al., 2013) - a function that, if disrupted, may take time to have adverse effects on OPC behaviour. To explore this possibility, we delivered tamoxifen to young adult (P57) control and *Lrp1*-deleted mice and waited a further 28 days before administering EdU via the drinking water for 4 consecutive days. Coronal brain cryosections were collected from P57+32 control (**Fig. 18k**) and *Lrp1*-deleted (**Fig. 18l**) mice and processed to detect PDGFRα$^+$ OPCs (green) and EdU (red). The proportion of OPCs that incorporated EdU over the 4-day labelling period was significantly higher in the corpus callosum of *Lrp1*-deleted mice than controls (**Fig. 18m**). This increase in OPC proliferation was not accompanied

Figure 18: *Lrp1* deletion leads to a delayed change in OPC proliferation

Coronal brain sections from control (*Pdgfrα-CreER^{TM}*) and *Lrp1* deleted mice (*Pdgfrα-CreER^{TM}:: Lrp1$^{fl/fl}$)* were immunolabelled to detect OPCs (PDGFRα, green) and EdU (red). (**a-h**) Confocal images showing EdU labelled OPCs in the corpus callosum after 2,4,6 and 20 days of EdU exposure. Graphical representation of the rate of EdU incorporation into OPCs in the corpus callosum (**i,** p=0.7, n= minimum of 3 mice per timepoint; m= 9.2 ± 1.80 and R^2 = 0.71 for control and m= 10.2 ± 1.77 and R^2 = 0.81 for *Lrp1*-del) and motor cortex (**j** p=0.3 ,n= minimum of 3 mice per timepoint; m= 2.9 ± 0.26 and R^2 = 0.92 for control and m= 3.4 ± 0.32 and R^2 = 0.88 for *Lrp1*-del). Coronal brain sections from control (**k**,*Pdgfrα-CreER^{TM}*) and *Lrp1*-deleted (**l**,*Pdgfrα-CreER^{TM}:: Lrp1$^{fl/fl}$*) mice that received EdU via the drinking water for 4 consecutive days (from P57+28) were immunolabelled to detect OPCs (PDGFRα, green) and EdU (red). (**m**) graphical representation showing the percentage of EdU$^+$ OPCs in the corpus callosum (mean ±SD, n=3 mice per genotype; unpaired t-test, p=0.008). (**n**) Quantification of the density of OPCs in the CC of P57+28 control and *Lrp1$^{fl/fl}$* mice (mean ±SD, n=3 mice per genotype; unpaired t-test, p= 0.6). Scale bar represents 17μm (a-h) and 70μm (k,l) White arrow heads indicate EdU-neg OPCs, yellow arrowheads indicate EdU$^+$ OPCs. CC= corpus callosum.

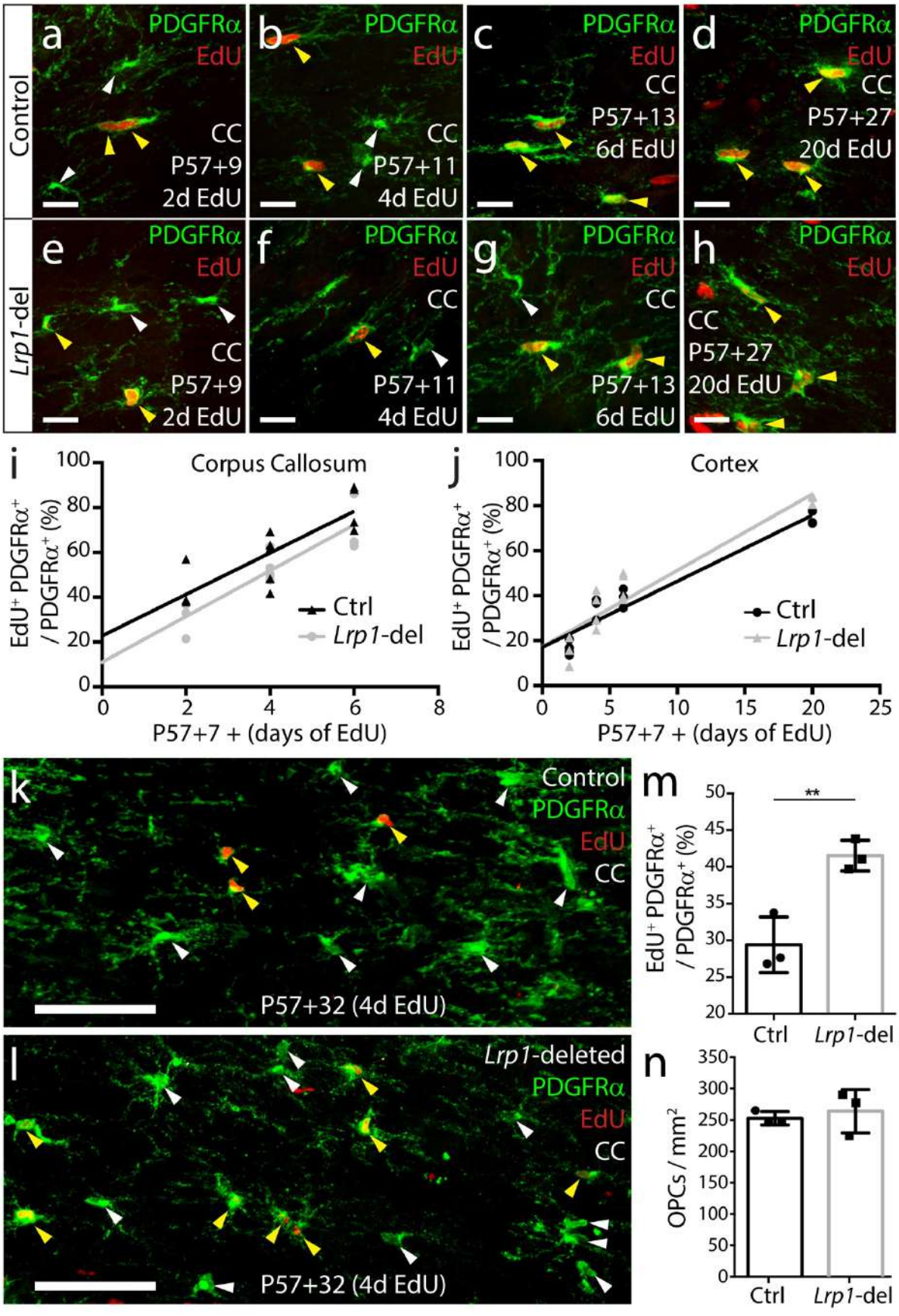
Control
Lrp1-del
a
b
c
d
e
f
g
h
PDGFRα
EdU
CC
P57+9
2d EdU
P57+11
4d EdU
P57+13
6d EdU
P57+27
20d EdU
i
Corpus Callosum
j
Cortex
EdU+ PDGFRα+ / PDGFRα+ (%)
P57+7 + (days of EdU)
Ctrl
Lrp1-del
k
l
Control
Lrp1-deleted
P57+32 (4d EdU)
m
n
**
OPCs / mm2

by a change in the density of PDGFRα^+ OPCs, which was equivalent in the corpus callosum of control and *Lrp1*-deleted mice (**Fig. 18n**). These data suggest that *Lrp1* deletion from adult OPCs results in a delayed increase in OPC proliferation, that must be accompanied by an increase in new OL generation i.e. OPC differentiation, or an increase in the number of newborn cells that die.

4.2.3 LRP1 is a negative regulator of adult oligodendrogenesis

An increase in OPC proliferation without a change in OPCs density could be the result of enhanced OPC differentiation. To determine whether LRP1 regulates OL production by adult OPCs, tamoxifen was given to P57 control (*Pdgfrα-CreER^{TM} :: Rosa26-YFP)* and *Lrp1*-deleted (*Pdgfrα-CreER^{TM} :: Rosa26-YFP :: Lrp1$^{fl/fl}$*) mice, to fluorescently label adult OPCs and the new OLs they produce. Coronal brain cryosections were generated from P57+14 mice and immunolabeled to detect YFP (green), PDGFRα (red) and OLIG2 (blue) and confirmed the specificity of labelling by demonstrating that YFP$^+$ cells were cells of the oligodendrocyte lineage (**Fig. 19**). Consistent with our previous findings in control mice (O'Rourke et al., 2016), all YFP$^+$ cells in the corpus callosum were either PDGFRα$^+$ OLIG2$^+$ OPCs or PDGFRα-negative OLIG2$^+$ newborn OLs (in control mice: 100% $\pm$ 0% of YFP$^+$ cells were OLIG2$^+$; In *Lrp1*-deleted mice; 100% $\pm$ 0% YFP$^+$ cells were OLIG2$^+$; avg ± SD for n=3 mice per genotype; **Fig. 19c**). In the motor cortex of P57+14 control and *Lrp1*-deleted mice, essentially all YFP$^+$ cells were also found to be OLIG2$^+$ (avg ± SD for n=3 mice per genotype; 96.2% $\pm$ 0.91 and 94.3% $\pm$ 1.02 respectively). The small number of YFP$^+$ OLIG2-negative cells identified in the cortex were neurons (data not shown), and these YFP$^+$ OLIG2-negative cells were excluded from all subsequent analyses.

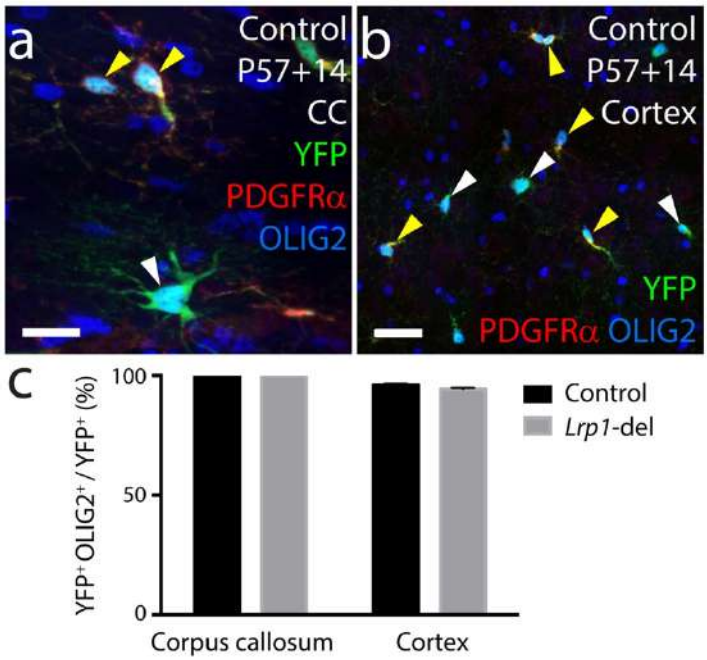

Figure 19: Almost all YFP labelled cells are of the oligodendrocyte lineage.

Coronal brain sections were taken from control (*Pdgfrα-CreER^{TM} :: Rosa26YFP*) mice 14 days post tamoxifen and immunolabelled to detect OPCs (PDGFRα, red), YFP (green) and oligodendrocyte lineage cells (OLIG2, blue). Representative images from the cortex (**a**) and corpus callosum (**b**) showing colocalization between YFP$^+$ cells and OLIG2$^+$ cells (white arrowheads, oligodendrocytes) and YFP$^+$, OLIG2$^+$ and PDGFRα$^+$ cells (yellow arrow heads, OPCs). (**c**) graphical representation showing proportion (%) of YFP$^+$ cells that also express OLIG2 in the corpus callosum and cortex of control and *Lrp1*-deleted mice (mean ± SEM,). Scale bar represents: 34μm (**a**) and 17μm (**b**). Ctx = cortex, CC= corpus callosum.

To determine whether LRP1 influences oligodendrogenesis, we next determined the proportion of YFP^+ cells that were PDGFRα-negative $OLIG2^+$ newborn OLs in the corpus callosum (**Fig. 20a-f**) or motor cortex (**Fig. 20g-l**) of P57+7, P57+14, P57+30 and P57+45 control and *Lrp1*-deleted mice. At P57+7 and P57+14, oligodendrogenesis was equivalent in the corpus callosum of control and *Lrp1*-deleted mice, however by P57+30, a larger proportion of YFP^+ cells had become newborn OLs in the corpus callosum of *Lrp1*-deleted mice, and this effect was sustained at P57+45 (**Fig. 20m**). Similarly, for the first two weeks, OL production was equivalent for OPCs in the motor cortex of control and *Lrp1*-deleted mice, however, by P57+30, the proportion of YFP^+ cells that were newborn OLs was higher in the motor cortex of *Lrp1*-deleted mice relative to controls (**Fig. 20n**). At P57+30, we also performed cell density measurements and found that new oligodendrocyte density was also significantly increased in the corpus callosum (control 107.2 ± 14.9 cell/mm^2 *Lrp1*-del 161.8 ± 27.4 cell/mm^2; avg $\pm$ SD, n= >4 mice per genotype; t-test, p= 0.001) and motor cortex (control 42.55 ± 9.2 cell/mm^2 *Lrp1*-del 61.34 ± 7.0cell/mm^2; avg $\pm$ SD, n= >4 mice per genotype; t-test; p= 0.01) of *Lrp1*-deleted mice compared to controls at P57+30 (data not shown). These results suggest that in the healthy adult mouse brain CNS, LRP1 is a negative regulator of OPC differentiation.

4.2.4 LRP1 reduces the generation of mature, myelinating oligodendrocytes

As OPCs differentiate, they rapidly downregulate their expression of PDGFRα, the NG2 proteoglycan and voltage-gated sodium channels (NaV) (Richardson et al., 1988; Pringle et al., 1989; De Biase et al., 2010; Kukley et al., 2010; Clarke et al., 2012), and become highly ramified pre-myelinating OLs, that either die or continue to mature into myelinating OLs, that are characterised by the elaboration of myelin internodes (Trapp et al., 1997; Psachoulia et al., 2009; Hughes et al., 2013; Young et al., 2013; Tripathi et al., 2017). In order to determine

Figure 20: LRP1 suppresses adult oligodendrogenesis in the adult mouse corpus callosum and motor cortex

Immunohistochemical analysis of coronal brain sections from P57+7 (**a**, **d**) P57+14 (**b**, **e**) and P57+30 (**c**, **f**) control (*Pdgfrα-CreER^{TM} :: Rosa26-YFP*) and *Lrp1*-deleted *(Pdgfrα-CreER^{TM} :: Rosa26-YFP :: Lrp1$^{fl/fll}$*) mice to detect PDGFRα (red) and YFP (green) in the corpus callosum (CC). Yellow arrows indicate YFP^{+}, PDGFRα^{+} OPCs and white arrows indicate the newborn YFP^{+}, PDGFRα-neg oligodendrocytes they produce during the tracing period. (**m**) Graphical representation of the proportion (%) of YFP^{+} cells in the corpus callosum of 7,14,30 and 45 days post tamoxifen in control and *Lrp1* deleted mice that are YFP^{+} PDGFRα-neg OLIG2^{+} newborn oligodendrocytes (mean ± SEM, n=4-6 mice per genotype per timepoint; [2-way ANOVA *genotype F (1,28)=22.3,p = <0.0001; Time F (3,28) =109.7, p = <0.0001; interaction F(3, 28)= 1.902, p = 0.15]* with Bonferroni multiple comparisons; 30 days p= 0.004, 45 days p= 0.006). Coronal brain sections were taken from *Pdgfrα-CreER^{TM} :: Rosa26-YFP* (control) and *Pdgfrα-CreER^{TM} :: Rosa26-YFP :: Lrp1$^{fl/fl}$* (*Lrp1$^{fl/fl}$*) mice and immunolabelled to detect PDGFRα (red) and YFP (green) at 7 (**g**,**j**) 14 (**h**,**k**) and 30 days (**i**,**l**) post tamoxifen. Yellow arrows indicate OPCs (YFP^{+}, PDGFRα^{+} cells) and white arrows indicate newly formed oligodendrocytes (YFP^{+}, PDGFRα-neg). (**n**) graphical representation depicting the proportion of newly formed oligodendrocytes over total YFP+ cells at 7, 14, 30 and 45 days post tamoxifen (mean ± SEM); [2-way ANOVA *genotype F (1,26)=22.5, p = <0.0001; Time F (3,26) =23.4, p = <0.0001; interaction F(3, 26)= 4.56, p = 0.011]* with Bonferroni multiple comparisons; 30 days p= <0.0001 and 45 days p= 0.027). The nuclear marker Hoescht 33342 was used to label cell nuclei (blue). Scale bars = 17μm (a-f) and 34μm (g-l). CC = corpus callosum, Ctx= cortex

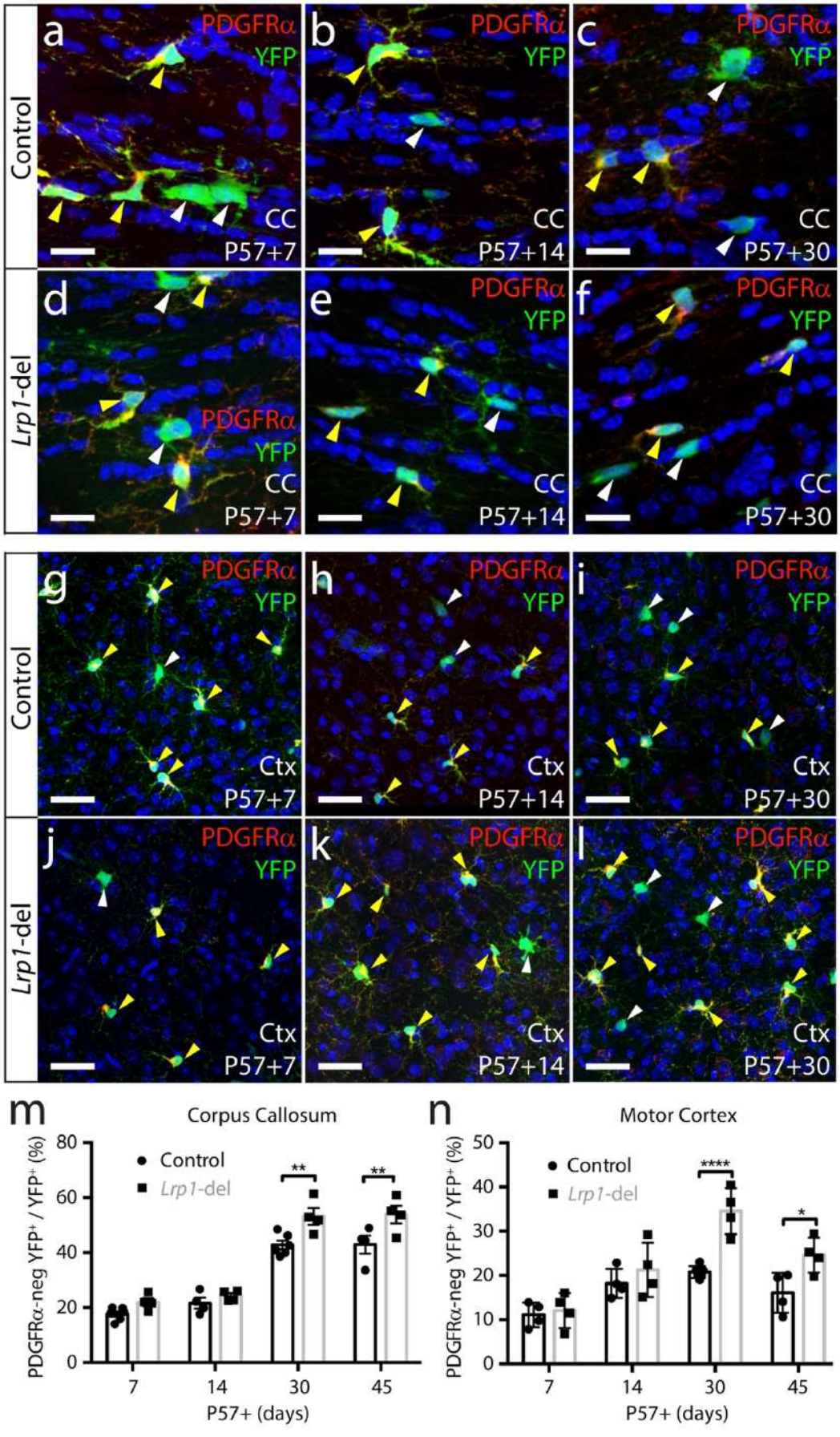
Control
Lrp1-del
a
b
c
d
e
f
g
h
i
j
k
l
PDGFRα
YFP
CC
Ctx
P57+7
P57+14
P57+30
m
Corpus Callosum
n
Motor Cortex
Control
Lrp1-del
PDGFRα-neg YFP+ / YFP+ (%)
P57+ (days)
**
****
*

whether *Lrp1*-deletion increases the number of myelinating OLs, we fluorescently labelled a subset of OPCs in the adult mouse brain with a membrane-targeted from of green fluorescent protein (GFP), allowing us to visualise the full morphology of the OPCs and the OLs they produce. We have previously shown that tamoxifen delivery to adult *Pdgfrα-CreER*^{TM} :: *Tau-GFP* mice does not result in the specific fluorescent labelling of OPCs and their progeny (Pitman et al., 2019). Therefore, for this study, we instead delivered tamoxifen to adult LE-control (*Pdgfrα-CreER*^{T2} *:: Tau-GFP*) and LE-*Lrp1*-deleted (*Pdgfrα-CreER*^{T2} *:: Tau-GFP :: Lrp1*$^{fl/fl}$) transgenic mice. The *Pdgfrα-CreER*^{T2} transgenic mouse (Rivers et al., 2008) has a lower recombination efficiency (LE) than the *Pdgfrα-CreER*^{TM} transgenic mouse (Kang et al., 2010), so we first evaluated the efficiency of *Lrp1* deletion using this mouse model. Coronal brain cryosections from P57+30 LE-control and LE-*Lrp1*-deleted mice were immunolabelled to detect PDGFRα (green) and LRP1 (red) (**Fig. 21 a, b**), and while 100% of PDGFRα^{+} OPCs expressed LRP1 in the motor cortex of LE-control mice, only 35% ± 9% of PDGFRα^{+} OPCs in the motor cortex expressed LRP1 in the LE-*Lrp1*-deleted mice with similar results in the corpus callosum (100% ± 0% for LE-control 37% ± 7 for LE-*Lrp1*-deleted mice) (**Fig. 21c**).

While only ~65% of OPCs lacked LRP1 in the LE-*Lrp1*-deleted mice, this was sufficient to increase adult oligodendrogenesis beyond that of LE-control mice. Brain cryosections from P57+30 LE-control and LE-*Lrp1*-deleted mice were immunolabelling to detect GFP (green), PDGFRα (red) and OLIG2 (blue) (**Fig. 21d, e**), and we found that the proportion of GFP^{+} cells have become PDGFRα-negative, OLIG2^{+} newborn OLs in the motor cortex was significantly elevated [(p= 0.03, n= 4 mice per genotype, t-test)] in the LE-*Lrp1*-deleted mice (56.3% ± 2.06%) compared to controls (49.2% ± 1.51). Furthermore, by examining the morphology of newborn GFP^{+} OLs in LE-control (**Fig. 21g**) and LE-*Lrp1*-deleted mice (**Fig. 21h**), we determined that *Lrp1*-deletion was associated with the generation of more myelinating OLs (**Fig. 21f**),

Figure 21: *Lrp1*-deletion increases the number of mature, myelinating oligodendrocytes added to the motor cortex of adult mice

Confocal image of the corpus callosum (CC) of P57+30 low efficiency control (**a**, LE-*Pdgfr*-*CreER*^{T2}) and low efficiency *Lrp1* deleted (***b***,*LE-Pdgfr*α*-CreER*^{T2} *:: Lrp1*$^{fl/lf}$) mice immunolabelled to detect OPCs (PDGFRα, green), LRP1 (red) and Hoescht 33342 (blue). (**c**) Graphical representation of the proportion of PDGFRα^+ OPCs that express LRP1 in the CC of LE-control and the LE-*Lrp1*-del mice (mean $\pm$ SD, n= 3 mice per group; unpaired t-test, *** p =0.0008). (**d**) Confocal image from the motor cortex (Ctx) of a P57+30 control (LE-*Pdgfrα-CreER*^{T2} *:: Tau-mGFP*) mouse immunolabelled to detect PDGFRα (red) and GFP (green). Yellow arrow heads indicate GFP-labelled OPCs. (**e**) Confocal image from the Ctx of a P57+30 control (LE-*Pdgfrα-CreER*^{T2} *:: Tau-mGFP*) mouse immunolabelled to detect PDGFRα (red) and GFP (green) showing the two distinct morphologies of premyelinating (arrowhead) and mature (arrow), myelinating oligodendrocytes (arrow). (**f**) Quantification of the proportion (%) of GFP$^+$ cells that are PDGFRα$^+$ OLIG2$^+$ OPCs, PDGFRα-neg OLIG2$^+$ premyelinating oligodendrocytes and PDGFRα-neg OLIG2$^+$ mature, myelinating oligodendrocytes (mean $\pm$ SEM, n = 4 mice per genotype; [2-way ANOVA *cell stage F (2,18)=193.3, p = <0.0001; genotype F (1,18) = 2.008e-005, p = 1; interaction F(2, 18)= 17.9, p <0.0001]* with Bonferroni multiple comparisons, * p = 0.024 and *** p = 0.004). Confocal image of GFP$^+$ myelinating oligodendrocytes in the Ctx of P57+30 control (**g, g'**) and LE-*Lrp1*-deleted (**h, h'**) mice. (**i**) The number of internodes elaborated by individual GFP$^+$ myelinating oligodendrocytes in control and LE-*Lrp1*-deleted mice (mean $\pm$ SEM, n= 10-12 oligodendrocytes from n=3 mice per genotype; unpaired t-test, p= 0.3). (**j**) The average length of internodes elaborated by individual GFP$^+$ myelinating oligodendrocyte in control and LE-*Lrp1*-deleted mice (n=10-12 OL oligodendrocytes from 3 mice per genotype; unpaired t-test, p= 0.6 respectively). (**k**) Internode length distribution for

GFP^{+} internodes measured in the Ctx of P57+30 control and LE-*Lrp1*-deleted mice (n= 519 control and n= 408 LE-*Lrp1*$^{fl/fl}$ GFP^{+} internodes measured; K-S test, D= 0.053, p= 0.5). Scale bars = 34μm. CC = corpus callosum, Ctx = cortex.

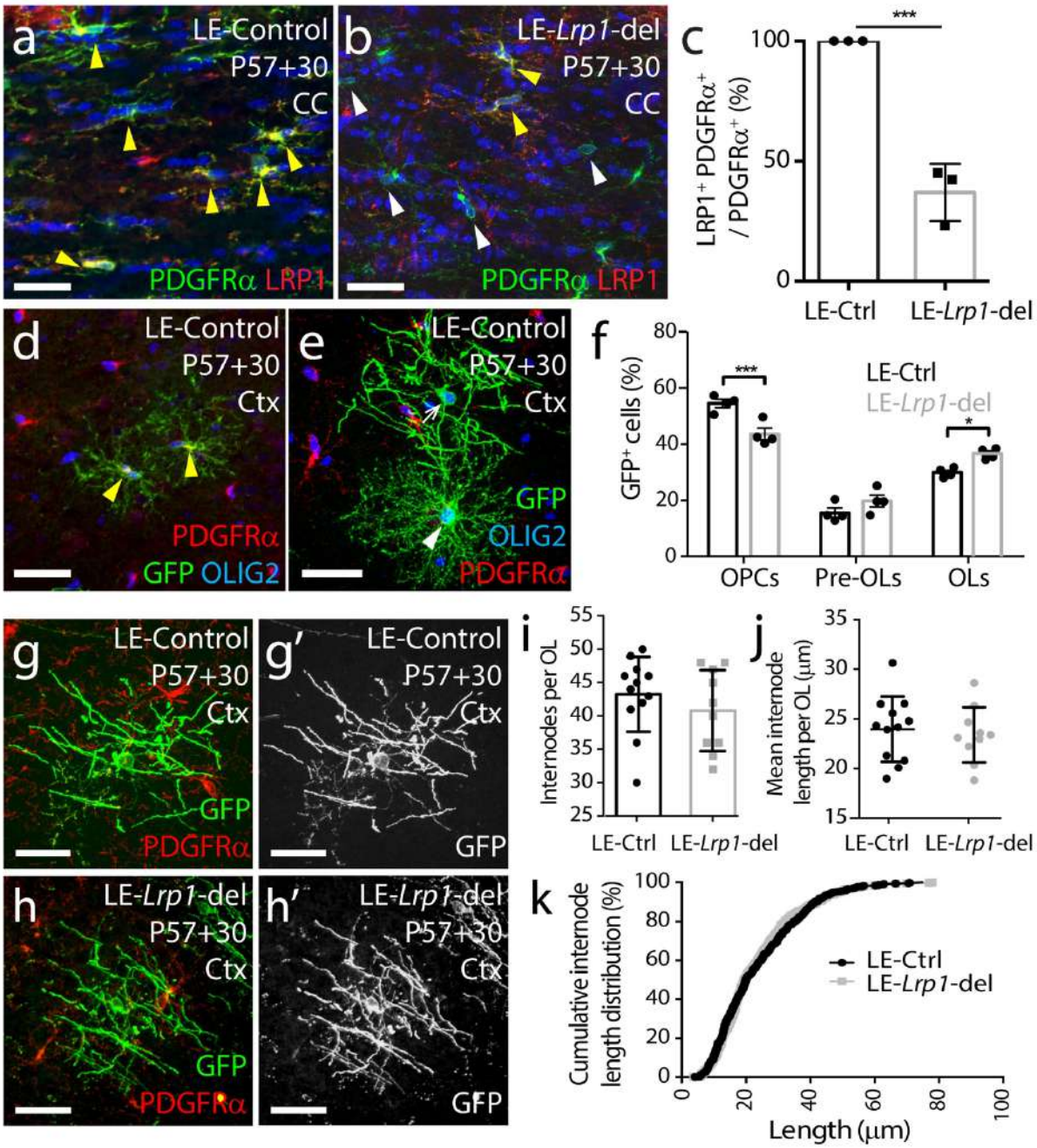
a
LE-Control
P57+30
CC
PDGFRα LRP1
b
LE-Lrp1-del
P57+30
CC
PDGFRα LRP1
c
***
100
50
0
LRP1+ PDGFRα+ / PDGFRα+ (%)
LE-Ctrl
LE-Lrp1-del
d
LE-Control
P57+30
Ctx
PDGFRα
GFP OLIG2
e
LE-Control
P57+30
Ctx
GFP
OLIG2
PDGFRα
f
80
60
40
20
0
GFP+ cells (%)
***
*
LE-Ctrl
LE-Lrp1-del
OPCs
Pre-OLs
OLs
g
LE-Control
P57+30
Ctx
GFP
PDGFRα
g'
LE-Control
P57+30
Ctx
GFP
i
55
50
45
40
35
30
25
Internodes per OL
LE-Ctrl
LE-Lrp1-del
j
35
30
25
20
15
Mean internode length per OL (µm)
LE-Ctrl
LE-Lrp1-del
h
LE-Lrp1-del
P57+30
Ctx
GFP
PDGFRα
h'
LE-Lrp1-del
P57+30
Ctx
GFP
k
100
80
60
40
20
0
Cumulative internode length distribution (%)
LE-Ctrl
LE-Lrp1-del
0
20
40
60
80
100
Length (µm)

while the proportion of YFP$^+$,PDGFRα-negative cells that are mature OLs was unchanged between control and *Lrp1*-deleted mice. Detailed morphological analysis of individual GFP$^+$ myelinating OLs in the motor cortex of LE-control and LE-*Lrp1*-deleted mice revealed that the myelinating profile of OLs was not affected by *Lrp1* deletion. The average number of internodes elaborated by GFP$^+$ myelinating OLs (**Fig. 21i**) or the mean length of internodes elaborated by GFP$^+$ myelinating OLs (**Fig. 21j**) was equivalent in LE-control and LE-*Lrp1*-deleted mice. Additionally, the length distribution for internodes elaborated by GFP$^+$ myelinating OLs was also the same in the motor cortex of LE-control and LE-*Lrp1*-deleted mice (**Fig. 21k**). These data indicate that in the healthy adult mouse brain, LRP1 negatively regulates the number of myelinating OLs produces from OPCs, but does not influence internode elaboration or maintenance by the resulting cells.

4.2.5 LRP1 does not influence NaV, AMPA receptor, L- or T-Type VGCC, PDGFRα or LRP2 expression by OPCs

LRP1 could influence a number of signaling pathways known to directly or indirectly regulate OPC proliferation and / or the number of newborn OLs present in the brain. The conditional deletion of *Lrp1* from neurons *in vitro* and *in vivo* has been shown to increase AMPA receptor turnover and reduce expression of the GluA1 subunit of the AMPA receptor (Gan et al., 2014). Adult OPCs express AMPA receptors (Gallo et al., 1996; Gudz, 2006; Zonouzi et al., 2011) and glutamatergic signalling has been shown to influence OPC proliferation and differentiation (Gallo et al., 1996; Fannon et al., 2015), as well as migration (Gudz, 2006), and, AMPA receptor signalling has been shown to enhance the survival of premyelinating oligodendrocytes during development (Kougioumtzidou et al., 2017). To determine whether LRP1 regulates AMPA receptor signalling in OPCs, we obtained whole cell patch clamp recordings from GFP-labelled OPCs in the motor cortex of P57+30 control (*Lrp1$^{fl/fl}$ :: Pdgfrα-histGFP*) and *Lrp1*-deleted

(*Pdgfrα-CreER*^{TM} *:: Lrp1*$^{fl/fl}$ :: *Pdgfrα-histGFP*) mice (**Fig. 22**). OPCs elicit a large inward voltage-gated (sodium) current in response to a series of voltage-steps (**Fig. 22a**), and the I_{Na} amplitude was not affected by genotype (**Fig. 22b**). The resting membrane potential (**Fig. 22c**) and the capacitance (size; **Fig. 22d**) of OPCs was also unaffected by LRP1 expression. AMPA receptors were next activated by the bath application of 100μm kainate, which evoked a large and sustained inward current in control and *Lrp1*-deleted OPCs (**Fig. 22e**), and the amplitude of the evoked current was found to be equivalent for control and *Lrp1*-deleted OPCs across all voltages examined (**Fig. 22f**). These data indicate that *Lrp1*-deletion is unlikely to affect the composition or cell-surface expression of AMPA/kainate receptors in OPC in the healthy adult mouse brain.

LRP1 has also been shown to regulate the cell surface expression and distribution of N-Type voltage gated calcium channels (VGCC), by interacting with the $\alpha_2\delta$ subunit (Kadurin et al., 2017). In adult OPCs, the closely related L-Type VGCCs have been shown to reduce OPC proliferation in the motor cortex and corpus callosum (Pitman et al., 2019), and influence the maturation of OPCs into OLs *in vitro* (Cheli et al., 2015). OPCs also express the T-Type VGCC, commonly referred to as the low voltage activated Ca^{++} channel (Williamson et al., 1997; Fulton et al., 2010). To determine whether the distribution of L-Type or T-Type VGCCs in OPCs is altered following *Lrp1* deletion, we performed whole cell patch clamp electrophysiology and measured the current density (pA/pF) in control and *Lrp1*-deleted mice (**Fig. 22g**). We found that the L and T-Type VGCC current densities were equivalent for OPCs in the motor cortex of control and *Lrp1*-deleted mice (**Fig. 22h**), indicating that LRP1 does not influence L-Type or T-Type VGCC expression in adult OPCs.

LRP1 has also been shown to influence the cell surface expression of PDGFRβ (Takayama et al., 2005; Muratoglu et al., 2010), a receptor closely related to PDGFRα, an important

Figure 22: LRP1 does not alter NaV, VGCC, AMPA/kainate or PDGFRα receptor expression in OPCs

Control (*Pdgfrα-histGFP :: Lrp1*$^{fl/fl}$) and *Lrp1*-deleted (*Pdgfra-CreER*^{TM} *:: Pdgfrα-histGFP :: Lrp1*$^{fl/fl}$*)* mice were gavaged at P57 and were sacrificed at P57+30 for electrophysiological analysis. GFP^{+} cells in the motor cortex were whole-cell patch clamped and determined to be OPCs by the presence of a sodium spike greater than 100mv (**a**) Representative traces of voltage-gated sodium channels currents evoked in GFP^{+} OPCs from control and *Lrp1*-deleted mice. Graphical representation showing no change in peak inward sodium current (**b,** unpaired t-test, n = 8-9 cells across n= 3 animals per genotype, p= 0.8) and cell capacitance (**c**, unpaired t-test, n = 9-11 cells across n= 3 animals per genotype, p= 0.9). (**d**) Representative trace showing the leak subtracted L-type calcium current evoked in response to a depolarising step. (**e**) Graphical representation showing the current density-voltage relationship for leak subtracted L-Type VGGC currents recorded from controls (dark circles, n= 7 cells across n=3 mice) and *Lrp1* deleted (grey squares, n=11 cells across n=3 mice) (mean±SEM, [2-way ANOVA; Interaction F(10,176)=0.62, p=0.8; genotype F=(1,176)=1.03), p=0.3; voltage F(10,176)=66.8, p=<0.0001]). Graphical representation showing the current density-voltage relationship for leak subtracted T-Type VGGC currents recorded from control (dark circles, n= 11 cells across n=3 mice) and *Lrp1* deleted (grey squares, n=10 cells across n=3 mice) (mean±SEM, [2-way ANOVA; Interaction F(9,190)=1.14, p=0.3; genotype F=(1,190)=2.85), p=0.09; voltage F(9,190)=23.5, p= <0.0001]). (**g**) Example traces from control and *Lrp1*-del OPCs in response to bath application of 100μM kainate (**h**) Graphical representation showing the current voltage relationship of AMPA/kainate receptors in control (n= 3 cells) and *Lrp1*-deleted (n=3 cells) mice following bath application of kainate (mean±SEM; [2-way ANOVA; Interaction F(6,28)=0.25, p=0.9; genotype F=(1,28)=0.91), p=0.3; voltage F6,28)=31.3,

p=<0.0001]). Coronal brain sections from control and *Lrp1* deleted mice at P57+30 were immunolabelled to detect OPCs (PDGFRα). Representative confocal images from control (**i**) and *Lrp1*-deleted (**j**) mice showing typical PDGFRα expression in OPCs. (**e**) graphical representation showing the mean grey value of PDGFRα expression between control and *Lrp1*-deleted OPCs (mean± SD; n= a minimum of 24 cells across 3 animals per genotype; unpaired t-test, p= 0.8). Scale bar represents 17μm. Ctx = cortex

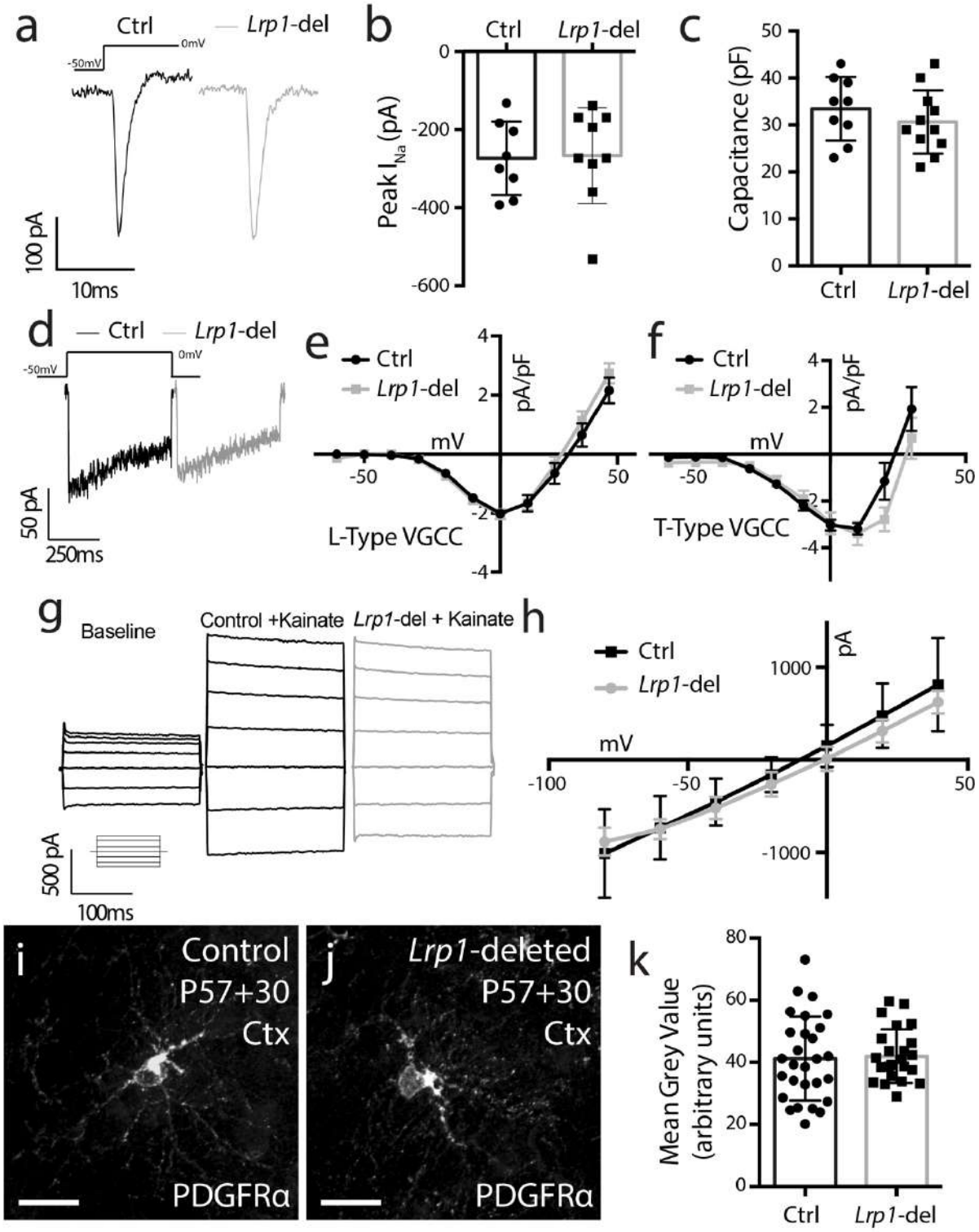
a
Ctrl
Lrp1-del
0mV
-50mV
100 pA
10ms
b
Ctrl
Lrp1-del
Peak I_Na (pA)
0
-200
-400
-600
c
Capacitance (pF)
50
40
30
20
10
0
Ctrl
Lrp1-del
d
Ctrl
Lrp1-del
0mV
-50mV
50 pA
250ms
e
Ctrl
Lrp1-del
pA/pF
mV
-50
50
L-Type VGCC
f
Ctrl
Lrp1-del
pA/pF
mV
-50
50
T-Type VGCC
g
Baseline
Control +Kainate
Lrp1-del + Kainate
500 pA
100ms
h
Ctrl
Lrp1-del
pA
mV
1000
-1000
-100
-50
50
i
Control
P57+30
Ctx
PDGFRα
j
Lrp1-deleted
P57+30
Ctx
PDGFRα
k
Mean Grey Value
(arbitrary units)
80
60
40
20
0
Ctrl
Lrp1-del

mitogenic receptor regulating OPC proliferation, survival and migration (Noble et al., 1988; Richardson et al., 1988; Pringle et al., 1989). To determine whether LRP1 is a negative regulator of PDGFRα expression, we performed immunohistochemistry to detect PDGFRα expression in the motor cortex of P57+30 control and *Lrp1*-deleted mice (**Fig. 22i-j**) and measured the mean grey value (**Fig. 22k**) and the maximum intensity for PDGFRα expression by OPCs (**Fig. 22l**), to determine that LRP1 did not influence PDGFRα expression.

The low-density lipoprotein receptor related protein 2 (LRP2) is a large cell surface receptor that is closely related to LRP1, with a number of common ligands (Spuch et al., 2012). It is unclear whether cells of the oligodendrocyte lineage express LRP2 (Cahoy et al., 2008; Zhang et al., 2014; Hrvatin et al., 2018), or whether *Lrp1*-deletion could alter *Lrp2* expression, however, LRP2 can increase the proliferation of neural precursor cells in the subependymal zone (Gajera et al., 2010), and the proliferation and survival of skin cancer cells (Andersen et al., 2015). By performing immunohistochemistry to detect LRP2 and PDGFRα or ASPA in coronal brain cryosections from P57+30 control and *Lrp1*-deleted mice, we determined that LRP2 is not expressed by OPCs or OLs in mice of either genotype (**Fig. 23a-d**). However, LRP2 was highly expressed by Iba1^{+} microglia (**Fig. 23e**). These data indicate that LRP2 is not responsible for the elevated OPC proliferation and differentiation observed in *Lrp1*-deleted mice.

4.2.6 LRP1 ligand-mediated activation and *Lrp1*-deletion do not alter OPC proliferation *in vitro*

Our data suggest that in the healthy adult mouse CNS, *Lrp1*-deletion either increases OPC proliferation which then results in an increase in the number of newborn OLs added to the brain over time, or increases OPC differentiation, which subsequently triggers a homeostatic increase in OPC proliferation to maintain the OPC population. Previous studies have shown

Figure 23: LRP2 is not expressed by wild type or Lrp1-deleted oligodendrocyte lineage cells

Brain sections from control (*Pdgfra-CreER^{TM})* and *Pdgfra-CreER^{TM} :: Lrp1$^{fl/fl}$* at P57+30 were taken and immunolabelled to detect OPCs (PDGFRα, red) and LRP2 (green) in the corpus corpus callosum (**a**,**b**). Brain sections from control (*Pdgfra-CreER^{TM})* and *Pdgfra-CreER^{TM} :: Lrp1$^{fl/fl}$* at P57+30 were taken and immunolabelled to detect oligodendrocytes (ASPA, red) and LRP2 (green) in the cortex (**c**,**d**). (**e**) brain sections from control (*Pdgfra-CreER^{TM})* mice were taken and immunolabelled to detect microglia (IBA1, green) and LRP2 (red) White arrows indicate PDGFRα^+ (a,b), ASPA$^+$ (c,d) or IBA1$^+$ (e) cells. Scale bar represents 17μm, CC= corpus callosum

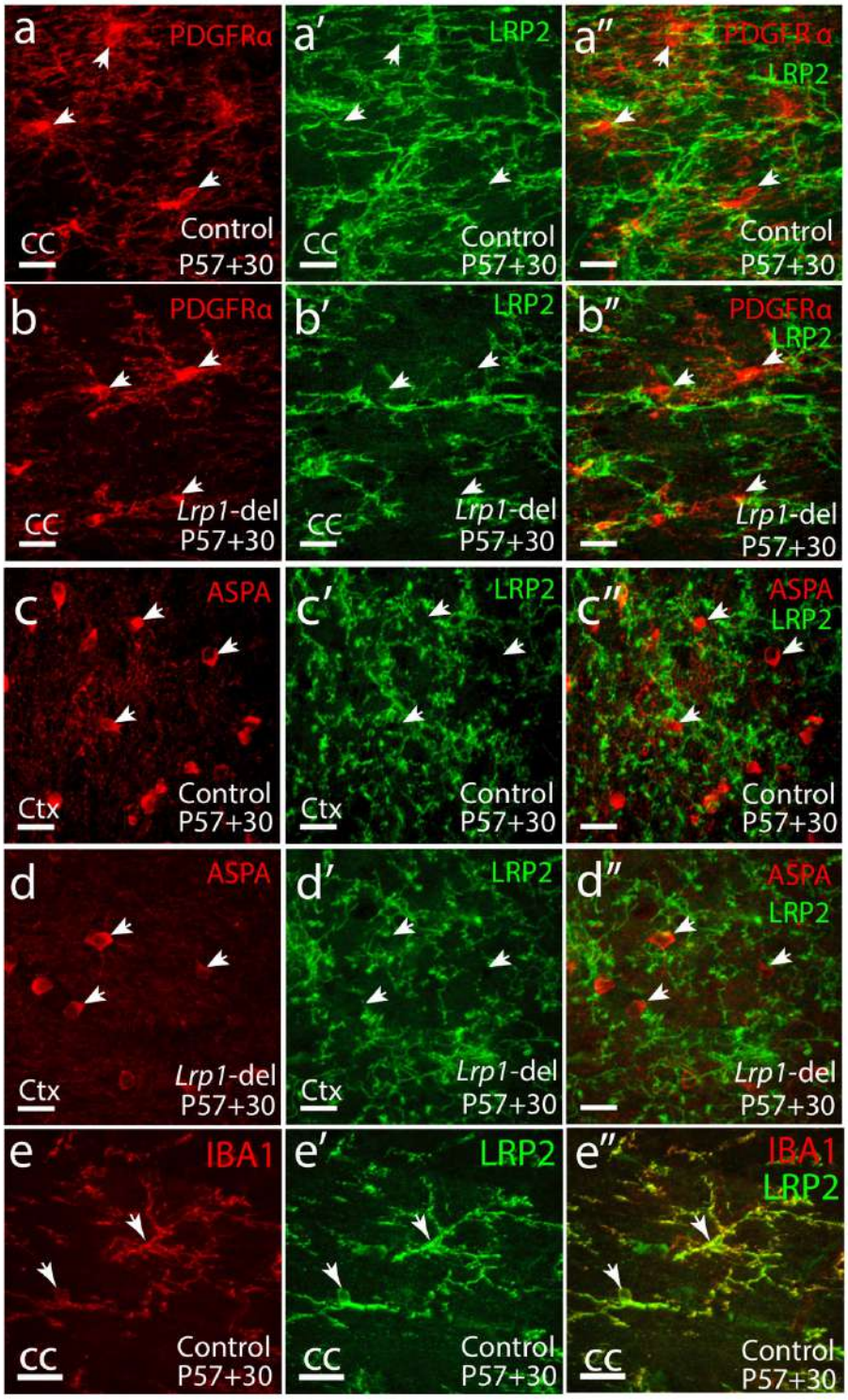
a
PDGFRα
CC
Control
P57+30
a′
LRP2
CC
Control
P57+30
a″
PDGFRα
LRP2
Control
P57+30
b
PDGFRα
CC
Lrp1-del
P57+30
b′
LRP2
CC
Lrp1-del
P57+30
b″
PDGFRα
LRP2
Lrp1-del
P57+30
c
ASPA
Ctx
Control
P57+30
c′
LRP2
Ctx
Control
P57+30
c″
ASPA
LRP2
Control
P57+30
d
ASPA
Ctx
Lrp1-del
P57+30
d′
LRP2
Ctx
Lrp1-del
P57+30
d″
ASPA
LRP2
Lrp1-del
P57+30
e
IBA1
CC
Control
P57+30
e′
LRP2
CC
Control
P57+30
e″
IBA1
LRP2
CC
Control
P57+30

that *Lrp1* deletion could enhance the proliferation of retinal endothelial cells (Mao et al., 2016), while the activation of LRP1 by its ligand tissue plasminogen activator (tPa), could enhance the proliferation of interstitial fibroblasts (Lin et al., 2010). To determine whether LRP1 directly suppresses OPC proliferation, we generated primary OPC cultures from the cortex of P0-P5 control (*Pdgfrα-hGFP)* or *Lrp1*-deleted (*Pdgfrα-hGFP :: Lrp1*$^{fl/fl}$) mice. At ~7DIV, OPCs were incubated with 1μM TAT-Cre for 90 min, and LRP1 expression was determined 2 days later by performing immunocytochemistry to detect PDGFRα (red), GFP (green) and LRP1 (blue) (**Fig. 24a**, **b**). All OPCs cultured from control mice expressed LRP1 (100% ± 0%), while only 21% ± 4% of PDGFRα^{+} OPCs cultured from *Lrp1*-deleted mice retained LRP1 expression following TAT-Cre treatment (**Fig. 24 c;** t-test, p<0.0001). At this same time-point, equivalent control and *Lrp1*-deleted OPC cultures were also exposed to EdU, to label all cells that enter s-phase of the cell cycle over a 10-hour period. By performing immunocytochemistry to detect GFP (green), LRP1 (red) and EdU (**Fig. 24d**, **e**), we found that the level of LRP1 expression did not influence OPC proliferation, as the fraction of PDGFRα^{+} OPCs that were EdU^{+} was equivalent in control and *Lrp1*-deleted cultures (**Fig. 24f**).

To further confirm that LRP1 activation by ligands does not directly influence OPC proliferation, we added the LRP1 ligands tPa (20nM) or activated alpha-2 macroglobulin (*α2M; 60mM), or vehicle (milliQ water) to OPC primary cultures for 10 hours, along with EdU (**Fig. 24**). We evaluated OPC proliferation by performing immunocytochemistry to detect (PDGFRα, green) and EdU (red) (**Fig. 24g, h, j**) and found that the proportion of EdU^{+} OPCs did not change with the addition of tPa or *α2M compared to vehicle treated controls (**Fig 24j**), indicating that LRP1 activation by these ligands is also unable to modify OPC proliferation *in vitro*.

Figure 24: *Lrp1* deletion and activation do not effect OPC proliferation *in vitro*

Purified OPCs from control (**a,** *Pdgfrα-histGFP*) and *Lrp1*-deleted (**b**, *Pdgfrα-histGFP :: Lrp1$^{fl/fl}$*) mice were treated with 1μM TAT-Cre for 90 minutes then left for 48 hours then immunolabelled with PDGFRα (red), LRP1 (blue) and GFP (green). (**c**) graphical representation comparing the percentage of LRP1^{+} OPCs 48 hours post TAT-Cre (mean ± SEM, n= 3 independent cultures for control and n= 4 independent cultures for *Lrp1*-deleted mice, unpaired t-test, p= <0.0001). Purified primary OPCs from control (**d,** *Pdgfrα-histGFP*) and *Lrp1* deleted (**e**, *Pdgfrα-histGFP :: Lrp1$^{fl/fl}$*) were treated with EdU for 10 hours then immunolabelled to detect GFP (green), LRP1 (red) and EdU (blue). (**f**) Graphical representation comparing the % of EdU^{+} GFP^{+} cells following TAT-Cre treatment (mean± SEM, n= 5-6 independent cultures, unpaired t-test p= 0.3). Example images from primary OPCs immunolabelled to detect PDGFRα (green) and EdU (red) following 10 hours of EdU exposure in combination with vehicle (**g**) 20nM tPa (**h**) or 60 nM *α2M (**j**). Graphical representation comparing the % of EdU^{+}, PDGFRα^{+} cells between vehicle and tPa treated cells (**i**, unpaired t-test, n= 4 independent cultures, p=0.2) or *α2M treated (**k**, unpaired t-test, n= 4 independent cultures p=0.8). Scalebar represents 17μm, DIV = Days *in vitro*, tPA = tissue plasminogen activator, *α2M = activated alpha-2 macroglobulin. The nuclear marker Hoescht 33342 was used to detect cell nuclei (**g**,**h**,**j**)

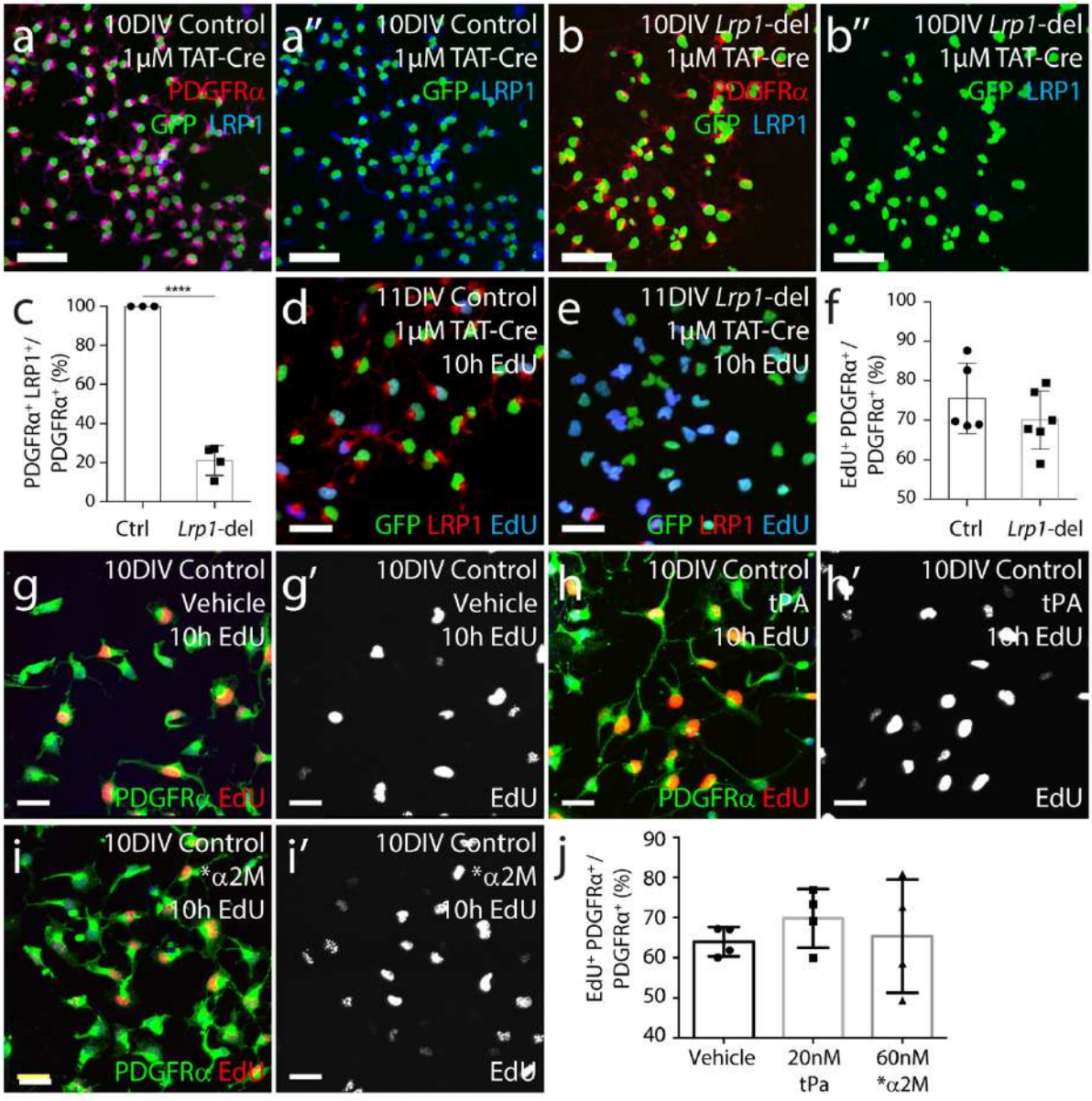
a
10DIV Control
1µM TAT-Cre
PDGFRα
GFP LRP1
a''
10DIV Control
1µM TAT-Cre
GFP LRP1
b
10DIV Lrp1-del
1µM TAT-Cre
PDGFRα
GFP LRP1
b''
10DIV Lrp1-del
1µM TAT-Cre
GFP LRP1
c
PDGFRα+ LRP1+ / PDGFRα+ (%)
****
Ctrl
Lrp1-del
d
11DIV Control
1µM TAT-Cre
10h EdU
GFP LRP1 EdU
e
11DIV Lrp1-del
1µM TAT-Cre
10h EdU
GFP LRP1 EdU
f
EdU+ PDGFRα+ / PDGFRα+ (%)
Ctrl
Lrp1-del
g
10DIV Control
Vehicle
10h EdU
PDGFRα EdU
g'
10DIV Control
Vehicle
10h EdU
EdU
h
10DIV Control
tPA
10h EdU
PDGFRα EdU
h'
10DIV Control
tPA
10h EdU
EdU
i
10DIV Control
*α2M
10h EdU
PDGFRα EdU
i'
10DIV Control
*α2M
10h EdU
EdU
j
EdU+ PDGFRα+ / PDGFRα+ (%)
Vehicle
20nM tPa
60nM *α2M

4.2.7 *Lrp1*-deletion but not LRP1 ligand-mediated activation influences OPC differentiation *in vitro*

In vitro, OPCs can be triggered to differentiate by withdrawing the mitogen PDGF-AA and providing triiodothyronine (T3) in the culture medium. To determine whether *Lrp1* deletion can enhance OPC differentiation, Tat-Cre-treated control and *Lrp1*-deleted cultures were transferred into differentiation medium for 4 days before they were immuno-labelled to detect PDGFRα OPCs (red) and MBP^+ OLs (green) (**Fig. 25a, b**). The proportion of cells that were $PDGFR\alpha^+$ OPCs was reduced in the *Lrp1*-deleted, and the number of cells that were MBP^+ OLs was significantly increased compared with control cultures (**Fig. 25c**).

To determine whether ligand activation of the LRP1 receptor was sufficient to suppress OPC differentiation, OPC primary cultures were instead transferred into differentiation medium containing vehicle, tPA (20nM) or *α2M (60nM) for 4 days. By performing immunocytochemistry to detect $PDGFR\alpha^+$ OPCs and MBP^+ OLs (**Fig. 25d-f**) we found that the activation of LRP1 by tPA or *α2M had no impact on the proportion of cells that differentiated over time (**Fig. 25g**). These data suggest that LRP1 normally acts to suppress OPC proliferation, however, this effect is independent of tPA and α2M signalling. Furthermore, the effect of LRP1 on OPCs proliferation is likely to be a secondary consequence of its ability to regulate OPC differentiation.

4.2.8 OPC specific *Lrp1* deletion in the cuprizone mouse model of demyelination results in reduced lesion volume

Having shown that *Lrp1* deletion increases OPC differentiation and consequently new OL addition, we wanted to determine whether the deletion of *Lrp1* from OPCs could improve remyelination. Control (*Pdgfrα-CreER^{TM} :: Rosa26-YFP)* and *Lrp1*-deleted (*PdgfrαCreER^{TM} :: Rosa26-YFP :: Lrp1$^{fl/fl}$*) mice received tamoxifen by oral gavage at P57, and were transferred

Figure 25: LRP1 expression reduces the OPC differentiation in vitro

Purified OPCs isolated from *Lrp1*$^{+/+}$(**a**) or *Lrp1*$^{fl/fl}$ (**b**) mice were treated with TAT-Cre then left for 48 hours before being exposed to differentiation media for 4 days. The cells were then immunostained to detect PDGFRα (red) and MBP (green) (**c**) graphical representation comparing the percentage of PDGFRα+ or MBP+ cells in control and *Lrp1*$^{fl/fl}$ cultures (mean $\pm$ SEM, n= 3 independent cultures; [2-way ANOVA *cell type* F (1,8)=395,p= <0.0001; interaction (F(1,8) = 37.7,p= 0.0003; genotype (F1,8) =0.0, p= 1] with Sidak's multiple comparisons test. OPCs from control (*Lrp1*$^{+/+}$) mice were exposed to differentiation media containing vehicle (**d**), tPa (**e**) or *α2M (**f**) for 4 days then immunostained to detect PDGFRα and MBP. (**g**) Graphical representation showing the percentage of PDGFRα^{+} or MBP^{+} cells after 4 days in differentiation medium (mean $\pm$ SEM, n= 3 independent cultures; [2-way ANOVA *cell type* F (1,10)=31.4, p= 0.0002; interaction (F (2,10) = 0.028, p= 0.9; genotype F(2,10) =2.04$^{10\text{-}0.12}$, p= 1]) . tPa = tissue plasminogen activator, *α2M = activated alpha 2 macroglobulin The nuclear marker Hoescht 33342 was used to label cell nuclei (blue). Scale bars represent 17μm.

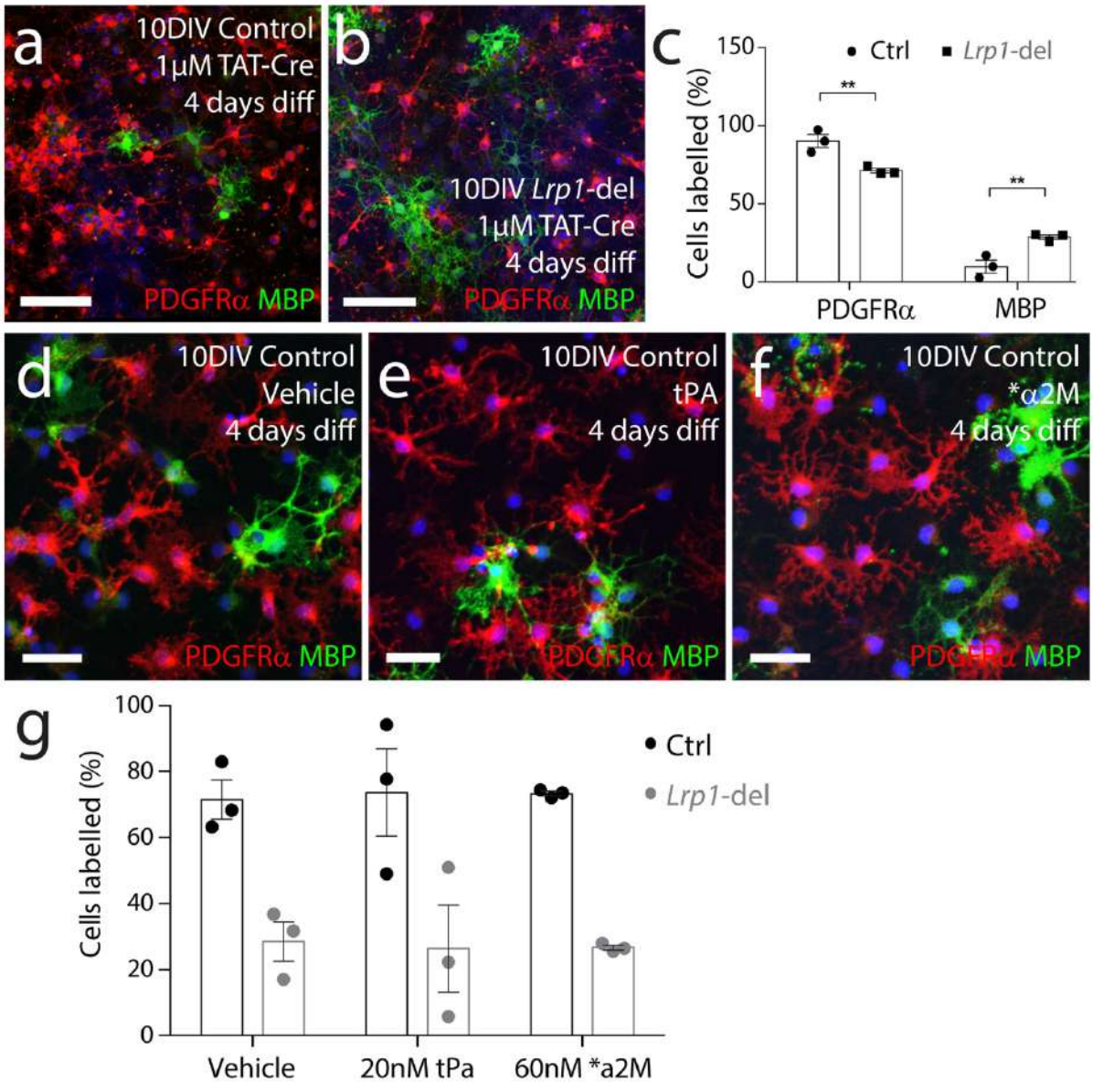
a
10DIV Control
1µM TAT-Cre
4 days diff
PDGFRα MBP
b
10DIV Lrp1-del
1µM TAT-Cre
4 days diff
PDGFRα MBP
c
Ctrl
Lrp1-del
Cells labelled (%)
150
100
50
0
**
**
PDGFRα
MBP
d
10DIV Control
Vehicle
4 days diff
PDGFRα MBP
e
10DIV Control
tPA
4 days diff
PDGFRα MBP
f
10DIV Control
*α2M
4 days diff
PDGFRα MBP
g
Cells labelled (%)
100
80
60
40
20
0
Ctrl
Lrp1-del
Vehicle
20nM tPa
60nM *a2M

onto a diet containing 0.2% (w/w) cuprizone at P64. After 5 weeks, mice were perfusion fixed and coronal brain sections stained to detect myelin (black-gold staining; **Fig. 26**), revealing overt demyelination in the corpus callosum of control and *Lrp1*-deleted mice (**Fig. 26a-d**). By quantifying the proportion of the corpus callosum with overt demyelination, we determined that *Lrp1*-deleted mice had less demyelination than controls (**Fig. 26e)**

Cuprizone initially causes OL death, yet oligodendrogenesis occurs during cuprizone delivery. When mice received EdU via their drinking water during weeks 2-5 of cuprizone feed, we found that the vast majority of OLIG2$^+$ cells were EdU$^+$ in control (146 of 154 cells counted) and *Lrp1*-deleted mice (97 of 106 cells counted) (**Fig 27**). Elucidating the role of LRP1 in myelin repair in the corpus callosum is complicated by the shared contribution of parenchymal OPCs and neural stem cell-derived OPCs to OL generation and remyelination (Xing et al., 2014). Indeed, when we perform immunohistochemistry to detect YFP-labelled cells (green), the OPC marker PDGFRα (red) and the oligodendrocyte lineage marker OLIG2 (blue), in coronal cryosections from control and *Lrp1*-deleted mice, we find large numbers of OPCs (PDGFRα^+ OLIG2$^+$ cells) and OLs (PDGFRα-neg OLIG2$^+$ cells) that are YFP-negative (**Fig. 26 f**,**g**), indicating that these cells were not derived from the YFP$^+$ parenchymal OPC population, but instead likely originate from neural stem cells in the subventricular zone (SVZ). The YFP$^+$ parenchymal OPCs lacked LRP1 (**Fig. 28b** 124 of 124 cells counted), however, the YFP-negative neural stem cell-derived OPCs had intact LRP1 expression (42 of 42 cells counted). We found no difference in the proportion of recombined parenchymal OPCs within the corpus callosum between control and *Lrp1*-delted mice (**Fig 26j;** t-test, p= 0.4, n= > 3 mice per genotype). Furthermore, 60% $\pm$ 15% of YFP$^+$ cells were PDGFRα-negative, OLIG2$^+$ newly generated OLs in control mice, and 65% $\pm$ 5% of YFP$^+$ cells were PDGFRα-negative, OLIG2$^+$ newly generated OLs in the *Lrp1*-deleted mice (**Fig. 26k**; unpaired t-test, p= 0.8, n=>3 mice per genotype). As the total density of OLIG2$^+$ PDGFRα-negative OLs present in the corpus callosum of control and *Lrp1*-deleted

Figure 26: Cuprizone induced lesion size is reduced in mice lacking LRP1 despite no change in new oligodendrocyte addition

Control (*Pdgfrα-CreER^{TM} :: Rosa26YFP*) and *Lrp1*-deleted (*Pdgfrα-CreER^{TM} :: Rosa26YFP :: Lrp1$^{fl/fl}$*) mice were fed a diet containing 0.2% cuprizone for 5 weeks. At the end of 5 weeks, brain sections were collected and stained with Black Gold to detect myelin. Examples of corpus callosal demyelination in control (**a,b**) and *Lrp1*-deleted (**c,d**) mice. (**e**) graphical representation showing the percentage of demyelination in the corpus callosum between the dotted white lines (mean±SD; n= minimum of 4 mice per genotype; unpaired-t- test with Welch's correction, p= 0.04). Control (**f**) and *Lrp1*-deleted (**g**) coronal brain sections immunolabelled to detect YFP (green), PDGFRα (red) and OLIG2 (blue). White dashed line indicates the boundary of the corpus callosum. (**f**) representative confocal image from the corpus callosum of cuprizone treated control (**h**) and *Lrp1*-deleted (**i**) mice immunolabelled to detect OPCs (PDGFRα, red), YFP (green) and OLIG2 (blue). (**j**) graphical representation showing the percentage of YFP$^+$, PDGFRα$^+$ over total PDGFRα$^+$ cells after 5 weeks of cuprizone (mean± SD; n= minimum of 3 mice per genotype; unpaired t-test, p=0.4) (**k**) graphical representation showing the percentage of newly formed oligodendrocytes over total YFP$^+$ cells in GFP$^+$ regions after 5 weeks of cuprizone (mean± SD; n= minimum of 3 mice per genotype; unpaired t-test, p=0.9). (**g**) graphical representation showing the density of oligodendrocytes in the corpus callosum after 5 weeks of cuprizone (mean± SD; n=minimum of 4 mice per genotype; unpaired t-test, p=0.8). Scale bar represents 150μm (a,c) 100μm (f,g) and 17μm (h,i). Regions of demyelination outlined by red dashed line. White arrow indicate PDGFRα$^+$ cells that don't express YFP, yellow arrowheads indicate PDGFRα$^+$ cells that also

express YFP^+ and white arrowheads indicate PDGFRα- negative YFP^+ cells . LV= lateral ventricle.

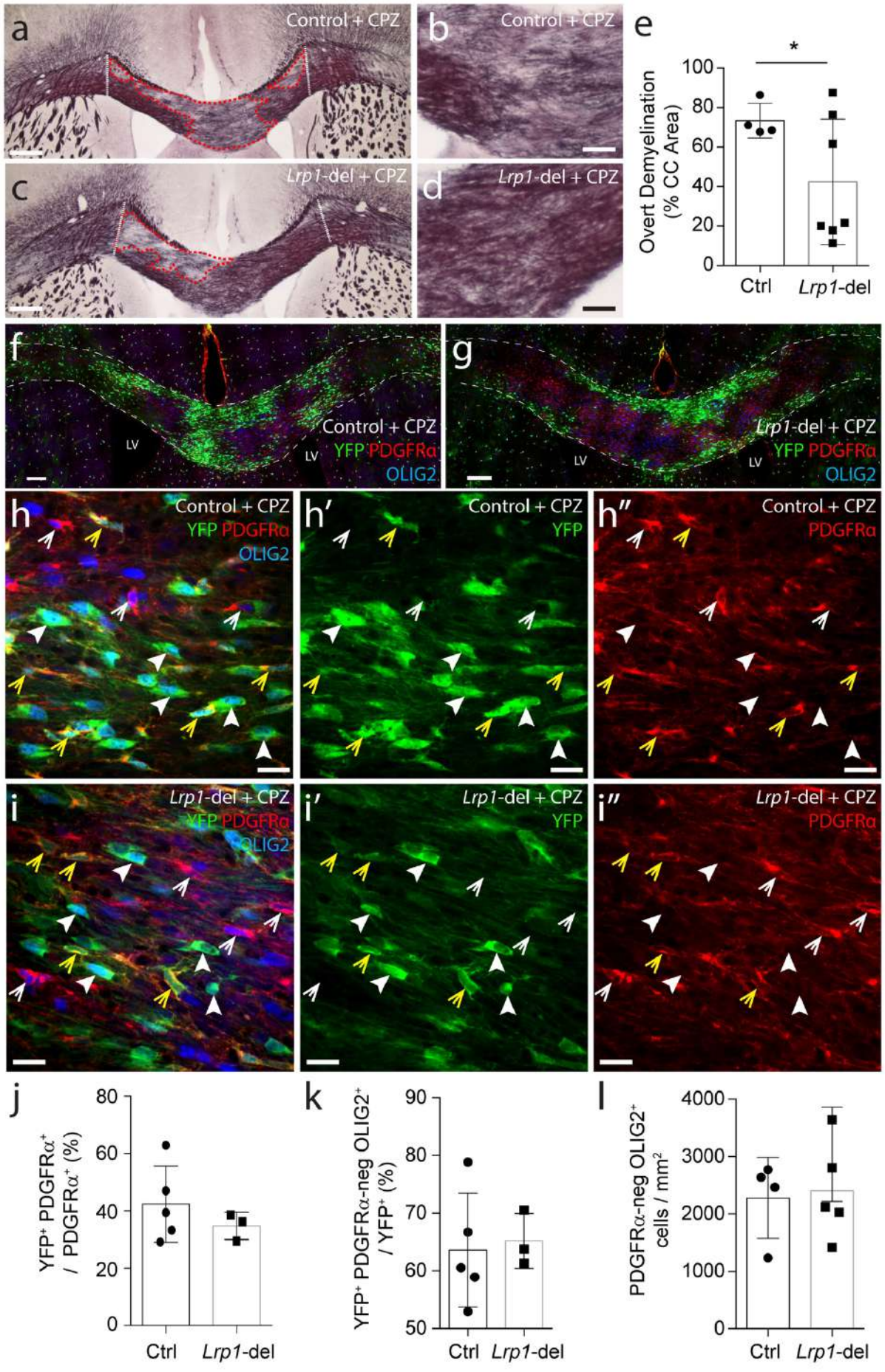
a
Control + CPZ
b
Control + CPZ
c
Lrp1-del + CPZ
d
Lrp1-del + CPZ
e
Overt Demyelination (% CC Area)
100
80
60
40
20
0
*
Ctrl
Lrp1-del
f
Control + CPZ
YFP PDGFRα
OLIG2
LV
LV
g
Lrp1-del + CPZ
YFP PDGFRα
OLIG2
LV
LV
h
Control + CPZ
YFP PDGFRα
OLIG2
h′
Control + CPZ
YFP
h″
Control + CPZ
PDGFRα
i
Lrp1-del + CPZ
YFP PDGFRα
OLIG2
i′
Lrp1-del + CPZ
YFP
i″
Lrp1-del + CPZ
PDGFRα
j
YFP⁺ PDGFRα⁺ / PDGFRα⁺ (%)
80
60
40
20
0
Ctrl
Lrp1-del
k
YFP⁺ PDGFRα-neg OLIG2⁺ / YFP⁺ (%)
90
80
70
60
50
Ctrl
Lrp1-del
l
PDGFRα-neg OLIG2⁺ cells / mm²
4000
3000
2000
1000
0
Ctrl
Lrp1-del

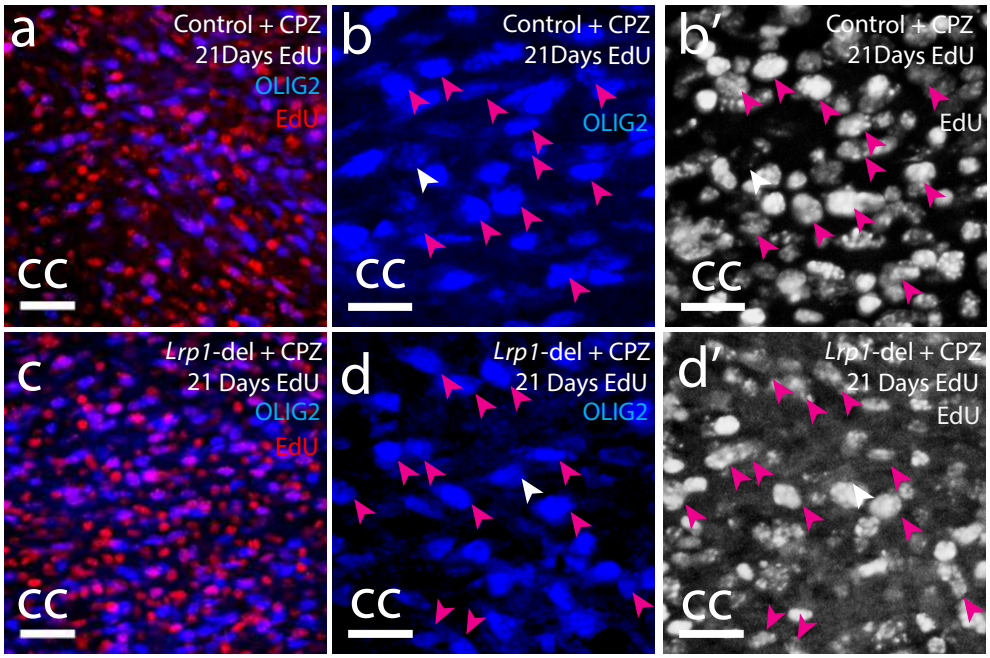

Figure 27: The vast majority of OLIG2 labelled cells are EdU^{+}
Control (*Pdgfrα-CreER^{TM}*) and *Lrp1*-deleted (*Pdgfrα-CreER^{TM} :: Lrp1$^{fl/fl}$*) mice were fed a diet containing 0.2% cuprizone for 5 weeks and administered EdU for the 3 finals weeks. Low (**a**) and high (**b,b'**) magnification images from the corpus callosum of control mice immunolabelled to detect OLIG2 (blue) and EdU (red). Low (**c**) and high (**d,d'**) magnification images from the corpus callosum of control mice immunolabelled to detect OLIG2 (blue) and EdU (red). Scale bar represents 34μm for a,c and 20μm for b and d. White arrowheads indicate OLIG2^{+} , EdU^{-} cells, magenta arrows represent OLIG2^{+} , EdU^{+} cells. CC = corpus callosum.

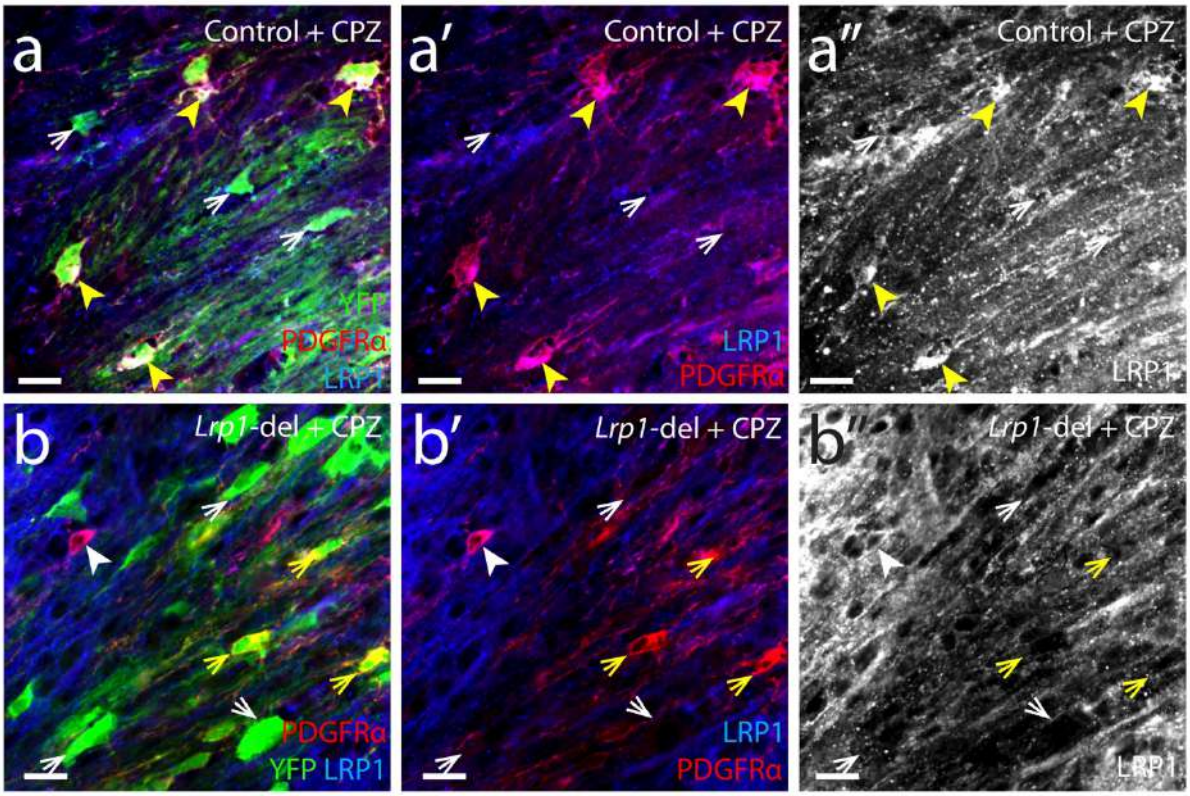

Figure 28: SVZ derived OPCs express LRP1 following cuprizone administration

Control (*Pdgfrα-CreER*^{TM} *:: Rosa26YFP*) and *Lrp1*-deleted (*Pdgfrα-CreER*^{TM} *:: Rosa26YFP :: Lrp1*$^{fl/fl}$) mice were fed a diet containing 0.2% cuprizone for 5 weeks. Representative images of the corpus callosum from control (**a**) and *Lrp1*-deleted (**b**) mice immunostained to detect OPCs (PDGFRα, red), YFP (green) and LRP1 (blue). Yellow arrowheads indicate PDGFRα^{+},YFP^{+} ,LRP1^{+} cells, white arrowheads indicate PDGFRα^{+}, YFP-negative, LRP1^{+} cells, yellow arrows indicate PDGFRα^{+}, YFP^{+}, LRP1-negative cells and white arrows indicate PDGFRα-negative, YFP^{+} LRP1-negative cells. Scale bar represents 34μm

mice was also equivalent (**Fig. 26l**, t-test genotype, p=0.8, n=>4 mice per genotype) total OL production from parenchymal and stem cell-derived OPCs was equivalent in control and *Lrp1* deleted mice on a cuprizone diet.

These data suggest that LRP1 does not influence OPC differentiation in the same way in the healthy and injured CNS. Within the demyelinated environment, parenchymal OPCs lacking *Lrp1* appear to produce the same number of new OLs as those with intact LRP1, but the resulting OLs are less able to remyelinate the lesion site.

4.3 Discussion

Understanding the signalling pathways that regulate OPC and OL function is critical to improving myelin repair outcomes. LRP1 is highly expressed in OPCs, and while its function is yet to be fully elucidated, LRP1 expression is rapidly downregulated as OPCs differentiate into OLs (Cahoy et al., 2008; Zhang et al., 2014; Auderset et al., 2016a). In other cell types, LRP1 signals in a variety of different ways (Lillis et al., 2008; Auderset et al., 2016b; Bres and Faissner, 2019), regulating cellular functions including proliferation, differentiation (Boucher et al., 2007; Mao et al., 2016; Safina et al., 2016) and migration (Mantuano et al., 2010; Barcelona et al., 2013; Mantuano et al., 2015; Ferrer et al., 2016; Sayre and Kokovay, 2019). To examine the importance of LRP1 signalling for adult OPC function, we conditionally deleted *Lrp1* from essentially all OPCs in the adult mouse brain and examined the effect that *Lrp1*-deletion had on OPC proliferation, oligodendrogenesis, and adult myelination. We found that in the healthy CNS, *Lrp1* deletion led to a significant increase in the generation of new-born OLs with no impact on OL morphology. However, following demyelination, LRP1 no longer influenced the number of new OLs produced by OPCs, but instead influenced the capacity of the resulting OLs to remyelinate.

4.3.1 Why does *Lrp1*-deletion have a delayed effect on OPC proliferation in the healthy adult CNS?

In the healthy adult mouse CNS, most OPCs are in G_0 at any given time (Psachoulia et al., 2009). OPCs in the corpus callosum re-enter the cell cycle to divide once every ~10 days, while those in the cortex divide once every ~38 days (Young et al., 2013). We found that *Lrp1*-deletion did not immediately alter the proportion of OPCs in S-phase of the cell cycle, as the proportion of OPCs that became EdU labelled over time was equivalent between control and *Lrp1*-deleted mice in the corpus callosum and cortex. However, when EdU was instead delivered 32 days after *Lrp1* deletion, we found that more OPCs in the corpus callosum were in S-phase of the cell cycle in *Lrp1*-deleted mice compared with controls. LRP1 has been shown to influence the proliferation of other cell types (Boucher et al., 2007; Basford et al., 2009; Mao et al., 2016; Safina et al., 2016; Yang et al., 2018; Zucker et al., 2019), negatively influencing the hypoxia-induced proliferation of mouse and human retinal endothelial cells, by regulating the activity of poly (ADP-ribose) polymerase-1 (PARP-1) (Mao et al., 2016), and suppressing the proliferation of mouse vascular smooth muscle cells *in vivo*, by reducing PDGFRβ activity (Boucher et al., 2003; Basford et al., 2009). OPCs do not express PDGFRβ, and while they do express the closely related mitogenic cell surface receptor PDGFRα (Asakura et al., 1997), we found that PDGFRα expression by OPCs was not altered following *Lrp1*-deletion, indicating that LRP1 does not suppress OPC proliferation by influencing PDGFRα expression.

As *Lrp1*-deletion does not acutely influence OPC proliferation *in vivo*, the effect of LRP1 on OPC proliferation may be indirect. Indeed, deleting *Lrp1* from early postnatal OPCs *in vitro* does not alter their proliferation (EdU-incorporation), nor does exposure to the LRP1 ligands tPA or *α2M. *Lrp1*-deletion also failed to alter the proliferation of OPCs isolated from early postnatal *Olig-2Cre :: Lrp1*$^{fl/fl}$ mice (Lin et al., 2017). LRP1 could indirectly influence OPC proliferation by modulating the endocytosis, degradation and recycling of cell surface proteins

and their ligands (Takayama et al., 2005; Parkyn et al., 2008; Liu et al., 2010; Muratoglu et al., 2010; Capurro et al., 2012; Farfán et al., 2013; Maier et al., 2013; Mantuano et al., 2013b; Kadurin et al., 2017; Wujak et al., 2018; Schubert et al., 2019). For example, LRP1 can regulate VGCC receptor function and distribution in a human kidney cell line (Kadurin et al., 2017), and the targeted deletion of *Cacna1c* (L-Type VGCC), using *Pdgfrα-CreER*^{TM} *:: Cacna1c* $^{fl/fl}$ mice, increases OPC proliferation in the adult mouse corpus callosum and motor cortex (Pitman et al., 2019). Therefore, we hypothesised that *Lrp1*-deletion could alter the trafficking of VGCCs to ultimately influence OPC proliferation, however, we found no evidence that LRP1 regulated VGCC function or distribution in OPCs. The influence of *Lrp1*-deletion on OPC proliferation could alternatively result from compensation from another LDL receptor family member. Notably, LRP2 has been linked to the enhanced survival and proliferation of melanoma cells (Andersen et al., 2015) as well as an increased risk of relapses in MS (Zhou et al., 2017), and is similar in size and structure to LRP1 (Spuch et al., 2012). However, we found no evidence of LRP2 expression in oligodendrocyte lineage cells in the healthy brain of control or *Lrp1*-deleted mice.

As OPC differentiation can trigger OPC proliferation *in vivo* (Hughes et al., 2013), LRP1 could also have a secondary effect on OPC proliferation by influencing OPC differentiation. We found that the deletion of *Lrp1* from OPCs in the healthy adult mouse brain was associated with the increased addition of new (YFP-labelled) OLs. Furthermore, deleting *Lrp1* from early postnatal OPCs *in vitro* had a significant effect on the number of OPCs that became MBP^{+} OLs, suggesting that LRP1 is a direct negative regulator of OPC differentiation. These data appear to conflict with a previous study, that indicated that the expression of *Myrf*, *Mbp* and *CNPase* mRNA was equivalent in OPCs cultured from the cortex of early postnatal *Olig1-Cre* and *Olig1-Cre :: Lrp1*$^{fl/fl}$ mice (Fernandez-Castaneda et al., 2019). This discrepancy may be the result of our quantifying protein expression instead of gene expression, examining differentiation over

72 rather than 48 hours, or deleting *Lrp1* immediately prior to differentiation, rather than *in utero*. However, if *Lrp1*-deletion has a similar effect *in vivo*, leading to enhanced OPC differentiation, it could readily stimulate the homeostatic division of OPCs, increasing OPC proliferation to maintain a stable pool of progenitor cells (Hughes et al., 2013).

4.3.2 LRP1 is a negative regulator of adult oligodendrogenesis

New OLs are added to the adult mouse CNS throughout life (Dimou et al., 2008; Rivers et al., 2008; Kang et al., 2010b; Zhu et al., 2011), however, when we followed the fate of adult OPCs after *Lrp1* deletion, we observed a significant increase in the number of new OLs added to the corpus callosum and motor cortex within 30 and 45 days of gene deletion. By contrast, deleting *Lrp1* from cells of the OL lineage in the developing mouse (*Olig2-Cre :: Lrp1*$^{fl/fl}$) has been shown to reduce the number of OLs detected in the optic nerve and result in hypomyelination by P21 (Lin et al., 2017). This phenotype was attributed to a role for LRP1 in promoting cholesterol homeostasis and peroxisome function, and consequently developmental OPC differentiation (Lin et al., 2017). Differences in the developing and adult brain environments (Velez-Fort et al., 2010), or changes in gene expression between developmental and adult OPCs (Spitzer et al., 2019) could account for LRP1 promoting developmental OPC differentiation, but suppressing adult OPC differentiation. However, our *in vitro* data suggest that LRP1 can suppress the differentiation of developmental OPCs derived from the mouse cortex. As deleting *Lrp1* from neural stem and progenitor cell reduces the ability of these cells to generate cells of the OL lineage (Hennen et al., 2013; Safina et al., 2016), and *Olig2* can be expressed by murine radial glia and transiently expressed by neonatal astrocytes (Marshall et al., 2005; Cai et al., 2007), it is also possible that the developmental

deletion of *Lrp1* from *Olig2*$^{+}$ cells includes its deletion from some neural stem or progenitor cells during development, and limits the generation of OLs, impairing myelination.

In the adult mouse brain, *Lrp1*-deleted OPCs produced a larger number of YFP^{+} OLs for the corpus callosum and motor cortex than *Lrp1*-intact OPCs. However, YFP does not reveal the full morphology of the cell, so that it is not possible to determine whether *Lrp1* regulated the number of newly formed pre-myelinating OLs and / or the number of new mature OLs that contributed myelin to the CNS. In the healthy adult mouse brain, there is a significant population of pre-myelinating OLs (Xiao et al., 2016; Fard et al., 2017) that are constantly turned over, as ~78% of newly generated pre-myelinating OLs survive less than 2 days (Hughes et al., 2018). By instead performing lineage tracing, visualising the newly generated OLs using LE-*Pdgfrα-CreER^{T2} :: Tau-mGFP* mouse line, we confirmed that *Lrp1*-deletion was associated with an overall increase in new OL number. However, as the proportion of new YFP^{+} oligodendrocytes that were pre-myelinating and myelinating oligodendrocytes was equivalent in the context of healthy adult control and *Lrp1*-deleted mice, LRP1 appears to increase the overall number but not the rate at which new OLs mature. Furthermore, LRP1 does not influence the myelinating profile of resulting mature OLs in the healthy CNS.

4.3.3 LRP1 suppresses remyelination in the cuprizone-model of demyelination

As *Lrp1*-deletion increased OPC differentiation, we predicted that *Lrp1*-deletion would also enhance the ability of OPCs to generate new OLs in response to a demyelinating injury. However, we instead found that the generation of new OLs from parenchymal OPCs was unaffected by LRP1 expression following cuprizone administration. As cuprizone-demyelination itself robustly stimulates OPC differentiation (Xing et al., 2014; Baxi et al., 2017), it is possible that this repair response masks the effect of LRP1 on oligodendrogenesis. Alternatively, the discrepancy between the effect of *Lrp1*-deletion in health and following

injury may be explained by demyelination triggering new OPC generation from neural stem cells in the SVZ. During cuprizone administration, a significant proportion of SVZ-derived OPCs enter the corpus callosum and contribute to oligodendrogenesis (Xing et al., 2014). Within the corpus callosum of *Lrp1*-deleted mice, the migration of SVZ-derived OPCs results in a mixed population of $LRP1^+$ and LRP1-negative OPCs, which may limit the stimulatory effect of *Lrp1*-deletion on OPC differentiation. However, this seems unlikely, as *Lrp1*-deletion increased the number of new OLs added to the cortex of healthy adult LE-*Lrp1*-deleted mice, despite the presence of a mixed population of $LRP1^+$ and LRP1-negative OPCs, resulting from the lower recombination efficiency observed in these mice.

Following cuprizone-induced demyelination, we determined that both the number of parenchymal OPC-derived YFP^+ OLs and the total number of OLs in the corpus callosum was equivalent for control and *Lrp1*-deleted mice. However, the *Lrp1*-deleted mice showed a marked reduction in the proportion of the corpus callosum that was demyelinated. While this could be explained by a difference in the behaviour or pre-existing, surviving OLs contributing more new myelin sheaths, as has been described to occur in humans (Yeung et al., 2019) this is unlikely as the vast majority of OLs detected in the corpus callosum were newborn EdU^+ cells. It is more likely that the reduced lesion size results from a change in the rate of maturation of the adult-born OLs, such that a larger proportion of them are already myelinating in the corpus callosum of *Lrp1*-deleted mice. A separate study has found that 3.5 days following cuprizone withdrawal, *Olig1-Cre :: Lrp1*$^{fl/fl}$ mice have more OLs and increased MBP coverage in the corpus callosum relative to *Olig1-Cre* controls (Fernandez-Castaneda et al., 2019). As parenchymal OPCs and neural stem cell-derived OPCs all lack LRP1 in this model, these data support our finding that LRP1-expression by OPCs impacts remyelination. However, the expression of LRP1 by OPCs is unlikely to directly affect the maturing OLs, as OLs

still lack LRP1 even following demyelination. It is more likely that LRP1 expression by OPCs indirectly regulates new born OL maturation within the injury environment.

Neuroinflammation has long been associated with impaired OL generation (Miron et al., 2011), and more recently OPCs have been identified as key modulators of the neuroinflammatory environment due to their ability to upregulate and express genes associated with antigen processing and presentation (Falcao et al., 2018; Kirby et al., 2019). Furthermore, expression of a key immunomodulatory receptor on OPCs, the Interleukin 17 receptor, was reported to be critical for EAE development, as it initiated cytokine release and propagated the pathology (Wang et al., 2017). RNA profiling of the remyelinating corpus callosum of *Olig1-Cre* and *Olig1-Cre :: Lrp1*$^{fl/fl}$ mice 3.5 days after cuprizone withdrawal revealed that inflammatory gene expression was suppressed in the environment containing *Lrp1*-deleted OPCs (Fernandez-Castaneda et al., 2019). As LRP1 expression by OPCs influences the inflammatory nature of the remyelinating environment, the enhanced remyelination we observe in *Lrp1*-deleted mice may reflect the level of influence that inflammation can exert on myelin repair in control versus *Lrp1*-deleted mice.

It is currently unclear how LRP1 expression by OPCs influences inflammation within the remyelinating corpus callosum, however, LRP1 could be cleaved from OPCs or result in their secretion of pro-inflammatory factors that then influence the function of other cell types. For example, when purified shed LRP1 (sLRP1) was added to microglia *in vitro* it induced a potent pro-inflammatory response (Brifault et al., 2017). Furthermore, *Lrp1* deletion from microglia *in vivo* significantly attenuated microglial activation and pro-inflammatory cytokine expression in the spinal dorsal horn following partial sciatic nerve ligation (Brifault et al., 2019). In light of these findings, it is possible that LRP1 shedding from OPCs may be acting on nearby microglia, amplifying inflammation within the local environment and impairing timely

remyelination. Alternatively, LRP1 may influence antigen presentation by OPCs, influencing the activity of other inflammatory cells (Fernadez-Castaneda et al., 2019). Therefore, while LRP1 appears to perform a cell-autonomous role in promoting OPC differentiation in the healthy brain, its role following demyelination appears to be more complex, and will require further research to fully elucidate the mechanism by which LRP1 expression by OPCs influences other cells within the demyelinated and remyelinating environment.

Chapter 5 – Final Discussion and Future Directions

Data presented in this thesis indicate that, consistent with microarray and RNA sequencing studies (Cahoy et al., 2008; Zhang et al., 2014), LRP1 is expressed by a number of CNS cell types throughout development and in adulthood, including neurons, astrocytes and microglia, however, LRP1 is not expressed by parvalbumin-expressing interneurons (Chapter 3). Within the OL lineage, LRP1 is expressed by OPCs and rapidly downregulated as OPCs differentiate into OLs (Chapter 3). Furthermore, in the healthy adult CNS, LRP1 acts to suppress oligodendrogenesis, as a larger number of newborn OLs are derived from *Lrp1*-deleted OPCs compared to control OPCs (Chapter 4). Of the newborn OLs produced over a 30 day period, there was no change in the proportion of mature OLs compared to premyelinating OLs, suggesting that OPCs that lack *Lrp1* mature at the same rate as control OPCs. While LRP1 does influence the number of myelinating OLs, by analysing individual newborn myelinating OLs, we determined that LRP1 did not influence the myelin load of individual cells, having no impact on the number or length of internodes they ultimately elaborate (Chapter 4). By contrast, following cuprizone-induced demyelination of the corpus callosum, *Lrp1*-deletion did not affect the number of new OLs generated, but did reduce the area of the corpus callosum that was demyelinated, suggesting that LRP1 expression by OPCs acts (presumably indirectly) to reduce the maturation of or myelination by newborn OLs in an inflammatory environment (Chapter 4).

5.1 Does LRP1 expression by OPCs suppress newborn OL maturation and myelination following CNS injury?

Having shown that LRP1 inhibits oligodendrocyte generation in the healthy adult CNS, I wanted to look at its role in the demyelinated CNS. I found that lesion area was reduced in *Pdgfrα-CreER^{T2} ::Rosa-26YFP :: Lrp1$^{fl/fl}$* mice following cuprizone administration compared to controls, however, surprisingly there was no associated increase in oligodendrogenesis (Chapter 4). This suggests that the newborn OLs are able to mature more quickly and remyelinate more efficiently in the *Lrp1*-deleted mice following cuprizone administration. Visualisation of newly formed premyelinating and mature myelinating OLs in the remyelinated region would answer the question of enhanced maturation of *Lrp1* deficient OPCs.

OL maturation could be visualised using the LE-control and LE- *Lrp1*-del mice. However, this is unlikely to be successful a high level of recombination is needed to evaluate the effect of *Lrp1* deletion, and this will also result in GFP labelling of a large number of newborn callosal OLs precluding the visualisation of isolated OL for morphological analysis. An alternate approach would be to further analyse control and *Lrp1* deleted mice, examining expression of specific markers that label premyelinating OLs such, as BCAS1 or *Enpp6* for *in situ* hybridisation detection.

One downside to using the inducible *Pdgfrα-CreER^{T2} :: Lrp1$^{fl/fl}$* mouse is that the new SVZ-derived OPCs born during cuprizone administration expressed intact LRP1, creating a mixed population of LRP1^{+} and Lrp1-negative OPCs within the corpus callosum. Other studies looking at the role of LRP1 in oligodendrocyte lineage cells did not have this problem as they were using a constitutively active *Olig1-Cre* or *Olig2-Cre* mouse. However, this ultimately means that *Lrp1* is deleted from oligodendrocyte lineage cells throughout development, making it difficult to look specifically at LRP1 function during adulthood. One way to eliminate the influence of SVZ-derived OPCs would be to repeat the experiments using the EAE model of

neuroinflammation. EAE primarily effects the spinal cord and the contribution of NSPCs to OPC addition and remyelination is minimal (Maeda et al., 2019).

5.2 LRP1 as an inflammatory mediator

The immunomodulatory role of OPCs is an emerging area of research (Falcao et al., 2018; Kirby et al., 2019) and it would be interesting to better understand the role that LRP1 plays in regulating the inflammatory response. A previous study has proposed that in a demyelinated environment, LRP1 is required for the internalisation of antigen which leads to processing and cross presentation via MHC1 and subsequent activation of CD8 lymphocytes, exacerbating the inflammatory response (Fernandez-Castaneda et al., 2019). The upregulation of antigen presenting molecules on OPCs following cuprizone would be interesting to visualise immunohistochemically but would be difficult to observe due to the increased activation of microglia. Isolating OPCs *in vitro* and adding conditioned medium containing myelin debris and inflammatory cytokines may provide a better way to visualise antigen presentation. Additionally, it would be interesting to see whether OPCs that lack LRP1 are able to participate in antigen presentation as effectively as control OPCs. Another intriguing aspect of LRP1 signalling is the formation of soluble LRP1 (sLRP1) following cleavage of the extracellular domain (Quinn et al., 1999; Arnim et al., 2005). sLRP1 can be found in plasma and CSF and is upregulated following LPS exposure as well as in patients with rheumatoid arthritis (Liu et al., 2009; Yamamoto et al., 2017). In myeloid cells, proteolytic shedding of LRP1 is thought to be a key step in the conversion of LRP1 from an anti-inflammatory to a pro-inflammatory molecule (Gorovoy et al., 2010; Brifault et al., 2017). There is currently no evidence to show that LRP1 can be shed from OPCs but if something in the demyelinated environment is causing LRP1 to be released from OPCs then it may contribute to the level of neuroinflammation. Testing this on OPCs should be quite simple, as previous studies have shown that the addition

of LPS to cultured microglia is sufficient to stimulate the release of sLRP1 (Brifault et al., 2017). Following on from that, it would be interesting to look at the overall level of microglial activation and the presence of inflammatory cytokines in the corpus callosum of control and *Lrp1*-deleted mice after cuprizone administration. If there is an observable difference, it may be due to impaired antigen presentation and/or reduced shedding of LRP1 from OPCs, creating an environment that is more accommodating to remyelination.

5.3 How does LRP2 contribute to MS pathology?

The possibility of compensation from other LDL family receptors was thought to contribute to the delayed generation of a phenotype following *Lrp1* deletion. This hypothesis was strengthened by the discovery of a mutation in *Lrp2* that led to an increased risk of developing relapse in people with MS (Zhou et al., 2017). However, when looking in the CNS of control and *Lrp1*-deleted mice, I found no evidence that LRP2 was expressed by OPCs or OLs, suggesting that the mutation found in people with MS is unlikely to affect cells of the oligodendrocyte lineage (Chaper 4). I did however find that LRP2 is highly expressed by $IBA1^{+}$ microglia and, to my knowledge, this is the first time that LRP2 has been shown to be expressed by these cells. This discovery opens up a number of questions relating to its potential role in MS progression and warrants further investigation. LRP2 is most widely known for its in renal function but it is also a significant player in neural development due to its role in facilitating the endocytosis of Shh (Christ et al., 2012). In the injured and inflamed CNS, upregulation of Shh has been shown to promote neural repair (Bambakidis et al., 2003; Amankulor et al., 2009) and silence the immune system in mice with EAE (Alvarez et al., 2011). As activated microglia are abundant in actively demyelinating lesions (Mycko et al., 2003; Sun et al., 2006), it is possible that deficiencies in Shh signalling result from an *Lrp2* gene mutation and may worsen demyelination, leading to increased occurrence of relapse. A follow up study

deleting *Lrp2* specifically from microglia using a *Cx3cr1-CreER^{T2} :: Lrp2$^{fl/fl}$* mice prior to the induction EAE or cuprizone induced demyelination may uncover a novel role of microglial LRP2 signalling in the demyelinated CNS.

5.4 Conclusion

By deleting LRP1 from OPCs in the adult CNS, this thesis builds upon the growing body of evidence that outlines the genes involved in regulating OPC behaviour in the healthy adult CNS. Further studies are needed in order to determine how LRP1 alters the behaviour of OPCs in an inflammatory environment and ultimately determine whether the inhibition of LRP1 signalling on OPCs could be a useful therapeutic intervention for demyelinating diseases.

Appendix

PCR Primers

Primer Name	Sequence
LRP1 5'	CATAC CCTCT CAAACC CCTT CCTG
LRP1 3'	GCAAG CTCC CTGCTCA GACC TGGA
Cre 5'	CAGGT CTCAG GAGCT ATGTC CAATT TACTG ACCGTA
Cre 3'	GGTGT TATAAG CAATCC CCAGAA
Rosa26 5' WT	AAAGT CGCTC TGAGT TGTTA
Rosa26 5' Mut	GCGAA GAGTT TGTCC TCAACC
Rosa26 3' WT	GGAGC GGGAG AAATG GATATG
GFP 5'	CCCTG AAGTTC ATCTG CACCAC
GFP 3'	TTCTC GTTGG GGTCT TTGCTC
LRP1 reco 5'	CCCAA GGAAAA TCAGG CCTCCGC
LRP1 reco 3'	CGCGG CAATCC TGACA GTGCG

Antibodies for immunofluorescence

Antibody	Species	Concentration	Manufacturer	Catalogue Number
LRP1	Rabbit	1:1000	Abcam	AB92544
PDGFRα	Goat	1:100	R&D Systems	AF1062
PSANCAM	Mouse	1:500	Millipore	MAB5324
RC2	Mouse	1:100	Millipore	MAB5740
GFAP	Mouse	1:2000	BD Pharmigen	556327
IBA1	Guinea Pig	1:250	Synaptic Systems	234004
CC1	Mouse	1:200	Millipore	MABC200
NeuN	Mouse	1:200	Millipore	MAB337
GFP	Rat	1:2000	Nacalitesque	04404-26
OLIG2	Rabbit	1:400	Millipore	AB9610
Parvalbumin	Mouse	1:1000	Millipore	MAB1572
LRP2	Rabbit	1:100	Abcam	AB76967

Cell culture medium

OPC medium (50ml)	Volume	Final Conc.
DMEM	~44ml	-
PDGF-AA	20µl	20ng/ml
FGF	5µl	10ng/ml
CNTF	25µl	10ng/ml
NAC	50µl	5µg/ml
NT3	5µl	1ng/ml
Biotin	10µl	1ng/ml
Forskolin	25µl	10µM
10X SATO Stock	5ml	1X
Pen/Strep	500µl	1X
B27	1ml	2%

SATO Stock

10X SATO Stock (100ml)		Final Conc
Transferrin	100mg	1mg/ml
BSA	100mg	1mg/ml
Progesterone (1mg/ml in EtOH)	60µl	600ng/ml
Sodium selenite 1mg/ml in 0.1M NaOH)	40µl	400ng/ml
Putrescine	16mg	160µg/ml
Insulin (10mg/ml in 10% Acetic Acid)	500µl	50µg/ml

OPC differentiation medium

Differentiation medium (50ml)	Volume	Final Conc.
DMEM	~44ml	-
T3	66µl	4µg/ml
FGF	5µl	10ng/ml
CNTF	25µl	10ng/ml
NAC	50µl	5µg/ml
NT3	5µl	1ng/ml
Biotin	10µl	1ng/ml
Forskolin	25µl	10µM
10X SATO Stock	5ml	1X
Pen/Strep	500µl	1X
B27	1ml	2%

RIPA cell lysis buffer

RIPA Buffer (10ml)	Volume	Final Conc
MilliQ	8190µl	-
1M Tris-HCl (pH7.4)	500µl	50mM
5M NaCl	300µl	150mM
10% NP-40	1ml	1%
Sodium deoxycholate	100mg	1%
10% SDS	10µl	0.10%
Protease inhibitor tablet	1 per 10ml	-

References

Alberti S, Krause SM, Kretz O, Philippar U, Lemberger T, Casanova E, Wiebel FF, Schwarz H, Frotscher M, Schütz G, Nordheim A (2005) Neuronal migration in the murine rostral migratory stream requires serum response factor. Proc Natl Acad Sci USA 102:6148–6153.

Alcántara S, Ruiz M, D'Arcangelo G, Ezan F, de Lecea L, Curran T, Sotelo C, Soriano E (1998) Regional and cellular patterns of reelin mRNA expression in the forebrain of the developing and adult mouse. Journal of Neuroscience 18:7779–7799.

Alvarez JI, Dodelet-Devillers A, Kebir H, Ifergan I, Fabre PJ, Terouz S, Sabbagh M, Wosik K, Bourbonniere L, Bernard M, van Horssen J, de Vries HE, Charron F, Prat A (2011) The Hedgehog Pathway Promotes Blood-Brain Barrier Integrity and CNS Immune Quiescence. Science 334:1727–1731.

Amankulor NM, Hambardzumyan D, Pyonteck SM, Becher OJ, Joyce JA, Holland EC (2009) Sonic Hedgehog Pathway Activation Is Induced by Acute Brain Injury and Regulated by Injury-Related Inflammation. Journal of Neuroscience 29:10299–10308.

Ambjørn M, Asmussen JW, Lindstam M, Gotfryd K, Jacobsen C, Kiselyov VV, Moestrup SK, Penkowa M, Bock E, Berezin V (2008) Metallothionein and a peptide modeled after metallothionein, EmtinB, induce neuronal differentiation and survival through binding to receptors of the low-density lipoprotein receptor family. Journal of Neurochemistry 104:21–37.

Andersen RK, Hammer K, Hager H, Christensen JN, Ludvigsen M, Honoré B, Thomsen M-BH, Madsen M (2015) Melanoma tumors frequently acquire LRP2/megalin expression, which modulates melanoma cell proliferation and survival rates. Pigment Cell Melanoma Res 28:267–280.

Andrade N, Komnenovic V, Blake SM, Jossin Y, Howell B, Goffinet A, Schneider WJ, Nimpf J (2007) ApoER2/VLDL receptor and Dab1 in the rostral migratory stream function in postnatal neuronal migration independently of Reelin. PNAS 104:8508–8513.

Aranda JF, Canfran-Duque A, Goedeke L, Suarez Y, Fernandez-Hernando C (2015) The miR-199-dynamin regulatory axis controls receptor-mediated endocytosis. J Cell Sci 128:3197–3209.

Arnim von CAF, Kinoshita A, Peltan ID, Tangredi MM, Herl L, Lee BM, Spoelgen R, Hshieh TT, Ranganathan S, Battey FD, Liu CX, Bacskai BJ, Sever S, Irizarry MC, Strickland DK, Hyman BT (2005) The Low Density Lipoprotein Receptor-related Protein (LRP) Is a Novel -Secretase (BACE1) Substrate. Journal of Biological Chemistry 280:17777–17785.

Asakura K, Hunter SF, Rodriguez M (1997) Effects of transforming growth factor-beta and platelet-derived growth factor on oligodendrocyte precursors: insights gained from a neuronal cell line. Journal of Neurochemistry 68:2281–2290.

Assémat E, Châtelet F, Chandellier J, Commo F, Cases O, Verroust P, Kozyraki R (2005) Overlapping expression patterns of the multiligand endocytic receptors cubilin and megalin in the CNS, sensory organs and developing epithelia of the rodent embryo. Gene Expr Patterns 6:69–78.

Auderset L, Cullen CL, Young KM (2016a) Low Density Lipoprotein-Receptor Related Protein 1 Is Differentially Expressed by Neuronal and Glial Populations in the Developing and Mature Mouse Central Nervous System. Coulson EJ, ed. PLoS ONE 11:e0155878–22.

Auderset L, Landowski LM, Foa L, Young KM (2016b) Low Density Lipoprotein Receptor Related Proteins as Regulators of Neural Stem and Progenitor Cell Function. Stem Cells International 2016:2108495–16.

Auer F, Vagionitis S, Czopka T (2018) Evidence for Myelin Sheath Remodeling in the CNS Revealed by In Vivo Imaging. Curr Biol 28:549–559.e3.

Avrov K, Kazlauskas A (2003) The role of c-Src in platelet-derived growth factor alpha receptor internalization. Experimental Cell Research 291:426–434.

Bacmeister CM, Barr HJ, McClain CR, Thornton MA, Nettles D, Welle CG, Hughes EG (2020) Motor Learning Promotes Remyelination via New and Surviving Oligodendrocytes. bioRxiv, p. 2020.01.28.923656.

Balabanov R, Strand K, Goswami R, McMahon E, Begolka W, Miller SD, Popko B (2007) Interferon-gamma-oligodendrocyte interactions in the regulation of experimental autoimmune encephalomyelitis. J Neurosci 27:2013–2024.

Bambakidis NC, Wang RZ, Franic L, Miller RH (2003) Sonic hedgehog-induced neural precursor proliferation after adult rodent spinal cord injury. J Neurosurg 99:70–75.

Baraban M, Koudelka S, Lyons DA (2018) Ca 2+ activity signatures of myelin sheath formation and growth in vivo. Nature Publishing Group 21:19–23.

Barcelona PF, Jaldin-Fincati JR, Sanchez MC, Chiabrando GA (2013) Activated 2-macroglobulin induces Muller glial cell migration by regulating MT1-MMP activity through LRP1. The FASEB Journal 27:3181–3197.

Barrera K, Chu P, Abramowitz J, Steger R, Ramos RL, Brumberg JC (2013) Organization of myelin in the mouse somatosensory barrel cortex and the effects of sensory deprivation. Devel Neurobio 73:297–314.

Bartzokis G (2004) Age-related myelin breakdown: a developmental model of cognitive decline and Alzheimer's disease. Neurobiology of Aging 25:5–18–authorreply49–62.

Basford JE, Moore ZWQ, Zhou L, Herz J, Hui DY (2009) Smooth muscle LDL receptor-related protein-1 inactivation reduces vascular reactivity and promotes injury-induced neointima formation. Arteriosclerosis, Thrombosis, and Vascular Biology 29:1772–1778.

Baxi EG, DeBruin J, Jin J, Strasburger HJ, Smith MD, Orthmann-Murphy JL, Schott JT, Fairchild AN, Bergles DE, Calabresi PA (2017) Lineage tracing reveals dynamic changes in oligodendrocyte precursor cells following cuprizone-induced demyelination. Glia 65:2087–2098.

Bechler ME, Byrne L, ffrench-Constant C (2015) CNS Myelin Sheath Lengths Are an Intrinsic Property of Oligodendrocytes. Curr Biol 25:2411–2416.

Beisiegel U, Weber W, Ihrke G, Herz J, Stanley KK (1989) The LDL-receptor-related protein, LRP, is an apolipoprotein E-binding protein. Nature 341:162–164.

Beniac DR, Wood DD, Palaniyar N, Ottensmeyer FP, Moscarello MA, Harauz G (2000) Cryoelectron microscopy of protein-lipid complexes of human myelin basic protein charge isomers differing in degree of citrullination. J Struct Biol 129:80–95.

Bentley D, O'Connor TP (1994) Cytoskeletal events in growth cone steering. Current Opinion in Neurobiology 4:43–48.

Bento-Abreu A, Velasco A, Polo-Hernández E, Lillo C, Kozyraki R, Tabernero A, Medina JM (2009) Albumin endocytosis via megalin in astrocytes is caveola- and Dab-1 dependent and is required for the synthesis of the neurotrophic factor oleic acid. Journal of Neurochemistry 111:49–60.

Bento-Abreu A, Velasco A, Polo-Hernndez E, Prez-Reyes PL, Tabernero A, Medina JM (2008) Megalin is a receptor for albumin in astrocytes and is required for the synthesis of the neurotrophic factor oleic acid. Journal of Neurochemistry 106:1149–1159.

Bergles DE, Roberts J, Somogyi P, Jahr CE (2000) Glutamatergic synapses on oligodendrocyte precursor cells in the hippocampus. Nature 405:187–191.

Bhat RV, Axt KJ, Fosnaugh JS, Smith KJ, Johnson KA, Hill DE, Kinzler KW, Baraban JM (1998) Expression of the APC tumor suppressor protein in oligodendroglia. Glia, vol. 17 (2) pp. 169-174.

Biemesderfer D (2006) Regulated intramembrane proteolysis of megalin: linking urinary protein and gene regulation in proximal tubule? Kidney International 69:1717–1721.

Biname F, Sakry D, Dimou L, Jolivel V, Trotter J (2013) NG2 Regulates Directional Migration of Oligodendrocyte Precursor Cells via Rho GTPases and Polarity Complex Proteins. Journal of Neuroscience 33:10858–10874.

Binder RJ, Han DK, Srivastava PK (2000) CD91: a receptor for heat shock protein gp96. Nat Immunol 1:151–155.

Birey F, Kloc M, Chavali M, Hussein I, Wilson M, Christoffel DJ, Chen T, Frohman MA, Robinson JK, Russo SJ, Maffei A, Aguirre A (2015) Genetic and Stress-Induced Loss of NG2 Glia Triggers Emergence of Depressive-like Behaviors through Reduced Secretion of FGF2. Neuron 88:–956.

Blake SM, Strasser V, Andrade N, Duit S, Hofbauer R, Schneider WJ, Nimpf J (2008) Thrombospondin-1 binds to ApoER2 and VLDL receptor and functions in postnatal neuronal migration. EMBO J 27:3069–3080.

Bolos M, Fernandez S, Torres-Aleman I (2010) Oral Administration of a GSK3 Inhibitor Increases Brain Insulin-like Growth Factor I Levels. Journal of Biological Chemistry 285:17693–17700.

Boucher P, Gotthardt M, Li WP, Anderson R, Herz J (2003) LRP: Role in vascular wall integrity and protection from atherosclerosis. Science 300:329–332.

Boucher P, Li W-P, Matz RL, Takayama Y, Auwerx J, Anderson RGW, Herz J (2007) LRP1 Functions as an Atheroprotective Integrator of TGFβ and PDGF Signals in the Vascular Wall: Implications for Marfan Syndrome. PLoS ONE 2:e448.

Boucher P, Liu P, Gotthardt M, Hiesberger T, Anderson RGW, Herz J (2002) Platelet-derived growth factor mediates tyrosine phosphorylation of the cytoplasmic domain of the low Density lipoprotein receptor-related protein in caveolae. Journal of Biological Chemistry 277:15507–15513.

Boyles JK, Pitas RE, Wilson E, Mahley RW, Taylor JM (1985) Apolipoprotein E associated with astrocytic glia of the central nervous system and with nonmyelinating glia of the peripheral nervous system. J Clin Invest 76:1501–1513.

Bradford CM, Ramos I, Cross AK, Haddock G, McQuaid S, Nicholas AP, Woodroofe MN (2014) Localisation of citrullinated proteins in normal appearing white matter and lesions in the central nervous system in multiple sclerosis. J Neuroimmunol 273:85–95.

Bres EE, Faissner A (2019) Low Density Receptor-Related Protein 1 Interactions With the Extracellular Matrix: More Than Meets the Eye. Front Cell Dev Biol 7:1916.

Brifault C, Gilder AS, Laudati E, Banki M, Gonias SL (2017) Shedding of membrane-associated LDL receptor-related protein-1 from microglia amplifies and sustains neuroinflammation. Journal of Biological Chemistry 292:18699–18712.

Brifault C, Kwon H, Campana WM, Gonias SL (2019) LRP1 deficiency in microglia blocks neuro-inflammation in the spinal dorsal horn and neuropathic pain processing. Glia 67:1210–1224.

Brown MS, Goldstein JL (1986) A Receptor-Mediated Pathway for Cholesterol Homeostasis. Science 232:34–47.

Brown SD, Twells R, Hey PJ, Cox RD, Levy ER, Soderman AR, Metzker ML, Caskey CT, Todd JA, Hess JF (1998) Isolation and characterization of LRP6, a novel member of the low density lipoprotein receptor gene family. Biochem Biophys Res Commun 248:879–888.

Bu G, Geuze HJ, Strous GJ, Schwartz AL (1995) 39 kDa receptor-associated protein is an ER resident protein and molecular chaperone for LDL receptor-related protein. EMBO J 14:2269–2280.

Bu G, Maksymovitch EA, Nerbonne JM, Schwartz AL (1994) Expression and function of the low density lipoprotein receptor-related protein (LRP) in mammalian central neurons. Journal of Biological Chemistry 269:18521–18528.

Bu G, Maksymovitch EA, Schwartz AL (1993) Receptor-mediated endocytosis of tissue-type plasminogen activator by low density lipoprotein receptor-related protein on human hepatoma HepG2 cells. Journal of Biological Chemistry 268:13002–13009.

Bu GJ, Marzolo MP (2000) Role of RAP in the biogenesis of lipoprotein receptors. Trends Cardiovasc Med 10:148–155.

Butt SJB, Fuccillo M, Nery S, Noctor S, Kriegstein A, Corbin JG, Fishell G (2005) The Temporal and Spatial Origins of Cortical Interneurons Predict Their Physiological Subtype. Neuron 48:591–604.

Cahoy JD, Emery B, Kaushal A, Foo LC, Zamanian JL, Christopherson KS, Xing Y, Lubischer JL, Krieg PA, Krupenko SA, Thompson WJ, Barres BA (2008) A Transcriptome Database for Astrocytes, Neurons, and Oligodendrocytes: A New Resource for Understanding Brain Development and Function. Journal of Neuroscience 28:264–278.

Cai J, Chen Y, Cai W-H, Hurlock EC, Wu H, Kernie SG, Parada LF, Lu QR (2007) A crucial role for Olig2 in white matter astrocyte development. Development 134:1887–1899.

Cai J, Qi Y, Hu X, Tan M, Liu Z, Zhang J, Li Q, Sander M, Qiu M (2005) Generation of oligodendrocyte precursor cells from mouse dorsal spinal cord independent of Nkx6 regulation and Shh signaling. Neuron 45:41–53.

Cam JA, Zerbinatti CV, Li Y, Bu G (2005) Rapid Endocytosis of the Low Density Lipoprotein Receptor-related Protein Modulates Cell Surface Distribution and Processing of the -Amyloid Precursor Protein. Journal of Biological Chemistry 280:15464–15470.

Campana WM, Li X, Dragojlovic N, Janes J, Gaultier A, Gonias SL (2006) The Low-Density Lipoprotein Receptor-Related Protein Is a Pro-Survival Receptor in Schwann Cells: Possible Implications in Peripheral Nerve Injury. Journal of Neuroscience 26:11197–11207.

Capurro MI, Shi W, Filmus J (2012) LRP1 mediates Hedgehog-induced endocytosis of the GPC3-Hedgehog complex. J Cell Sci 125:3380–3389.

Casse F, Bardou I, Danglot L, Briens A, Montagne A, Parcq J, Alahari A, Galli T, Vivien D, Docagne F (2012) Glutamate Controls tPA Recycling by Astrocytes, Which in Turn Influences Glutamatergic Signals. Journal of Neuroscience 32:5186–5199.

Castellano J, Aledo R, Sendra J, Costales P, Juan-Babot O, Badimon L, Llorente-Cortes V (2011) Hypoxia Stimulates Low-Density Lipoprotein Receptor-Related Protein-1 Expression Through Hypoxia-Inducible Factor-1 in Human Vascular Smooth Muscle Cells. Arteriosclerosis, Thrombosis, and Vascular Biology 31:1411–1420.

Caudy M, Bentley D (1986) Pioneer growth cone morphologies reveal proximal increases in substrate affinity within leg segments of grasshopper embryos. Journal of Neuroscience 6:364–379.

Chae T, Kwon YT, Bronson R, Dikkes P, Li E, Tsai LH (1997) Mice lacking p35, a neuronal specific activator of Cdk5, display cortical lamination defects, seizures, and adult lethality. Neuron 18:29–42.

Chanas-Sacré G, Thiry M, Pirard S, Rogister B, Moonen G, Mbebi C, Verdière-Sahuqué M, Leprince P (2000) A 295-kDA intermediate filament-associated protein in radial glia and developing muscle cells in vivo and in vitro. Dev Dyn 219:514–525.

Chandran S (2003) FGF-dependent generation of oligodendrocytes by a hedgehog-independent pathway. Development 130:6599–6609.

Chang A, Tourtellotte WW, Rudick R, Trapp BD (2002) Premyelinating oligodendrocytes in chronic lesions of multiple sclerosis. N Engl J Med 346:165–173.

Chari DM, Blakemore WF (2002) Efficient recolonisation of progenitor-depleted areas of the CNS by adult oligodendrocyte progenitor cells. Glia 37:307–313.

Chazal G, Durbec P, Jankovski A, Rougon G, Cremer H (2000) Consequences of neural cell adhesion molecule deficiency on cell migration in the rostral migratory stream of the mouse. Journal of Neuroscience 20:1446–1457.

Cheli VT, Santiago González DA, Spreuer V, Paez PM (2015) Voltage-gated Ca2+ entry promotes oligodendrocyte progenitor cell maturation and myelination in vitro. Experimental Neurology 265:69–83.

Chen WJ, Goldstein JL, BROWN MS (1990) Npxy, a Sequence Often Found in Cytoplasmic Tails, Is Required for Coated Pit-Mediated Internalization of the Low-Density-Lipoprotein Receptor. Journal of Biological Chemistry 265:3116–3123.

Chetrit D, Barzilay L, Horn G, Bielik T, Smorodinsky NI, Ehrlich M (2011) Negative regulation of the endocytic adaptor disabled-2 (Dab2) in mitosis. J Biol Chem 286:5392–5403.

Chew L-J, Coley W, Cheng Y, Gallo V (2010) Mechanisms of regulation of oligodendrocyte development by p38 mitogen-activated protein kinase. J Neurosci 30:11011–11027.

Choudhry Z, Rikani AA, Choudhry AM, Tariq S, Zakaria F, Asghar MW, Sarfraz MK, Haider K, Shafiq AA, Mobassarah NJ (2014) Sonic hedgehog signalling pathway: a complex network. ANS 21:1–4.

Christ A, Christa A, Kur E, Lioubinski O, Bachmann S, Willnow TE, Hammes A (2012) LRP2 Is an Auxiliary SHH Receptor Required to Condition the Forebrain Ventral Midline for Inductive Signals. Developmental Cell 22:268–278.

Chuang T-Y, Guo Y, Seki SM, Rosen AM, Johanson DM, Mandell JW, Lucchinetti CF, Gaultier A (2016) LRP1 expression in microglia is protective during CNS autoimmunity. Acta Neuropathologica Communications 2016 4:1 4:68.

Chun JT, Wang L, Pasinetti GM, Finch CE, Zlokovic BV (1999) Glycoprotein 330/megalin (LRP-2) has low prevalence as mRNA and protein in brain microvessels and choroid plexus. Experimental Neurology 157:194–201.

Clarke LE, Young KM, Hamilton NB, Li H, Richardson WD, Attwell D (2012) Properties and fate of oligodendrocyte progenitor cells in the corpus callosum, motor cortex, and piriform cortex of the mouse. J Neurosci 32:8173–8185.

Craig J, Mikhailenko I, Noyes N, Migliorini M, Strickland DK (2013) The LDL Receptor-Related Protein 1 (LRP1) Regulates the PDGF Signaling Pathway by Binding the Protein Phosphatase SHP-2 and Modulating SHP-2- Mediated PDGF Signaling Events Buday L, ed. PLoS ONE 8:e70432–10.

Croy JE, Shin WD, Knauer MF, Knauer DJ, Komives EA (2003) All three LDL receptor homology regions of the LDL receptor-related protein bind multiple ligands. Biochemistry 42:13049–13057.

Cullen CL, Senesi M, Tang AD, Clutterbuck MT, Auderset L, O'Rourke ME, Rodger J, Young KM (2019) Low-intensity transcranial magnetic stimulation promotes the survival and maturation of newborn oligodendrocytes in the adult mouse brain. Glia 67:1462–1477.

Czekay RP, Orlando RA, Woodward L, Lundstrom M, Farquhar MG (1997) Endocytic trafficking of megalin/RAP complexes: Dissociation of the complexes in late endosomes. Mol Biol Cell 8:517–532.

Czopka T, ffrench-Constant C, Lyons DA (2013) Individual oligodendrocytes have only a few hours in which to generate new myelin sheaths in vivo. Developmental Cell 25:599–609.

D'Arcangelo G, Nakajima K, Miyata T, Ogawa M, Mikoshiba K, Curran T (1997) Reelin is a secreted glycoprotein recognized by the CR-50 monoclonal antibody. Journal of Neuroscience 17:23–31.

Dahmane N, Ruiz i Altaba A (1999) Sonic hedgehog regulates the growth and patterning of the cerebellum. Development 126:3089–3100.

Dai J, Bercury KK, Ahrendsen JT, Macklin WB (2015) Olig1 Function Is Required for Oligodendrocyte Differentiation in the Mouse Brain. Journal of Neuroscience 35:4386–4402.

Dailey ME, Bridgman PC (1989) Dynamics of the endoplasmic reticulum and other membranous organelles in growth cones of cultured neurons. Journal of Neuroscience 9:1897–1909.

Daly NL, Scanlon MJ, Djordjevic JT, Kroon PA, Smith R (1995) 3-Dimensional Structure of a Cysteine-Rich Repeat From the Low-Density-Lipoprotein Receptor. PNAS 92:6334–6338.

Dawson M (2003) NG2-expressing glial progenitor cells: an abundant and widespread population of cycling cells in the adult rat CNS. Molecular and Cellular Neuroscience 24:476–488.

De Biase LM, Nishiyama A, Bergles DE (2010) Excitability and Synaptic Communication within the Oligodendrocyte Lineage. Journal of Neuroscience 30:3600–3611.

Demerens C, Stankoff B, Logak M, Anglade P, Allinquant B, Couraud F, Zalc B, Lubetzki C (1996) Induction of myelination in the central nervous system by electrical activity. Proc Natl Acad Sci USA 93:9887–9892.

Deutsch SI, Burket JA, Katz E (2010) Does subtle disturbance of neuronal migration contribute to schizophrenia and other neurodevelopmental disorders? Potential genetic mechanisms with possible treatment implications. Eur Neuropsychopharmacol 20:281–287.

Dickson BJ (2002) Molecular mechanisms of axon guidance. Science 298:1959–1964.

Dimou L, Simon C, Kirchhoff F, Takebayashi H, Gotz M (2008) Progeny of Olig2-Expressing Progenitors in the Gray and White Matter of the Adult Mouse Cerebral Cortex. Journal of Neuroscience 28:10434–10442.

Doetsch F, Caillé I, Lim DA, Garcia-Verdugo JM, Alvarez-Buylla A (1999) Subventricular zone astrocytes are neural stem cells in the adult mammalian brain. Cell 97:703–716.

Donoso M, Cancino J, Lee J, van Kerkhof P, Retamal C, Bu G, Gonzalez A, Cáceres A, Marzolo M-P (2009) Polarized traffic of LRP1 involves AP1B and SNX17 operating on Y-dependent sorting motifs in different pathways. Gruenberg JE, ed. Mol Biol Cell 20:481–497.

Drakew A, Frotscher M, Deller T, Ogawa M, Heimrich B (1998) Developmental distribution of a reeler gene-related antigen in the rat hippocampal formation visualized by CR-50 immunocytochemistry. Neuroscience 82:1079–1086.

Duncan GJ, Plemel JR, Assinck P, Manesh SB, Muir FGW, Hirata R, Berson M, Liu J, Wegner M, Emery B, Moore GRW, Tetzlaff W (2017) Myelin regulatory factor drives remyelination in multiple sclerosis. Acta Neuropathol 134:403–422.

Duncan ID, Radcliff AB, Heidari M, Kidd G, August BKA, Wierenga LA. The adult (2018) oligodendrocyte can participate in remyelination. Proc Natl Acad Sci USA, vol. 115 (50) pp. E11807-E11816.

Emery B, Dugas JC (2013) Purification of oligodendrocyte lineage cells from mouse cortices by immunopanning. Cold Spring Harb Protoc 2013:854–868.

Falcao AM, Meijer M, Scaglione A, Rinwa P, Agirre E, Liang J, Larsen SC, Heskol A, Frawley R, Klingener M, Varas-Godoy M, Raposo AASF, Ernfors P, Castro DS, Nielsen ML, Casaccia P, Castelo-Branco G (2019) PAD2-Mediated Citrullination Contributes to Efficient Oligodendrocyte Differentiation and Myelination. CellReports 27:1090–1102.e10.

Falcao AM, van Bruggen D, Marques S, Meijer M, Jäkel S, Agirre E, Samudyata, Floriddia EM, Vanichkina DP, ffrench-Constant C, Williams A, Guerreiro-Cacais AO, Castelo-Branco G (2018) Disease-specific oligodendrocyte lineage cells arise in multiple sclerosis. Nature Medicine 24:1837–1844.

Fancy SPJ, Kotter MR, Harrington EP, Huang JK, Zhao C, Rowitch DH, Franklin RJM (2010) Overcoming remyelination failure in multiple sclerosis and other myelin disorders. Experimental Neurology 225:18–23.

Fannon J, Tarmier W, Fulton D (2015) Neuronal activity and AMPA-type glutamate receptor activation regulates the morphological development of oligodendrocyte precursor cells. Glia 63:1021–1035.

Fard MK, van der Meer F, Sánchez P, Cantuti-Castelvetri L, Mandad S, Jäkel S, Fornasiero EF, Schmitt S, Ehrlich M, Starost L, Kuhlmann T, Sergiou C, Schultz V, Wrzos C, Brück W, Urlaub H, Dimou L, Stadelmann C, Simons M (2017) BCAS1 expression defines a population of early myelinating oligodendrocytes in multiple sclerosis lesions. Sci Transl Med 9:eaam7816.

Farfán P, Lee J, Larios J, Sotelo P, Bu G, Marzolo M-P (2013) A sorting nexin 17-binding domain within the LRP1 cytoplasmic tail mediates receptor recycling through the basolateral sorting endosome. Traffic 14:823–838.

Fernandez-Castaneda A, Chappell MS, Rosen DA, Seki SM, Beiter RM, Johanson DM, Liskey D, Farber E, Onengut-Gumuscu S, Overall CC, Dupree JL, Gaultier A (2019) The active contribution of OPCs to neuroinflammation is mediated by LRP1. Acta Neuropathol 14:1142–18.

Ferrer DG, Actis Dato V, Jaldín Fincati JR, Lorenc VE, Sánchez MC, Chiabrando GA (2016) Activated α2 -Macroglobulin Induces Mesenchymal Cellular Migration of Raw264.7 Cells through Low-Density Lipoprotein Receptor-Related Protein 1. J Cell Biochem.

ffrench-Constant C, Raff MC (1986) Proliferating bipotential glial progenitor cells in adult rat optic nerve. Nature 319:499–502.

Fogarty M (2005) A subset of oligodendrocytes generated from radial glia in the dorsal spinal cord. Development 132:1951–1959.

Fogarty M, Grist M, Gelman D, Marin O, Pachnis V, Kessaris N (2007) Spatial Genetic Patterning of the Embryonic Neuroepithelium Generates GABAergic Interneuron Diversity in the Adult Cortex. Journal of Neuroscience 27:10935–10946.

Fok-Seang J, Miller RH (1994) Distribution and differentiation of A2B5+ glial precursors in the developing rat spinal cord. Journal of Neuroscience Research 37:219–235.

Franklin R, Gilson JM, Blakemore WF (1997) Local recruitment of remyelinating cells in the repair of demyelination in the central nervous system. Journal of Neuroscience Research 50:337–344.

Franklin RJM, ffrench-Constant C (2008) Remyelination in the CNS: from biology to therapy. Nat Rev Neurosci 9:839–855.

Frotscher M (1998) Cajal-Retzius cells, Reelin, and the formation of layers. Current Opinion in Neurobiology 8:570–575.

Fuccillo M, Joyner AL, Fishell G (2006) Morphogen to mitogen: the multiple roles of hedgehog signalling in vertebrate neural development. Nat Rev Neurosci 7:772–783.

Fukushi J, Makagiansar IT, Stallcup WB (2004) NG2 proteoglycan promotes endothelial cell motility and angiogenesis via engagement of galectin-3 and alpha 3 beta 1 integrin. Mol Biol Cell 15:3580–3590.

Fulton D, Paez PM, Fisher R, Handley V, Colwell CS, Campagnoni AT (2010) Regulation of L-type Ca++ currents and process morphology in white matter oligodendrocyte precursor cells by golli-myelin proteins. Glia 58:1292–1303.

Gajera CR, Emich H, Lioubinski O, Christ A, Beckervordersandforth-Bonk R, Yoshikawa K, Bachmann S, Christensen EI, Götz M, Kempermann G, Peterson AS, Willnow TE, Hammes A (2010) LRP2 in ependymal cells regulates BMP signaling in the adult neurogenic niche. J Cell Sci 123:1922–1930.

Gallo V, Zhou JM, McBain CJ, Wright P, Knutson PL, Armstrong RC (1996) Oligodendrocyte progenitor cell proliferation and lineage progression are regulated by glutamate receptor-mediated K+ channel block. Journal of Neuroscience 16:2659–2670.

Gan M, Jiang P, McLean P, Kanekiyo T, Bu G (2014) Low-Density Lipoprotein Receptor-Related Protein 1 (LRP1) Regulates the Stability and Function of GluA1 α-Amino-3-Hydroxy-5-Methyl-4-Isoxazole Propionic Acid (AMPA) Receptor in Neurons Tang Y-P, ed. PLoS ONE 9:e113237–18.

Gao L, Miller RH (2006) Specification of Optic Nerve Oligodendrocyte Precursors by Retinal Ganglion Cell Axons. Journal of Neuroscience 26:7619–7628.

Gaultier A, Wu X, Le Moan N, Takimoto S, Mukandala G, Akassoglou K, Campana WM, Gonias SL (2009) Low-density lipoprotein receptor-related protein 1 is an essential receptor for myelin phagocytosis. J Cell Sci 122:1155–1162.

Genoud S, Lappe-Siefke C, Goebbels S, Radtke F, Aguet M, Scherer SS, Suter U, Nave KA, Mantei N (2002) Notch1 control of oligodendrocyte differentiation in the spinal cord. J Cell Biol 158:709–718.

Gibson EM, Purger D, Mount CW, Goldstein AK, Lin GL, Wood LS, Inema I, Miller SE, Bieri G, Zuchero JB, Barres BA, Woo PJ, Vogel H, Monje M (2014) Neuronal Activity Promotes Oligodendrogenesis and Adaptive Myelination in the Mammalian Brain. Science 344:1252304–1252304.

Givogri MI, Costa RM, Schonmann V, Silva AJ, Campagnoni AT, Bongarzone ER (2002) Central nervous system myelination in mice with deficient expression of notch1 receptor. Journal of Neuroscience Research 67:309–320.

Gopal U, Bohonowych JE, Lema-Tome C, Liu A, Garrett-Mayer E, Wang B, Isaacs JS (2011) A Novel Extracellular Hsp90 Mediated Co-Receptor Function for LRP1 Regulates EphA2 Dependent Glioblastoma Cell Invasion Lesniak M, ed. PLoS ONE 6:e17649–14.

Gorovoy M, Gaultier A, Campana WM, Firestein GS, Gonias SL (2010) Inflammatory mediators promote production of shed LRP1/CD91, which regulates cell signaling and cytokine expression by macrophages. J Leukoc Biol 88:769–778.

Gotthardt M, Trommsdorff M, Nevitt MF, Shelton J, Richardson JA, Stockinger W, Nimpf J, Herz J (2000) Interactions of the Low Density Lipoprotein Receptor Gene Family with Cytosolic Adaptor and Scaffold Proteins Suggest Diverse Biological Functions in Cellular Communication and Signal Transduction. Journal of Biological Chemistry 275:25616–25624.

Grana TR, LaMarre J, Kalisch BE (2012) Nerve Growth Factor-Mediated Regulation of Low Density Lipoprotein Receptor-Related Protein Promoter Activation. Cell Mol Neurobiol 33:269–282.

Granda B, Tabernero A, Tello V, Medina JM (2003) Oleic acid induces GAP-43 expression through a protein kinase C-mediated mechanism that is independent of NGF but synergistic with NT-3 and NT-4/5. Brain Research 988:1–8.

Grier MD, West KL, Kelm ND, Fu C, Does MD, Parker B, McBrier E, Lagrange AH, Ess KC, Carson RP (2017) Loss of mTORC2 signaling in oligodendrocyte precursor cells delays myelination de Castro F, ed. PLoS ONE 12.

Grobmyer SR, Kuo A, Orishimo M, Okada SS, Cines DB, Barnathan ES (1993) Determinants of binding and internalization of tissue-type plasminogen activator by human vascular smooth muscle and endothelial cells. Journal of Biological Chemistry 268:13291–13300.

Gudz TI (2006) Glutamate Stimulates Oligodendrocyte Progenitor Migration Mediated via an v Integrin/Myelin Proteolipid Protein Complex. Journal of Neuroscience 26:2458–2466.

Hack I, Bancila M, Loulier K, Carroll P, Cremer H (2002) Reelin is a detachment signal in tangential chain-migration during postnatal neurogenesis. Nat Neurosci 5:939–945.

Haldipur P, Bharti U, Govindan S, Sarkar C, Iyengar S, Gressens P, Mani S (2012) Expression of Sonic hedgehog during cell proliferation in the human cerebellum. Stem Cells Dev 21:1059–1068.

Hamilton TG, Klinghoffer RA, Corrin PD, Soriano P (2003) Evolutionary Divergence of Platelet-Derived Growth Factor Alpha Receptor Signaling Mechanisms. Molecular and Cellular Biology 23:4013–4025.

Hanover JA, Willingham MC, Pastan I (1983) Receptor-mediated endocytosis of alpha 2-macroglobulin: solubilization and partial purification of the fibroblast alpha 2-macroglobulin receptor. Ann N Y Acad Sci 421:410–423.

Hastings NB, Gould E (1999) Rapid extension of axons into the CA3 region by adult-generated granule cells. J Comp Neurol 413:146–154.

Henley JR, Huang K-H, Wang D, Poo M-M (2004) Calcium mediates bidirectional growth cone turning induced by myelin-associated glycoprotein. Neuron 44:909–916.

Hennen E, Safina D, Haussmann U, Worsdorfer P, Edenhofer F, Poetsch A, Faissner A (2013) A LewisX Glycoprotein Screen Identifies the Low Density Lipoprotein Receptor-related Protein 1 (LRP1) as a Modulator of Oligodendrogenesis in Mice. Journal of Biological Chemistry 288:16538–16545.

Herz J, Clouthier DE, Hammer RE (1992) LDL receptor-related protein internalizes and degrades uPA-PAI-1 complexes and is essential for embryo implantation. Cell 71:411–421.

Herz J, Strickland DK (2001) LRP: a multifunctional scavenger and signaling receptor. J Clin Invest 108:779–784.

Hey PJ, Twells R, Phillips MS, Nakagawa Y, Brown SD, Kawaguchi Y, Cox R, Xie GC, Dugan V, Hammond H, Metzker ML, Todd JA, Hess JF (1998) Cloning of a novel member of the low-density lipoprotein receptor family. Gene 216:103–111.

Hidalgo J, Aschner M, Zatta P, Vasák M (2001) Roles of the metallothionein family of proteins in the central nervous system. Brain Res Bull 55:133–145.

Hiesberger T, Trommsdorff M, Howell BW, Goffinet A, Mumby MC, Cooper JA, Herz J (1999) Direct binding of Reelin to VLDL receptor and ApoE receptor 2 induces tyrosine phosphorylation of disabled-1 and modulates tau phosphorylation. Neuron 24:481–489.

Hill RA, Li AM, Grutzendler J (2018) Lifelong cortical myelin plasticity and age-related degeneration in the live mammalian brain. Nature Publishing Group 21:683–695.

Hines JH, Abu-Rub M, Henley JR (2010) Asymmetric endocytosis and remodeling of beta1-integrin adhesions during growth cone chemorepulsion by MAG. Nature Publishing Group 13:829–837.

Hippenmeyer S, Vrieseling E, Sigrist M, Portmann T, Laengle C, Ladle DR, Arber S (2005) A developmental switch in the response of DRG neurons to ETS transcription factor signaling. Sanes JR, ed. PLoS Biol 3:e159.

Hrvatin S, Hochbaum DR, Nagy MA, Cicconet M, Robertson K, Cheadle L, Zilionis R, Ratner A, Borges-Monroy R, Klein AM, Sabatini BL, Greenberg ME (2018) Single-cell analysis of experience-dependent transcriptomic states in the mouse visual cortex. Nature Publishing Group 21:120–129.

Hu H, Tomasiewicz H, Magnuson T, Rutishauser U (1996) The role of polysialic acid in migration of olfactory bulb interneuron precursors in the subventricular zone. Neuron 16:735–743.

Hughes EG, Kang SH, Fukaya M, Bergles DE (2013) Oligodendrocyte progenitors balance growth with self-repulsion to achieve homeostasis in the adult brain. Nature Publishing Group 16:668–676.

Hughes EG, Orthmann-Murphy JL, Langseth AJ, Bergles DE (2018) Myelin remodeling through experience-dependent oligodendrogenesis in the adult somatosensory cortex. Nature Publishing Group 21:696–706.

Ito D, Imai Y, Ohsawa K, Nakajima K, Fukuuchi Y, Kohsaka S (1998) Microglia-specific localisation of a novel calcium binding protein, Iba1. Brain Res Mol Brain Res vol. 57 (1) pp. 1-9.

Jakovcevski I, Filipovic R, Mo Z, Rakic S, Zecevic N (2009) Oligodendrocyte development and the onset of myelination in the human fetal brain. Front Neuroanatomy .

Jäkel S, Agirre E, Mendanha Falcão A, van Bruggen D, Lee KW, Knuesel I, Malhotra D, ffrench-Constant C, Williams A, Castelo-Branco G (2019) Altered human oligodendrocyte heterogeneity in multiple sclerosis. Nature 566:543–547.

Jeon H, Kim J-H, Kim J-H, Lee W-H, Lee M-S, Suk K (2012) Plasminogen activator inhibitor type 1 regulates microglial motility and phagocytic activity. J Neuroinflammation 9:149.

Jeon H, Meng WY, Takagi J, Eck MJ, Springer TA, Blacklow SC (2001) Implications for familial hypercholesterolemia from the structure of the LDL receptor YWTD-EGF domain pair. Nat Struct Biol 8:499–504.

Jiang M, Liu L, He X, Wang H, Lin W, Wang H, Yoon SO, Wood TL, Lu QR (2016) Regulation of PERK-eIF2α signalling by tuberous sclerosis complex-1 controls homoeostasis and survival of myelinating oligodendrocytes. Nature Communications 7:12185.

Kadurin I, Rothwell SW, Lana B, Nieto-Rostro M, Dolphin AC (2017) LRP1 influences trafficking of N-type calcium channels via interaction with the auxiliary α2δ-1 subunit. Sci Rep 7:43802.

Kang SH, Fukaya M, Yang JK, Rothstein JD, Bergles DE (2010a) NG2+ CNS Glial Progenitors Remain Committed to the Oligodendrocyte Lineage in Postnatal Life and following Neurodegeneration. Neuron 68:668–681.

Kang SH, Fukaya M, Yang JK, Rothstein JD, Bergles DE (2010b) NG2+ CNS Glial Progenitors Remain Committed to the Oligodendrocyte Lineage in Postnatal Life and following Neurodegeneration. Neuron 68:668–681.

Kang Z, Wang C, Zepp J, Wu L, Sun K, Zhao J, Chandrasekharan U, DiCorleto PE, Trapp BD, Ransohoff RM, Li X (2013) Act1 mediates IL-17-induced EAE pathogenesis selectively in NG2+ glial cells. Nature Publishing Group 16:1401–1408.

Kantarci S, Al-Gazali L, Hill RS, Donnai D, Black GCM, Bieth E, Chassaing N, Lacombe D, Devriendt K, Teebi A, Loscertales M, Robson C, Liu T, MacLaughlin DT, Noonan KM, Russell MK, Walsh CA, Donahoe PK, Pober BR (2007) Mutations in LRP2, which encodes the multiligand receptor megalin, cause Donnai-Barrow and facio-oculo-acoustico-renal syndromes. Nature Genetics 1999 21:1 39:957–959.

Kawaguchi Y, Kubota Y (1997) GABAergic cell subtypes and their synaptic connections in rat frontal cortex. Cerebral Cortex 7:476–486.

Kessaris N, Fogarty M, Iannarelli P, Grist M, Wegner M, Richardson WD (2005) Competing waves of oligodendrocytes in the forebrain and postnatal elimination of an embryonic lineage. Nat Neurosci 9:173–179.

Kessaris N, Pringle N, Richardson WD (2008) Specification of CNS glia from neural stem cells in the embryonic neuroepithelium. Philosophical Transactions of the Royal Society B: Biological Sciences 363:71–85.

Kim SU, de Vellis J (2005) Microglia in health and disease. Journal of Neuroscience Research 81:302–313.

Kinoshita A, Shah T, Tangredi MM, Strickland DK, Hyman BT (2003) The intracellular domain of the low density lipoprotein receptor-related protein modulates transactivation mediated by amyloid precursor protein and Fe65. Journal of Biological Chemistry 278:41182–41188.

Kirby L, Jin J, Cardona JG, Smith MD, Martin KA, Wang J, Strasburger H, Herbst L, Alexis M, Karnell J, Davidson T, Dutta R, Goverman J, Bergles D, Calabresi PA (2019) Oligodendrocyte precursor cells present antigen and are cytotoxic targets in inflammatory demyelination. Nature Communications 10:3887–20.

Ko KW, McLeod RS, Avramoglu RK, Nimpf J, FitzGerald DJ, Vukmirica J, Yao Z (1998) Mutation at the processing site of chicken low density lipoprotein receptor-related protein impairs efficient endoplasmic reticulum exit, but proteolytic cleavage is not essential for its endocytic functions. Journal of Biological Chemistry 273:27779–27785.

Korey CA, Van Vactor D (2000) From the growth cone surface to the cytoskeleton: one journey, many paths. J Neurobiol 44:184–193.

Kougioumtzidou E, Shimizu T, Hamilton NB, Tohyama K, Sprengel R, Monyer H, Attwell D, Richardson WD (2017) Signalling through AMPA receptors on oligodendrocyte precursors promotes myelination by enhancing oligodendrocyte survival. Elife 6:31.

Krasnow AM, Ford MC, Valdivia LE, Wilson SW, Attwell D (2018) Regulation of developing myelin sheath elongation by oligodendrocyte calcium transients in vivo. Nature Publishing Group 21:24–28.

Kriegstein A, Noctor S, Martínez-Cerdeño V (2006) Patterns of neural stem and progenitor cell division may underlie evolutionary cortical expansion. Nat Rev Neurosci 7:883–890.

Kuhlmann T, Miron V, Cui Q, Wegner C, Antel J, Brueck W (2009) Differentiation block of oligodendroglial progenitor cells as a cause for remyelination failure in chronic multiple sclerosis (vol 131, pg 1749, 2008). Brain 132:1118–1118.

Kukley M, Nishiyama A, Dietrich D (2010) The fate of synaptic input to NG2 glial cells: neurons specifically downregulate transmitter release onto differentiating oligodendroglial cells. J Neurosci 30:8320–8331.

Laatsch A, Panteli M, Sornsakrin M, Hoffzimmer B, Grewal T, Heeren J (2012) Low Density Lipoprotein Receptor-Related Protein 1 Dependent Endosomal Trapping and Recycling of Apolipoprotein E Johannes L, ed. PLoS ONE 7:e29385–10.

Landowski LM, Pavez M, Brown LS, Gasperini R, Taylor BV, West AK, Foa L (2016) Low-density Lipoprotein Receptor-related Proteins in a Novel Mechanism of Axon Guidance and Peripheral Nerve Regeneration. Journal of Biological Chemistry 291:1092–1102.

Lavdas AA, Grigoriou M, Pachnis V, Parnavelas JG (1999) The medial ganglionic eminence gives rise to a population of early neurons in the developing cerebral cortex. J Neurosci 19:7881–7888.

Le Marrec-Croq F, Bocquet-Garcon A, Vizioli J, Vancamp C, Drago F, Franck J, Wisztorski M, Salzet M, Sautiere P-E, Lefebvre C (2014) Calreticulin contributes to C1q-dependent recruitment of microglia in the leech Hirudo medicinalis following a CNS injury. Med Sci Monit 20:644–653.

Lecca D, Trincavelli ML, Gelosa P, Sironi L, Ciana P, Fumagalli M, Villa G, Verderio C, Grumelli C, Guerrini U, Tremoli E, Rosa P, Cuboni S, Martini C, Buffo A, Cimino M, Abbracchio MP (2008) The recently identified P2Y-like receptor GPR17 is a sensor of brain damage and a new target for brain repair. Hashimoto K, ed. PLoS ONE 3:e3579.

Lee D, Walsh JD, Mikhailenko I, Yu P, Migliorini M, Wu Y, Krueger S, Curtis JE, Harris B, Lockett S, Blacklow SC, Strickland DK, Wang Y-X (2006) RAP uses a histidine switch to regulate its interaction with LRP in the ER and Golgi. Mol Cell 22:423–430.

Lee S, Leach MK, Redmond SA, Chong SYC, Mellon SH, Tuck SJ, Feng Z-Q, Corey JM, Chan JR (2012) A culture system to study oligodendrocyte myelination processes using engineered nanofibers. Nat Meth 9:917–922.

Lee Y, Morrison BM, Li Y, Lengacher S, Farah MH, Hoffman PN, Liu Y, Tsingalia A, Jin L, Zhang P-W, Pellerin L, Magistretti PJ, Rothstein JD (2017) Oligodendroglia metabolically support axons and contribute to neurodegeneration. Nature 487:443–448.

Lehtonen S, Shah M, Nielsen R, Iino N, Ryan JJ, Zhou H, Farquhar MG (2008) The endocytic adaptor protein ARH associates with motor and centrosomal proteins and is involved in centrosome assembly and cytokinesis. Zheng Y, ed. Mol Biol Cell 19:2949–2961.

Letinic K, Zoncu R, Rakic P (2002) Origin of GABAergic neurons in the human neocortex. Nature 417:645–649.

Leung JYK, Bennett WR, Herbert RP, West AK, Lee PR, Wake H, Fields RD, Chuah MI, Chung RS (2011) Metallothionein promotes regenerative axonal sprouting of dorsal root ganglion neurons after physical axotomy. Cell Mol Life Sci 69:809–817.

Levine JM, Reynolds R (1999) Activation and proliferation of endogenous oligodendrocyte precursor cells during ethidium bromide-induced demyelination. Experimental Neurology 160:333–347.

Lewis AK, Bridgman PC (1992) Nerve growth cone lamellipodia contain two populations of actin filaments that differ in organization and polarity. J Cell Biol 119:1219–1243.

Li Q, Brus-Ramer M, Martin JH, McDonald JW (2010) Electrical stimulation of the medullary pyramid promotes proliferation and differentiation of oligodendrocyte progenitor cells in the corticospinal tract of the adult rat. Neurosci Lett 479:128–133.

Li Y (2000) The YXXL Motif, but Not the Two NPXY Motifs, Serves as the Dominant Endocytosis Signal for Low Density Lipoprotein Receptor-related Protein. Journal of Biological Chemistry 275:17187–17194.

Li Y, van Kerkhof P, Marzolo MP, Strous GJ, Bu G (2001) Identification of a Major Cyclic AMP-Dependent Protein Kinase A Phosphorylation Site within the Cytoplasmic Tail of the Low-Density Lipoprotein Receptor-Related Protein: Implication for Receptor-Mediated Endocytosis. Molecular and Cellular Biology 21:1185–1195.

Lillis AP, Van Duyn LB, Murphy-Ullrich JE, Strickland DK (2008) LDL Receptor-Related Protein 1: Unique Tissue-Specific Functions Revealed by Selective Gene Knockout Studies. Physiological Reviews 88:887–918.

Lim DA, Tramontin AD, Trevejo JM, Herrera DG, Garcia-Verdugo JM, Alvarez-Buylla A (2000) Noggin antagonizes BMP signaling to create a niche for adult neurogenesis. Neuron 28:713–726.

Lin J-P, Mironova YA, Shrager P, Giger RJ (2017) LRP1 regulates peroxisome biogenesis and cholesterol homeostasis in oligodendrocytes and is required for proper CNS myelin development and repair. Elife 6:e30498.

Lin L, Bu G, Mars WM, Reeves WB, Tanaka S, Hu K (2010) tPA activates LDL receptor-related protein 1-mediated mitogenic signaling involving the p90RSK and GSK3beta pathway. The American Journal of Pathology 177:1687–1696.

Lin S, Racz J, Tai MF, Brooks KM, Rzeczycki P, Heath LJ, Newstead MW, Standiford TJ, Rosania GR, Stringer KA (2016) A Role for Low Density Lipoprotein Receptor-Related Protein 1 in the Cellular Uptake of Tissue Plasminogen Activator in the Lungs. Pharm Res 33:72–82.

Lin S-C, Bergles DE (2004) Synaptic signaling between GABAergic interneurons and oligodendrocyte precursor cells in the hippocampus. Nat Neurosci 7:24–32.

Liu C-C, Hu J, Zhao N, Wang J, Na W, Cirrito JR, Kanekiyo T, Holtzman DM, Bu G (2017) Astrocytic LRP1 Mediates Brain Aβ Clearance and Impacts Amyloid Deposition. J Neurosci 37:3442–16–4031.

Liu C-X, Musco S, Lisitsina NM, Yaklichkin SY, Lisitsyn NA (2000) Genomic Organization of a New Candidate Tumor Suppressor Gene, LRP1B. Genomics 69:271–274.

Liu CC, Hu J, Tsai CW, Yue M, Melrose HL, Kanekiyo T, Bu G (2015) Neuronal LRP1 Regulates Glucose Metabolism and Insulin Signaling in the Brain. Journal of Neuroscience 35:5851–5859.

Liu Q, Trotter J, Zhang J, Peters MM, Cheng H, Bao J, Han X, Weeber EJ, Bu G (2010) Neuronal LRP1 knockout in adult mice leads to impaired brain lipid metabolism and progressive, age-dependent synapse loss and neurodegeneration. J Neurosci 30:17068–17078.

Liu Q, Zerbinatti CV, Zhang J, Hoe H-S, Wang B, Cole SL, Herz J, Muglia L, Bu G (2007) Amyloid precursor protein regulates brain apolipoprotein E and cholesterol metabolism through lipoprotein receptor LRP1. Neuron 56:66–78.

Liu Q, Zhang J, Tran H, Verbeek MM, Reiss K, Estus S, Bu G (2009) LRP1 shedding in human brain: roles of ADAM10 and ADAM17. Molecular Neurodegeneration 4:17–17.

Liu Y, Aguzzi A (2019) NG2 glia are required for maintaining microglia homeostatic state. Glia 70:31.

Llorente-Cortes V, Costales P, Bernués J, Camino-Lopez S, Badimon L (2006) Sterol Regulatory Element-binding Protein-2 Negatively Regulates Low Density Lipoprotein Receptor-related Protein Transcription. Journal of Molecular Biology 359:950–960.

Loukinova E (2002) Platelet-derived Growth Factor (PDGF)-induced Tyrosine Phosphorylation of the Low Density Lipoprotein Receptor-related Protein (LRP). Evidence For Integrated Co-receptor Function Between Lrp and the Pdgf receptor. Journal of Biological Chemistry 277:15499–15506.

Lu QR, Yuk D, Alberta JA, Zhu Z, Pawlitzky I, Chan J, McMahon AP, Stiles CD, Rowitch DH (2000) Sonic hedgehog--regulated oligodendrocyte lineage genes encoding bHLH proteins in the mammalian central nervous system. Neuron 25:317–329.

Ma Y (2006) Distinct Subtypes of Somatostatin-Containing Neocortical Interneurons Revealed in Transgenic Mice. Journal of Neuroscience 26:5069–5082.

Maeda Y, Nakagomi N, Nakano-Doi A, Ishikawa H, Tatsumi Y, Bando Y, Yoshikawa H, Matsuyama T, Gomi F, Nakagomi T (2019) Potential of Adult Endogenous Neural

Stem/Progenitor Cells in the Spinal Cord to Contribute to Remyelination in Experimental Autoimmune Encephalomyelitis. Cells 8.

Maier W, Bednorz M, Meister S, Roebroek A, Weggen S, Schmitt U, Pietrzik CU (2013) LRP1 is critical for the surface distribution and internalization of the NR2B NMDA receptor subtype. Molecular Neurodegeneration 8:1–1.

R Marmur, P C Mabie, S Gokhan, Q Song, J A Kessler, and M F Mehler
Isolation and developmental characterization of cerebral cortical multipotent progenitors Dev Biol, 1998 vol. 204 (2) pp. 577-591.

Makinodan M, Rosen KM, Ito S, Corfas G (2012) A critical period for social experience-dependent oligodendrocyte maturation and myelination. Science 337:1357–1360.

Mantuano E, Jo M, Gonias SL, Campana WM (2010) Low density lipoprotein receptor-related protein (LRP1) regulates Rac1 and RhoA reciprocally to control Schwann cell adhesion and migration. J Biol Chem 285:14259–14266.

Mantuano E, Lam MS, Gonias SL (2013a) LRP1 Assembles Unique Co-receptor Systems to Initiate Cell Signaling in Response to Tissue-type Plasminogen Activator and Myelin-associated Glycoprotein. Journal of Biological Chemistry 288:34009–34018.

Mantuano E, Lam MS, Gonias SL (2013b) LRP1 assembles unique co-receptor systems to initiate cell signaling in response to tissue-type plasminogen activator and myelin-associated glycoprotein. J Biol Chem 288:34009–34018.

Mantuano E, Lam MS, Shibayama M, Campana WM, Gonias SL (2015) The NMDA receptor functions independently and as an LRP1 co-receptor to promote Schwann cell survival and migration. J Cell Sci 128:3478–3488.

Mañes S, Martínez-A C (2004) Cholesterol domains regulate the actin cytoskeleton at the leading edge of moving cells. Trends in Cell Biology 14:275–278.

Mañes S, Mira E, Gómez-Moutón C, Lacalle RA, Keller P, Labrador JP, Martínez-A C (1999) Membrane raft microdomains mediate front-rear polarity in migrating cells. EMBO J 18:6211–6220.

Mao H, Lockyer P, Townley-Tilson WHD, Xie L, Pi X (2016) LRP1 Regulates Retinal Angiogenesis by Inhibiting PARP-1 Activity and Endothelial Cell Proliferation. Arteriosclerosis, Thrombosis, and Vascular Biology 36:350–360.

Marín-Padilla M (1998) Cajal-Retzius cells and the development of the neocortex. Trends in Neurosciences 21:64–71.

Marques S, van Bruggen D, Vanichkina DP, Floriddia EM, Munguba H, Varemo L, Giacomello S, Falcao AM, Meijer M, Bjorklund AK, Hjerling-Leffler J, Taft RJ, Castelo-Branco G (2018) Transcriptional Convergence of Oligodendrocyte Lineage Progenitors during Development. Developmental Cell 46:504–.

Marschang P, Brich J, Weeber EJ, Sweatt JD, Shelton JM, Richardson JA, Hammer RE, Herz J (2004) Normal Development and Fertility of Knockout Mice Lacking the Tumor

Suppressor Gene LRP1b Suggest Functional Compensation by LRP1. Molecular and Cellular Biology 24:3782–3793.

Marshall CAG, Novitch BG, Goldman JE (2005) Olig2 directs astrocyte and oligodendrocyte formation in postnatal subventricular zone cells. Journal of Neuroscience 25:7289–7298.

Marynen P, Van Leuven F, Cassiman JJ, Van den Berghe H (1984) Solubilization and affinity purification of the alpha 2-macroglobulin receptor from human fibroblasts. Journal of Biological Chemistry 259:7075–7079.

Marzban H, Del Bigio MR, Alizadeh J, Ghavami S, Zachariah RM, Rastegar M (2014) Cellular commitment in the developing cerebellum. Front Cell Neurosci 8:450.

Marzolo M-P, Bernhardi von R, Bu G, Inestrosa NC (2000) Expression of α2-macroglobulin receptor/low density lipoprotein receptor-related protein (LRP) in rat microglial cells. Journal of Neuroscience Research 60:401–411.

Marzolo M-P, Farfán P (2011) New insights into the roles of megalin/LRP2 and the regulation of its functional expression. Biol Res 44:89–105.

May P (2002a) Proteolytic Processing of Low Density Lipoprotein Receptor-related Protein Mediates Regulated Release of Its Intracellular Domain. Journal of Biological Chemistry 277:18736–18743.

May P (2002b) Proteolytic Processing of Low Density Lipoprotein Receptor-related Protein Mediates Regulated Release of Its Intracellular Domain. Journal of Biological Chemistry 277:18736–18743.

May P, Rohlmann A, Bock HH, Zurhove K, Marth JD, Schomburg ED, Noebels JL, Beffert U, Sweatt JD, Weeber EJ, Herz J (2004) Neuronal LRP1 functionally associates with postsynaptic proteins and is required for normal motor function in mice. Molecular and Cellular Biology 24:8872–8883.

McCarthy RA (2002) Megalin Functions as an Endocytic Sonic Hedgehog Receptor. Journal of Biological Chemistry 277:25660–25667.

McKinnon RD (2005) PDGF -Receptor Signal Strength Controls an RTK Rheostat That Integrates Phosphoinositol 3'-Kinase and Phospholipase C Pathways during Oligodendrocyte Maturation. Journal of Neuroscience 25:3499–3508.

Menn B, Garcia-Verdugo JM, Yaschine C, Gonzalez-Perez O, Rowitch D, Alvarez-Buylla A (2006) Origin of Oligodendrocytes in the Subventricular Zone of the Adult Brain. Journal of Neuroscience 26:7907–7918.

Mensch S, Baraban M, Almeida R, Czopka T, Ausborn J, Manira El A, Lyons DA (2015) Synaptic vesicle release regulates myelin sheath number of individual oligodendrocytes in vivo. Nature Publishing Group 18:628–630.

Miron VE, Kuhlmann T, Antel JP (2011) Cells of the oligodendroglial lineage, myelination, and remyelination. BBA - Molecular Basis of Disease 1812:184–193.

Mitew S, Gobius I, Fenlon LR, McDougall SJ, Hawkes D, Xing YL, Bujalka H, Gundlach AL, Richards LJ, Kilpatrick TJ, Merson TD, Emery B (2018) Pharmacogenetic stimulation of neuronal activity increases myelination in an axon-specific manner. Nature Communications 9:–16.

Miyamoto Y, Yamauchi J, Tanoue A (2008) Cdk5 Phosphorylation of WAVE2 Regulates Oligodendrocyte Precursor Cell Migration through Nonreceptor Tyrosine Kinase Fyn. Journal of Neuroscience 28:8326–8337.

Moestrup SK, Gliemann J, Pallesen G (1992) Distribution of the alpha 2-macroglobulin receptor/low density lipoprotein receptor-related protein in human tissues. Cell Tissue Res 269:375–382.

Morales CR (2006) Epithelial Trafficking of Sonic Hedgehog By Megalin. Journal of Histochemistry and Cytochemistry 54:1115–1127.

Morrisett JD, Jackson RL, Gotto AM (1975) Lipoproteins: structure and function. Annu Rev Biochem 44:183–207.

Mulder M, Jansen PJ, Janssen BJA, van de Berg WDJ, van der Boom H, Havekes LM, de Kloet RE, Ramaekers FCS, Blokland A (2004) Low-density lipoprotein receptor-knockout mice display impaired spatial memory associated with a decreased synaptic density in the hippocampus. Neurobiol Dis 16:212–219.

Mullen RJ, Buck C R, and Smith A M. NeuN, a neuronal specific nuclear protein in vertebrates. Development, 1992 vol. 116 (1) pp. 201-211.

Murase S-I, Horwitz AF (2002) Deleted in colorectal carcinoma and differentially expressed integrins mediate the directional migration of neural precursors in the rostral migratory stream. J Neurosci 22:3568–3579.

Muratoglu SC, Mikhailenko I, Newton C, Migliorini M, Strickland DK (2010) Low density lipoprotein receptor-related protein 1 (LRP1) forms a signaling complex with platelet-derived growth factor receptor-beta in endosomes and regulates activation of the MAPK pathway. Journal of Biological Chemistry 285:14308–14317.

Murcia-Belmonte V, Medina-Rodríguez EM, Bribián A, de Castro F, Esteban PF (2014) ERK1/2 signaling is essential for the chemoattraction exerted by human FGF2 and human anosmin-1 on newborn rat and mouse OPCs via FGFR1. Glia 62:374–386.

Murray K, Calaora V, Rottkamp C, Guicherit O, Dubois-Dalcq M (2002) Sonic hedgehog is a potent inducer of rat oligodendrocyte development from cortical precursors in vitro. Mol Cell Neurosci 19:320–332.

Murtie JC, Zhou YX, Le TQ, Armstrong RC (2005) In vivo analysis of oligodendrocyte lineage development in postnatal FGF2 null nice. Glia 49:542–554.

Mycko MP, Papoian R, Boschert U, Raine CS, Selmaj KW (2003) cDNA microarray analysis in multiple sclerosis lesions: detection of genes associated with disease activity. Brain 126:1048–1057.

N'songo A, Kanekiyo T, Bu G (2013) LRP1 plays a major role in the amyloid-β clearance in microglia. Molecular Neurodegeneration 8:1–1.

Nagai J (2005) Mutually dependent localization of megalin and Dab2 in the renal proximal tubule. AJP: Renal Physiology 289:F569–F576.

Nagai M, Meerloo T, Takeda T, Farquhar MG (2003) The Adaptor Protein ARH Escorts Megalin to and through Endosomes. Mol Biol Cell 14:4984–4996.

Nakajima C, Kulik A, Frotscher M, Herz J, Schäfer M, Bock HH, May P (2013) Low Density Lipoprotein Receptor-related Protein 1 (LRP1) Modulates N-Methyl-d-aspartate (NMDA) Receptor-dependent Intracellular Signaling and NMDA-induced Regulation of Postsynaptic Protein Complexes. Journal of Biological Chemistry 288:21909–21923.

Nakano M, Tamura Y, Yamato M, Kume S, Eguchi A, Takata K, Watanabe Y, Kataoka Y (2017) NG2 glial cells regulate neuroimmunological responses to maintain neuronal function and survival. Sci Rep 7:42041.

Nakato M, Matsuo M, Kono N, Arita M, Arai H, Ogawa J, Kioka N, Ueda K (2015) Neurite outgrowth stimulation by n-3 and n-6 PUFAs of phospholipids in apoE-containing lipoproteins secreted from glial cells. J Lipid Res 56:1880–1890.

Nery S, Fishell G, Corbin JG (2002) The caudal ganglionic eminence is a source of distinct cortical and subcortical cell populations. Nat Neurosci 5:1279–1287.

Nery S, Wichterle H, Fishell G (2001) Sonic hedgehog contributes to oligodendrocyte specification in the mammalian forebrain. Development 128:527–540.

Newton CS, Loukinova E, Mikhailenko I, Ranganathan S, Gao Y, Haudenschild C, Strickland DK (2005) Platelet-derived Growth Factor Receptor- (PDGFR-) Activation Promotes Its Association with the Low Density Lipoprotein Receptor-related Protein (LRP): EVIDENCE FOR CO-RECEPTOR FUNCTION. Journal of Biological Chemistry 280:27872–27878.

Nguyen-Ba-Charvet KT (2004) Multiple Roles for Slits in the Control of Cell Migration in the Rostral Migratory Stream. Journal of Neuroscience 24:1497–1506.

Nichols AJ, Olson EC (2010) Reelin Promotes Neuronal Orientation and Dendritogenesis during Preplate Splitting. Cerebral Cortex 20:2213–2223.

Noble M, Murray K, Stroobant P, Waterfield MD, Riddle P (1988) Platelet-derived growth factor promotes division and motility and inhibits premature differentiation of the oligodendrocyte/type-2 astrocyte progenitor cell. Nature 333:560–562.

Noll E, Miller RH (1993) Oligodendrocyte precursors originate at the ventral ventricular zone dorsal to the ventral midline region in the embryonic rat spinal cord. Development 118:563–573.

Nykjaer A, Dragun D, Walther D, Vorum H, Jacobsen C, Herz J, Melsen F, Christensen EI, Willnow TE (1999) An endocytic pathway essential for renal uptake and activation of the steroid 25-(OH) vitamin D3. Cell 96:507–515.

O'Rourke M, Cullen CL, Auderset L, Pitman KA, Achatz D, Gasperini R, Young KM (2016) Evaluating Tissue-Specific Recombination in a Pdgfrα-CreERT2 Transgenic Mouse Line. PLoS ONE 11:e0162858.

O'Rourke M, Gasperini R, Young KM (2014) Adult myelination: wrapping up neuronal plasticity. Neural Regen Res 9:1261–1264.

Oleinikov AV, Zhao J, Makker SP (2000) Cytosolic adaptor protein Dab2 is an intracellular ligand of endocytic receptor gp600/megalin. Biochem J 347:613–621.

Orentas DM, Hayes JE, Dyer KL, Miller RH (1999) Sonic hedgehog signaling is required during the appearance of spinal cord oligodendrocyte precursors. Development 126:2419–2429.

Ortega MC, Cases O, Merchán P, Kozyraki R, Clemente D, de Castro F (2012) Megalin mediates the influence of sonic hedgehog on oligodendrocyte precursor cell migration and proliferation during development. Glia 60:851–866.

Osso LA, Chan JR (2017) Architecting the myelin landscape. Current Opinion in Neurobiology 47:1–7.

Pankov R, Endo Y, Even-Ram S, Araki M, Clark K, Cukierman E, Matsumoto K, Yamada KM (2005) A Rac switch regulates random versus directionally persistent cell migration. J Cell Biol 170:793–802.

Parkyn CJ, Vermeulen EGM, Mootoosamy RC, Sunyach C, Jacobsen C, Oxvig C, Moestrup S, Liu Q, Bu G, Jen A, Morris RJ (2008) LRP1 controls biosynthetic and endocytic trafficking of neuronal prion protein. J Cell Sci 121:773–783.

Parnavelas JG (2000) The origin and migration of cortical neurones: new vistas. Trends in Neurosciences 23:126–131.

Pepper RE, Pitman KA, Cullen CL, Young KM (2018) How Do Cells of the Oligodendrocyte Lineage Affect Neuronal Circuits to Influence Motor Function, Memory and Mood? Front Cell Neurosci 12:399.

Pfrieger FW (2003) Role of cholesterol in synapse formation and function. Biochimica et Biophysica Acta (BBA) - Biomembranes 1610:271–280.

Philips T, Rothstein JD (2017) Oligodendroglia: metabolic supporters of neurons. J Clin Invest 127:3271–3280.

Pi X, Schmitt CE, Xie L, Portbury AL, Wu Y, Lockyer P, Dyer LA, Moser M, Bu G, Flynn EJ, Jin S-W, Patterson C (2012) LRP1-dependent endocytic mechanism governs the signaling output of the bmp system in endothelial cells and in angiogenesis. Circ Res 111:564–574.

Pietrzik CU (2004) FE65 Constitutes the Functional Link between the Low-Density Lipoprotein Receptor-Related Protein and the Amyloid Precursor Protein. Journal of Neuroscience 24:4259–4265.

Pietrzik CU, Busse T, Merriam DE, Weggen S, Koo EH (2002) The cytoplasmic domain of the LDL receptor-related protein regulates multiple steps in APP processing. EMBO J 21:5691–5700.

Pitman KA, Ricci R, Gasperini R, Beasley S, Pavez M, Charlesworth J, Foa L, Young KM (2019) The voltage-gated calcium channel CaV1.2 promotes adult oligodendrocyte progenitor cell survival in the mouse corpus callosum but not motor cortex. Glia 22:54.

Pocivavsek A, Mikhailenko I, Strickland DK, Rebeck GW (2009) Microglial low-density lipoprotein receptor-related protein 1 modulates c-Jun N-terminal kinase activation. J Neuroimmunol 214:25–32.

Pollen AA, Nowakowski TJ, Chen J, Retallack H, Sandoval-Espinosa C, Nicholas CR, Shuga J, Liu SJ, Oldham MC, Diaz A, Lim DA, Leyrat AA, West JA, Kriegstein AR (2015) Molecular Identity of Human Outer Radial Glia during Cortical Development. Cell 163:55–67.

Polo-Hernández E, de Castro F, García-García AG, Tabernero A, Medina JM (2010) Oleic acid synthesized in the periventricular zone promotes axonogenesis in the striatum during brain development. Journal of Neurochemistry 114:1756–1766.

Polo-Hernández E, Tello V, Arroyo ÁA, Domínguez-Prieto M, de Castro F, Tabernero A, Medina JM (2014) Oleic acid synthesized by stearoyl-CoA desaturase (SCD-1) in the lateral periventricular zone of the developing rat brain mediates neuronal growth, migration and the arrangement of prospective synapses. Brain Research 1570:13–25.

Poncet C, Soula C, Trousse F, Kan P, Hirsinger E, Pourquié O, Duprat AM, Cochard P (1996) Induction of oligodendrocyte progenitors in the trunk neural tube by ventralizing signals: effects of notochord and floor plate grafts, and of sonic hedgehog. Mech Dev 60:13–32.

Pringle N, Collarini EJ, Mosley MJ, Heldin CH, Westermark B, Richardson WD (1989) PDGF A chain homodimers drive proliferation of bipotential (O-2A) glial progenitor cells in the developing rat optic nerve. EMBO J 8:1049–1056.

Pringle NP (2003) Fgfr3 expression by astrocytes and their precursors: evidence that astrocytes and oligodendrocytes originate in distinct neuroepithelial domains. Development 130:93–102.

Pringle NP, Richardson WD (1993) A singularity of PDGF alpha-receptor expression in the dorsoventral axis of the neural tube may define the origin of the oligodendrocyte lineage. Development 117:525–533.

Pringle NP, Yu WP, Guthrie S, Roelink H, Lumsden A, Peterson AC, Richardson WD (1996) Determination of neuroepithelial cell fate: induction of the oligodendrocyte lineage by ventral midline cells and sonic hedgehog. Developmental Biology 177:30–42.

Psachoulia K, Jamen F, Young KM, Richardson WD (2009) Cell cycle dynamics of NG2 cells in the postnatal and ageing brain. Neuron Glia Biol 5:57–67.

Quinn KA, Grimsley PG, Dai YP, Tapner M, Chesterman CN, Owensby DA (1997) Soluble low density lipoprotein receptor-related protein (LRP) circulates in human plasma. Journal of Biological Chemistry 272:23946–23951.

Quinn KA, Pye VJ, Dai YP, Chesterman CN, Owensby DA (1999) Characterization of the soluble form of the low density lipoprotein receptor-related protein (LRP). Experimental Cell Research 251:433–441.

Raff MC, Miller RH, Noble M (1983) A glial progenitor cell that develops in vitro into an astrocyte or an oligodendrocyte depending on culture medium. Nature 303:390–396.

Rajasekharan S (2008) Intracellular signaling mechanisms directing oligodendrocyte precursor cell migration. J Neurosci 28:13365–13367.

Ramanathan A, Nelson AR, Sagare AP, Zlokovic BV (2015) Impaired vascular-mediated clearance of brain amyloid beta in Alzheimer's disease: the role, regulation and restoration of LRP1. Front Aging Neurosci 7:1–12.

Reekmans SM, Pflanzner T, Gordts PLSM, Isbert S, Zimmermann P, Annaert W, Weggen S, Roebroek AJM, Pietrzik CU (2009) Inactivation of the proximal NPXY motif impairs early steps in LRP1 biosynthesis. Cell Mol Life Sci 67:135–145.

Richardson WD, Kessaris N, Pringle N (2006) Oligodendrocyte wars. Nat Rev Neurosci 7:11–18.

Richardson WD, Pringle N, Mosley MJ, Westermark B, Dubois-Dalcg M (1988) A role for platelet-derived growth factor in normal gliogenesis in the central nervous system. Cell 53:309–319.

Riddell DR, Vinogradiv DV, Stannard AK, Chadwick N, Owen JS (1999) Identification and characterization of LRP8 (apoER2) in human blood platelets. J Lipid Res 40:1925–1930.

Rivers LE, Young KM, Rizzi M, Jamen F, Psachoulia K, Wade A, Kessaris N, Richardson WD (2008) PDGFRA/NG2 glia generate myelinating oligodendrocytes and piriform projection neurons in adult mice. Nature Publishing Group 11:1392–1401.

Rosenberg SS, Kelland EE, Tokar E, la Torre De AR, Chan JR (2008) The geometric and spatial constraints of the microenvironment induce oligodendrocyte differentiation. Proc Natl Acad Sci USA 105:14662–14667.

Rosenkranz S, DeMali KA, Gelderloos JA, Bazenet C, Kazlauskas A (1999) Identification of the receptor-associated signaling enzymes that are required for platelet-derived growth factor-AA-dependent chemotaxis and DNA synthesis. Journal of Biological Chemistry 274:28335–28343.

Rowitch DH, Kriegstein AR (2010) Developmental genetics of vertebrate glial–cell specification. Nature 468:214–222.

Rönnstrand L, Arvidsson AK, Kallin A, Rorsman C, Hellman U, Engström U, Wernstedt C, Heldin CH (1999) SHP-2 binds to Tyr763 and Tyr1009 in the PDGF beta-receptor and mediates PDGF-induced activation of the Ras/MAP kinase pathway and chemotaxis. Oncogene 18:3696–3702.

Rudenko G, Henry L, Henderson K, Ichtchenko K, Brown MS, Goldstein JL, Deisenhofer J (2002) Structure of the LDL receptor extracellular domain at endosomal pH. Science 298:2353–2358.

Rudy B, Fishell G, Lee S, Hjerling-Leffler J (2010) Three groups of interneurons account for nearly 100% of neocortical GABAergic neurons McBain CJ, Fishell G, eds. Devel Neurobio 71:45–61.

Sabo JK, Kilpatrick TJ, Cate HS (2009) Effects of Bone Morphogenic Proteins on Neural Precursor Cells and Regulation during Central Nervous System Injury. Neurosignals 17:255–264.

Safaiyan S, Kannaiyan N, Snaidero N, Brioschi S, Biber K, Yona S, Edinger AL, Jung S, Rossner MJ, Simons M (2016) Age-related myelin degradation burdens the clearance function of microglia during aging. Nature Publishing Group 19:995–998.

Safina D, Schlitt F, Romeo R, Pflanzner T, Pietrzik CU, Narayanaswami V, Edenhofer F, Faissner A (2016) Low-density lipoprotein receptor-related protein 1 is a novel modulator of radial glia stem cell proliferation, survival, and differentiation. Glia 64:1363–1380.

Saito A, Pietromonaco S, Loo AK, Farquhar MG (1994) Complete cloning and sequencing of rat gp330/“megalin,” a distinctive member of the low density lipoprotein receptor gene family. PNAS 91:9725–9729.

Samson AL, Nevin ST, Croucher D, Niego B, Daniel PB, Weiss TW, Moreno E, Monard D, Lawrence DA, Medcalf RL (2008) Tissue-type plasminogen activator requires a co-receptor to enhance NMDA receptor function. Journal of Neurochemistry 107:1091–1101.

Sayre N, Kokovay E (2019) Loss of lipoprotein receptor LRP1 ablates neural stem cell migration to ischemic lesions. The FASEB Journal.

Schmidt C, Ohlemeyer C, Labrakakis C, Walter T, Kettenmann H, Schnitzer J (1997) Analysis of motile oligodendrocyte precursor cells in vitro and in brain slices. Glia 20:284–298.

Schubert K, Collins LE, Green P, Nagase H, Troeberg L (2019) LRP1 Controls TNF Release via the TIMP-3/ADAM17 Axis in Endotoxin-Activated Macrophages. J Immunol 202:1501–1509.

Sekine K, Kawauchi T, Kubo K-I, Honda T, Herz J, Hattori M, Kinashi T, Nakajima K (2012) Reelin Controls Neuronal Positioning by Promoting Cell-Matrix Adhesion via Inside-Out Activation of Integrin α5β1. Neuron 76:353–369.

Selvais C, D'Auria L, Tyteca D, Perrot G, Lemoine P, Troeberg L, Dedieu S, Noel A, Nagase H, Henriet P, Courtoy PJ, Marbaix E, Emonard H (2011) Cell cholesterol modulates metalloproteinase-dependent shedding of low-density lipoprotein receptor-related protein-1 (LRP-1) and clearance function. The FASEB Journal 25:2770–2781.

Shah M, Baterina OY Jr., Taupin V, Farquhar MG (2013) ARH directs megalin to the endocytic recycling compartment to regulate its proteolysis and gene expression. J Cell Biol 202:113–127.

Shi Y, Mantuano E, Inoue G, Campana WM, Gonias SL (2009) Ligand binding to LRP1 transactivates Trk receptors by a Src family kinase-dependent pathway. Sci Signal 2:ra18–ra18.

Simpson PB, Armstrong RC (1999) Intracellular signals and cytoskeletal elements involved in oligodendrocyte progenitor migration. Glia 26:22–35.

Snaidero N, Simons M (2014) Myelination at a glance. J Cell Sci 127:2999–3004.

Soriano E, del Río JA (2005) The Cells of Cajal-Retzius: Still a Mystery One Century After. Neuron 46:389–394.

Sousa MM, Berglund L, Saraiva MJ (2000) Transthyretin in high density lipoproteins: association with apolipoprotein A-I. J Lipid Res 41:58–65.

Spitzer SO, Sitnikov S, Kamen Y, Evans KA, Kronenberg-Versteeg D, Dietmann S, de Faria OJ, Agathou S, Karadottir RT (2019) Oligodendrocyte Progenitor Cells Become Regionally Diverse and Heterogeneous with Age. Neuron 101:459–.

Spoelgen R (2005) LRP2/megalin is required for patterning of the ventral telencephalon. Development 132:405–414.

Spuch C (2017) LRP-1 and LRP-2 receptors function in the membrane neuron. Trafficking mechanisms and proteolytic processing in Alzheimer's disease. :1–14.

Spuch C, Antequera D, Pascual C, Abilleira S, Blanco M, Jose Moreno-Carretero M, Romero-Lopez J, Ishida T, Antonio Molina J, Villarejo A, Bermejo-Pareja F, Carro E (2015) Soluble megalin is reduced in cerebrospinal fluid samples of Alzheimer's disease patients. Front Cell Neurosci 9.

Spuch C, Ortolano S, Navarro C (2012) LRP-1 and LRP-2 receptors function in the membrane neuron. Trafficking mechanisms and proteolytic processing in Alzheimer's disease. Front Physiol 3.

Srinivas S, Watanabe T, Lin CS, William CM, Tanabe Y, Jessell TM, Costantini F (2001) Cre reporter strains produced by targeted insertion of EYFP and ECFP into the ROSA26 locus. BMC Dev Biol 1:4.

Stallcup WB (1981) The NG2 antigen, a putative lineage marker: immunofluorescent localization in primary cultures of rat brain. Developmental Biology 83:154–165.

Stiles J, Jernigan TL (2010) The basics of brain development. Neuropsychol Rev 20:327–348.

Stiles TL, Dickendesher TL, Gaultier A, Fernandez-Castaneda A, Mantuano E, Giger RJ, Gonias SL (2013) LDL receptor-related protein-1 is a sialic-acid-independent receptor for myelin-associated glycoprotein that functions in neurite outgrowth inhibition by MAG and CNS myelin. J Cell Sci 126:209–220.

Su J, Klemm MA, Josephson AM, Fox MA (2013) Contributions of VLDLR and LRP8 in the establishment of retinogeniculate projections. Neural Development 8:1–1.

Sun LO, Mulinyawe SB, Collins HY, Ibrahim A, Li Q, Simon DJ, Tessier-Lavigne M, Barres BA (2018) Spatiotemporal Control of CNS Myelination by Oligodendrocyte Programmed Cell Death through the TFEB-PUMA Axis. Cell 175:1811–1826.e1821.

Sun SW, Liang HF, Trinkaus K, Cross AH, Armstrong RC, Song SK (2006) Noninvasive detection of cuprizone induced axonal damage and demyelination in the mouse corpus callosum. Magn Reson Med 55:302–308.

Suter DM, Forscher P (2000) Substrate-cytoskeletal coupling as a mechanism for the regulation of growth cone motility and guidance. J Neurobiol 44:97–113.

Tabernero A, Velasco A, Granda B, Lavado EM, Medina JM (2002) Transcytosis of Albumin in Astrocytes Activates the Sterol Regulatory Element-binding Protein-1, Which Promotes the Synthesis of the Neurotrophic Factor Oleic Acid. Journal of Biological Chemistry 277:4240–4246.

Takayama Y, May P, Anderson RGW, Herz J (2005) Low density lipoprotein receptor-related protein 1 (LRP1) controls endocytosis and c-CBL-mediated ubiquitination of the platelet-derived growth factor receptor beta (PDGFR beta). Journal of Biological Chemistry 280:18504–18510.

Takebayashi H, Nabeshima Y, Yoshida S, Chisaka O, Ikenaka K, Nabeshima Y-I (2002) The Basic Helix-Loop-Helix Factor Olig2 Is Essential for the Development of Motoneuron and Oligodendrocyte Lineages. Curr Biol 12:1157–1163.

Tekki-Kessaris N, Woodruff R, Hall AC, Gaffield W, Kimura S, Stiles CD, Rowitch DH, Richardson WD (2001) Hedgehog-dependent oligodendrocyte lineage specification in the telencephalon. Development 128:2545–2554.

Telese F, Ma Q, Perez PM, Notani D, Oh S, Li W, Comoletti D, Ohgi KA, Taylor H, Rosenfeld MG (2015) LRP8-Reelin-Regulated Neuronal Enhancer Signature Underlying Learning and Memory Formation. Neuron 86:696–710.

Tessier-Lavigne M, Goodman CS (1996) The molecular biology of axon guidance. Science 274:1123–1133.

Thornalley PJ, Vasák M (1985) Possible role for metallothionein in protection against radiation-induced oxidative stress. Kinetics and mechanism of its reaction with superoxide and hydroxyl radicals. Biochim Biophys Acta 827:36–44.

Tomasiewicz H, Ono K, Yee D, Thompson C, Goridis C, Rutishauser U, Magnuson T (1993) Genetic deletion of a neural cell adhesion molecule variant (N-CAM-180) produces distinct defects in the central nervous system. Neuron 11:1163–1174.

Tomassy GS, Berger DR, Chen H-H, Kasthuri N, Hayworth KJ, Vercelli A, Seung HS, Lichtman JW, Arlotta P (2014) Distinct profiles of myelin distribution along single axons of pyramidal neurons in the neocortex. Science 344:319–324.

Trapp BD, Nishiyama A, Cheng D, Macklin W (1997) Differentiation and death of premyelinating oligodendrocytes in developing rodent brain. J Cell Biol 137:459–468.

Traub LM (2009) Tickets to ride: selecting cargo for clathrin-regulated internalization. Nat Rev Mol Cell Biol 10:583–596.

Tripathi RB, Clarke LE, Burzomato V, Kessaris N, Anderson PN, Attwell D, Richardson WD (2011) Dorsally and Ventrally Derived Oligodendrocytes Have Similar Electrical Properties but Myelinate Preferred Tracts. Journal of Neuroscience 31:6809–6819.

Tripathi RB, Jackiewicz M, McKenzie IA, Kougioumtzidou E, Grist M, Richardson WD (2017) Remarkable Stability of Myelinating Oligodendrocytes in Mice. CellReports 21:316–323.

Trommsdorff M, Borg JP, Margolis B, Herz J (1998) Interaction of cytosolic adaptor proteins with neuronal apolipoprotein E receptors and the amyloid precursor protein. Journal of Biological Chemistry 273:33556–33560.

Trommsdorff M, Gotthardt M, Hiesberger T, Shelton J, Stockinger W, Nimpf J, Hammer RE, Richardson JA, Herz J (1999) Reeler/Disabled-like disruption of neuronal migration in knockout mice lacking the VLDL receptor and ApoE receptor 2. Cell 97:689–701.

Tsai H-H, Niu J, Munji R, Davalos D, Chang J, Zhang H, Tien A-C, Kuo CJ, Chan JR, Daneman R, Fancy SPJ (2016) Oligodendrocyte precursors migrate along vasculature in the developing nervous system. Science 351:379–384.

Tzartos JS, Friese MA, Craner MJ, Palace J, Newcombe J, Esiri MM, Fugger L (2008) Interleukin-17 production in central nervous system-infiltrating T cells and glial cells is associated with active disease in multiple sclerosis. The American Journal of Pathology 172:146–155.

Ulery PG, Beers J, Mikhailenko I, Tanzi RE, Rebeck GW, Hyman BT, Strickland DK (2000) Modulation of beta-amyloid precursor protein processing by the low density lipoprotein receptor-related protein (LRP). Evidence that LRP contributes to the pathogenesis of Alzheimer's disease. Journal of Biological Chemistry 275:7410–7415.

Vaillant C, Michos O, Orolicki S, Brellier F, Taieb S, Moreno E, Te H, Zeller R, Monard D (2007) Protease nexin 1 and its receptor LRP modulate SHH signalling during cerebellar development. Development 134:1745–1754.

Vallstedt A, Klos JM, Ericson J (2005) Multiple Dorsoventral Origins of Oligodendrocyte Generation in the Spinal Cord and Hindbrain. Neuron 45:55–67.

Van Gool B, Storck SE, Reekmans SM, Lechat B, Gordts PLSM, Pradier L, Pietrzik CU, Roebroek AJM (2019) LRP1 Has a Predominant Role in Production over Clearance of Aβ in a Mouse Model of Alzheimer's Disease. Mol Neurobiol 330:1774–12.

Van Uden E, Carlson G, St George-Hyslop P, Westaway D, Orlando R, Mallory M, Rockenstein E, Masliah E (1999) Aberrant presenilin-1 expression downregulates LDL receptor-related protein (LRP): is LRP central to Alzheimer's disease pathogenesis? Mol Cell Neurosci 14:129–140.

Velez-Fort M, Maldonado PP, Butt AM, Audinat E, Angulo MC (2010) Postnatal Switch from Synaptic to Extrasynaptic Transmission between Interneurons and NG2 Cells. Journal of Neuroscience 30:6921–6929.

Viganò F, Schneider S, Cimino M, Bonfanti E, Gelosa P, Sironi L, Abbracchio MP, Dimou L (2016) GPR17 expressing NG2-Glia: Oligodendrocyte progenitors serving as a reserve pool after injury. Glia 64:287–299.

Vogel C, Marcotte EM (2012) Insights into the regulation of protein abundance from proteomic and transcriptomic analyses. Nat Rev Genet 13:227–232.

Wake H, Lee PR, Fields RD (2011) Control of local protein synthesis and initial events in myelination by action potentials. Science 333:1647–1651.

Wang C, Zhang C-J, Martin BN, Bulek K, Kang Z, Zhao J, Bian G, Carman JA, Gao J, Dongre A, Xue H, Miller SD, Qian Y, Hambardzumyan D, Hamilton T, Ransohoff RM, Li X (2017) IL-17 induced NOTCH1 activation in oligodendrocyte progenitor cells enhances proliferation and inflammatory gene expression. Nature Communications 8:15508–15516.

Wang S, Young KM (2014) White matter plasticity in adulthood. Neuroscience 276:148–160.

Wechsler-Reya RJ, Scott MP (1999) Control of neuronal precursor proliferation in the cerebellum by Sonic Hedgehog. Neuron 22:103–114.

Weeber EJ, Beffert U, Jones C, Christian JM, Forster E, Sweatt JD, Herz J (2002) Reelin and ApoE Receptors Cooperate to Enhance Hippocampal Synaptic Plasticity and Learning. Journal of Biological Chemistry 277:39944–39952.

Wicher G, Aldskogius H (2008) Megalin deficiency induces critical changes in mouse spinal cord development. Neuroreport 19:559–563.

Wicher G, Larsson M, Fex Svenningsen A, Gyllencreutz E, Rask L, Aldskogius H (2006) Low density lipoprotein receptor-related protein-2/megalin is expressed in oligodendrocytes in the mouse spinal cord white matter. Journal of Neuroscience Research 83:864–873.

Wicher G, Larsson M, Rask L, Aldskogius H (2005) Low-density lipoprotein receptor-related protein (LRP)-2/megalin is transiently expressed in a subpopulation of neural progenitors in the embryonic mouse spinal cord. J Comp Neurol 492:123–131.

Williamson AV, Compston DA, Randall AD (1997) Analysis of the ion channel complement of the rat oligodendrocyte progenitor in a commonly studied in vitro preparation. Eur J Neurosci 9:706–720.

Willnow TE, ARMSTRONG SA, Hammer RE, Herz J (1995) Functional Expression of Low-Density-Lipoprotein Receptor-Related Protein Is Controlled by Receptor-Associated Protein in-Vivo. PNAS 92:4537–4541.

Willnow TE, Christ A, Hammes A (2012) Endocytic receptor-mediated control of morphogen signaling. Development 139:4311–4319.

Willnow TE, Goldstein JL, Orth K, BROWN MS, Herz J (1992) Low density lipoprotein receptor-related protein and gp330 bind similar ligands, including plasminogen activator-inhibitor complexes and lactoferrin, an inhibitor of chylomicron remnant clearance. Journal of Biological Chemistry 267:26172–26180.

Willnow TE, Hammes A, Eaton S (2007) Lipoproteins and their receptors in embryonic development: more than cholesterol clearance. Development 134:3239–3249.

Willnow TE, Hilpert J, ARMSTRONG SA, Rohlmann A, Hammer RE, Burns DK, Herz J (1996a) Defective forebrain development in mice lacking gp330/megalin. PNAS 93:8460–8464.

Willnow TE, Moehring JM, Inocencio NM, Moehring TJ, Herz J (1996b) The low-density-lipoprotein receptor-related protein (LRP) is processed by furin in vivo and in vitro. Biochem J 313 (Pt 1):71–76.

Woldt E, Matz RL, Terrand J, Mlih M, Gracia C, Foppolo S, Martin S, Bruban V, Ji J, Velot E, Herz J, Boucher P (2011) Differential signaling by adaptor molecules LRP1 and ShcA regulates adipogenesis by the insulin-like growth factor-1 receptor. J Biol Chem 286:16775–16782.

Wolf BB, Lopes MB, VandenBerg SR, Gonias SL (1992) Characterization and immunohistochemical localization of alpha 2-macroglobulin receptor (low-density lipoprotein receptor-related protein) in human brain. The American Journal of Pathology 141:37–42.

Wolff NA, Lee W-K, Abouhamed M, Thévenod F (2008) Role of ARF6 in internalization of metal-binding proteins, metallothionein and transferrin, and cadmium-metallothionein toxicity in kidney proximal tubule cells. Toxicology and Applied Pharmacology 230:78–85.

Wolswijk G (2002) Oligodendrocyte precursor cells in the demyelinated multiple sclerosis spinal cord. Brain 125:338–349.

Wu KY, Hengst U, Cox LJ, Macosko EZ, Jeromin A, Urquhart ER, Jaffrey SR (2005) Local translation of RhoA regulates growth cone collapse. Nature 436:1020–1024.

Wu W, Wong K, Chen J, Jiang Z, Dupuis S, Wu JY, Rao Y (1999) Directional guidance of neuronal migration in the olfactory system by the protein Slit. Nature 400:331–336.

Wu Y, Liu Y, Levine EM, Rao MS (2003) Hes1 but not Hes5 regulates an astrocyte versus oligodendrocyte fate choice in glial restricted precursors. Dev Dyn 226:675–689.

Wujak L, Böttcher RT, Pak O, Frey H, Agha El E, Chen Y, Schmitt S, Bellusci S, Schaefer L, Weissmann N, Fässler R, Wygrecka M (2018) Low density lipoprotein receptor-related protein 1 couples β1 integrin activation to degradation. Cell Mol Life Sci 75:1671–1685.

Xiao L, Ohayon D, McKenzie IA, Sinclair-Wilson A, Wright JL, Fudge AD, Emery B, Li H, Richardson WD (2016) Rapid production of new oligodendrocytes is required in the earliest stages of motor-skill learning. Nature Publishing Group 19:1210–1217.

Xing YL, Röth PT, Stratton JAS, Chuang BHA, Danne J, Ellis SL, Ng SW, Kilpatrick TJ, Merson TD (2014) Adult neural precursor cells from the subventricular zone contribute significantly to oligodendrocyte regeneration and remyelination. J Neurosci 34:14128–14146.

Yamamoto K, Santamaria S, Botkjaer KA, Dudhia J, Troeberg L, Itoh Y, Murphy G, Nagase H (2017) Inhibition of Shedding of Low-Density Lipoprotein Receptor-Related Protein 1

Reverses Cartilage Matrix Degradation in Osteoarthritis. Arthritis & Rheumatology 69:1246–1256.

Yamanaka Y, Faghihi MA, Magistri M, Alvarez-Garcia O, Lotz M, Wahlestedt C (2015) Antisense RNA Controls LRP1 Sense Transcript Expression through Interaction with a Chromatin- Associated Protein, HMGB2. CellReports 11:967–976.

Yang L, Liu C-C, Zheng H, Kanekiyo T, Atagi Y, Jia L, Wang D, N'songo A, Can D, Xu H, Chen X-F, Bu G (2016) LRP1 modulates the microglial immune response via regulation of JNK and NF-kappa B signaling pathways. J Neuroinflammation 13.

Yang T-H, St John LS, Garber HR, Kerros C, Ruisaard KE, Clise-Dwyer K, Alatrash G, Ma Q, Molldrem JJ (2018) Membrane-Associated Proteinase 3 on Granulocytes and Acute Myeloid Leukemia Inhibits T Cell Proliferation. J Immunol 201:1389–1399.

Yepes M, Sandkvist M, Moore EG, Bugge TH, Strickland DK, Lawrence DA (2003) Tissue-type plasminogen activator induces opening of the blood-brain barrier via the LDL receptor–related protein. J Clin Invest 112:1533–1540.

Yeung MSY, Djelloul M, Steiner E, Bernard S, Salehpour M, Possnert G, Brundin L, Frisén J (2019) Dynamics of oligodendrocyte generation in multiple sclerosis. Nature 566:538–542.

Yeung MSY, Zdunek S, Bergmann O, Bernard S, Salehpour M, Alkass K, Perl S, Tisdale J, Possnert G, Brundin L, Druid H, Frisén J (2014) Dynamics of oligodendrocyte generation and myelination in the human brain. Cell 159:766–774.

Young KM, Fogarty M, Kessaris N, Richardson WD (2007) Subventricular zone stem cells are heterogeneous with respect to their embryonic origins and neurogenic fates in the adult olfactory bulb. J Neurosci 27:8286–8296.

Young KM, Mitsumori T, Pringle N, Grist M, Kessaris N, Richardson WD (2010) An Fgfr3-iCreER T2transgenic mouse line for studies of neural stem cells and astrocytes. Glia:NA–NA.

Young KM, Psachoulia K, Tripathi RB, Dunn S-J, Cossell L, Attwell D, Tohyama K, Richardson WD (2013) Oligodendrocyte Dynamics in the Healthy Adult CNS: Evidence for Myelin Remodeling. Neuron 77:873–885.

Yuseff MI, Farfán P, Bu G, Marzolo M-P (2007) A cytoplasmic PPPSP motif determines megalin“s phosphorylation and regulates receptor”s recycling and surface expression. Traffic 8:1215–1230.

Zarbalis K, May SR, Shen Y, Ekker M, Rubenstein JLR, Peterson AS (2004) A Focused and Efficient Genetic Screening Strategy in the Mouse: Identification of Mutations That Disrupt Cortical Development Joshua R Sanes, ed. PLoS Biol 2:e219–11.

Zawadzka M, Rivers LE, Fancy SPJ, Zhao C, Tripathi R, Jamen F, Young K, Goncharevich A, Pohl H, Rizzi M, Rowitch DH, Kessaris N, Suter U, Richardson WD, Franklin RJM (2010) CNS-Resident Glial Progenitor/Stem Cells Produce Schwann Cells as well as Oligodendrocytes during Repair of CNS Demyelination. Stem Cell 6:578–590.

Zhang C, An J, Strickland DK, Yepes M (2017) The Low-Density Lipoprotein Receptor-Related Protein 1 Mediates Tissue-Type Plasminogen Activator-Induced Microglial Activation in the Ischemic Brain. The American Journal of Pathology 174:586–594.

Zhang Y, Argaw AT, Gurfein BT, Zameer A, Snyder BJ, Ge C, Lu QR, Rowitch DH, Raine CS, Brosnan CF, John GR (2009) Notch1 signaling plays a role in regulating precursor differentiation during CNS remyelination. Proc Natl Acad Sci USA 106:19162–19167.

Zhang Y, Chen K, Sloan SA, Bennett ML, Scholze AR, O'Keeffe S, Phatnani HP, Guarnieri P, Caneda C, Ruderisch N, Deng S, Liddelow SA, Zhang C, Daneman R, Maniatis T, Barres BA, Wu JQ (2014) An RNA-Sequencing Transcriptome and Splicing Database of Glia, Neurons, and Vascular Cells of the Cerebral Cortex. Journal of Neuroscience 34:11929–11947.

Zheng G, Bachinsky DR, Stamenkovic I, Strickland DK, Brown D, Andres G, McCluskey RT (1994) Organ distribution in rats of two members of the low-density lipoprotein receptor gene family, gp330 and LRP/alpha 2MR, and the receptor-associated protein (RAP). Journal of Histochemistry and Cytochemistry 42:531–542.

Zhou Q, Anderson DJ (2002) The bHLH transcription factors OLIG2 and OLIG1 couple neuronal and glial subtype specification. Cell 109:61–73.

Zhou Q, Wang S, Anderson DJ (2000) Identification of a novel family of oligodendrocyte lineage-specific basic helix-loop-helix transcription factors. Neuron 25:331–343.

Zhou Y, Graves JS, Simpson S, Charlesworth JC, van der Mei I, Waubant E, Barcellos LF, Belman A, Krupp L, Lucas R, Ponsonby A-L, Taylor BV, Investiga AA (2017) Genetic variation in the gene LRP2 increases relapse risk in multiple sclerosis. J Neurol Neurosurg Psychiatry 88:864–868.

Zhou Y-X, Flint NC, Murtie JC, Le TQ, Armstrong RC (2006) Retroviral lineage analysis of fibroblast growth factor receptor signaling in FGF2 inhibition of oligodendrocyte progenitor differentiation. Glia 54:578–590.

Zhu L, Su Q, Jie X, Liu A, Wang H, He B, Jiang H (2016) NG2 expression in microglial cells affects the expression of neurotrophic and proinflammatory factors by regulating FAK phosphorylation. Sci Rep 6.

Zhu X, Bergles DE, Nishiyama A (2008) NG2 cells generate both oligodendrocytes and gray matter astrocytes. Development 135:145–157.

Zhu X, Hill RA, Dietrich D, Komitova M, Suzuki R, Nishiyama A (2011) Age-dependent fate and lineage restriction of single NG2 cells. Development 138:745–753.

Zonouzi M, Renzi M, Farrant M, Cull-Candy SG (2011) Bidirectional plasticity of calcium-permeable AMPA receptors in oligodendrocyte lineage cells. Nature Publishing Group 14:1430–1438.

Zou Y, Jiang W, Wang J, Li Z, Zhang J, Bu J, Zou J, Zhou L, Yu S, Cui Y, Yang W, Luo L, Lu QR, Liu Y, Chen M, Worley PF, Xiao B (2014) Oligodendrocyte Precursor Cell-Intrinsic Effect of Rheb1 Controls Differentiation and Mediates mTORC1-Dependent Myelination in Brain. Journal of Neuroscience 34:15764–15778.

Zucker MM, Wujak L, Gungl A, Didiasova M, Kosanovic D, Petrovic A, Klepetko W, Schermuly RT, Kwapiszewska G, Schaefer L, Wygrecka M (2019) LRP1 promotes synthetic phenotype of pulmonary artery smooth muscle cells in pulmonary hypertension. Biochim Biophys Acta Mol Basis Dis 1865:1604–1616.

Zurhove K, Nakajima C, Herz J, Bock HH, May P (2008) Gamma-secretase limits the inflammatory response through the processing of LRP1. Sci Signal 1:ra15–ra15.